Satellite Observations of the Beaufort Sea Ice Cover
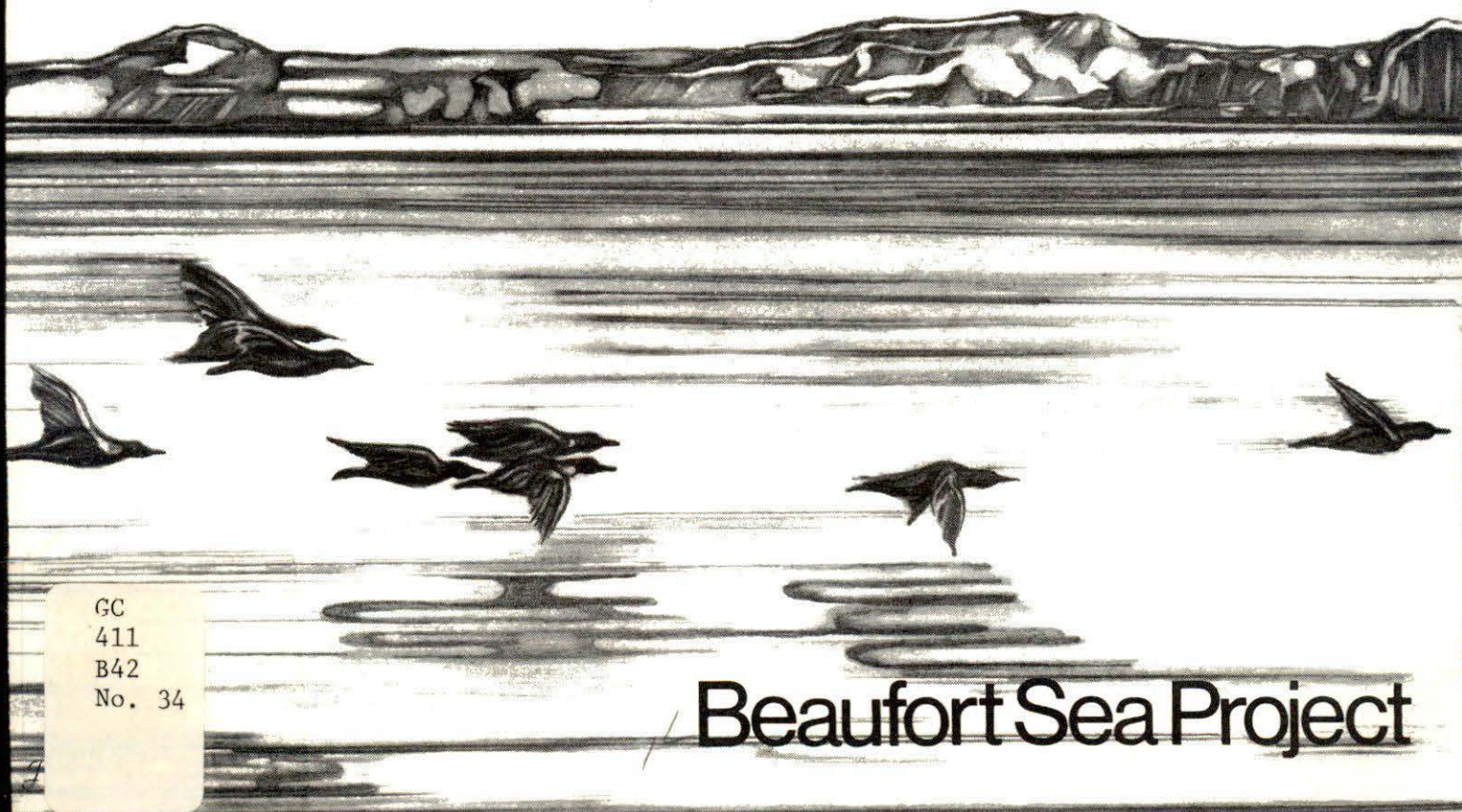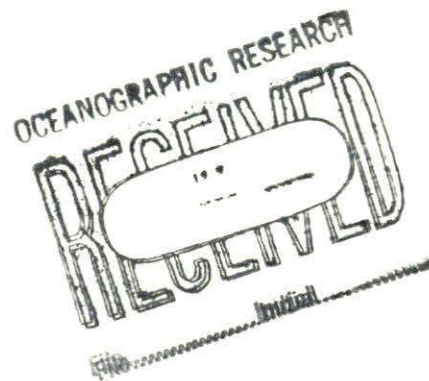
J. MARKO
Technical Report No. 34

Beaufort Sea Project

SATELLITE OBSERVATIONS OF THE

BEAUFORT SEA ICE COVER

J.R. Marko
Under Contract to

Dept. of the Environment
Victoria, B.C.

2 Beaufort Sea Technical Report #34

December 1975

TABLE OF CONTENTS

Page

LIST OF FIGURES

Page

1. SUMMARY

Using the NOAA and ERTS series of satellites, observations of the Beaufort Sea and encompassing Canada Basin ice cover have been carried out for the March through October periods of the years 1973-5. The seasonal trends in motion and appearance over each of these years were detailed for the defined landfast-ice, transition and gyral pack zones. The positionings of the summer ice pack boundaries, the leads at the edge of the landfast-ice and other surface features were determined. A systematic eastward progression of north-south leads was seen to be an early step in the spring break-up process. The close association of the individual steps in this progression with easterly wind allignments suggested the over-riding importance to a given ice configuration of the immediately preceding and contemporary atmospheric pressure patterns.

The ubiquitous presence of rectilinear leads in the gyral pack zone, sometimes arranged in macro-scale patterns of great extent and spatial periodicity, was discovered. These were found to be associated with localized, long period or monotonic shearing displacements. Arguments are given in support of the proposition that these features are produced by current shears in the surface water layer associated with propagating planetary waves. Consideration is given to alternative interpretations, specifically including the possibility that the observed patterns represent massive scale strike-slip faulting.

Observations of the patterns of movement of the turbid Mackenzie River water and smaller ice floes were used to determine the extent and directionality of the river's low salinity water distribution and the peculiarities of individual surface flow features such as the Herschel Island convergence. Relatively general studies of the relationship between isolated floe motion and wind were in basic agreement with the results of other workers. An observed anomalous wavelength dependence in the turbid-water reflected-light levels was attributed to the presence of a characteristic formation of thin cloud.

The data on ice movement and positioning in the landfast-ice and transition zones indicated the proposed 1976 drilling sites to be decidedly non-optimum locations in terms of both the likelihood of single-year drilling success and the minimizing of environmental damage from a possible blow-out. A scenario of oil pollutant transport is offered on the basis of the observed surface movements which, in the proposed drilling area, often averaged 5 to 10 km/day. Further data on these motions in the winter darkness period is required and should be available shortly from longer wavelength infrared satellite imagery.

2. INTRODUCTION

Imagery from the ERTS (Landsat) and NOAA series of observational satellites has been used in both independent and supportive research roles in the Beaufort Sea Project. The first of these systems offers images with approximately 100 m resolution covering a 185 km wide, northeast-southwesterly strip of earth surface. Nominally exact repeat coverage is obtained at 18-day intervals. However, orbital overlap north of 70°N allows a given Arctic ground point to be observed on at least four consecutive days, in the absence of cloud or fog obstruction. Images are available in each of four visible and near infrared wavelength bands: 4 (.5 to .6 μ), 5 (.6 to .7 μ), 6 (.7 to .8 μ) and 7 (.8 to 1.1 μ).* The two longest wavelength bands are generally used in studies directed toward establishing ice types and water-ice boundaries, while band 5 is nearly optimum for water-suspended sediment investigations.

The NOAA satellite systems offer twice-daily (1 day-time and 1 night-time pass) observation in two bands, one visible (.5 to .7 μ) and one "thermal" infrared (10.5 to 12.5 μ) with both coarse (10 km) and intermediate (1 km, in the VHRR** mode) resolution. The utility of this satellite system derives from its daily frequency of repeat observation and its coverage of 2000 km wide, nearly east-west ground swaths at Arctic latitudes. Imagery from both the ERTS and NOAA systems is readily available, not only in standard photographic forms but also in a variety of computer print-out formats which highlight or accent (by expansion and compression of the printed grey-scale) particular aspects of the original digital ground brightness data recorded on magnetic tape. The satellite systems were used individually and in common to explore phenomena of widely varying scales relevant to the Beaufort Sea Project.

The description of the scientific results of observation in the years 1973-5 will begin in Section 3 with an overview of the surface of the Canada Basin and its oceanic boundary areas as obtained primarily from the NOAA satellites. Attention will be paid in Subsection 3.1 to the apparently systematic aspects of the ice break-up process and the distributions of open water and floe ice. The satellite data has been exploited to obtain, for the first time, simultaneous ice displacement mapping over a wide area of the Arctic Ocean's surface. The implications of these results for models of ice and surface water current movement will be discussed in Subsection 3.2. In 3.3 a detailed presentation will be given of a newly discovered phenomenon whereby extremely long, rectilinear leads arrange themselves in criss-cross patterns of great extent, persistence and spatial regularity. Possible alternative explanations of these phenomena will be developed in terms of oceanic planetary waves and the ice cover rheology.

Section 4 will deal specifically with areas of immediate interest in the southeastern Beaufort Sea. Subsections 4.1 and 4.2 will describe the dependence of ice motion upon wind and floe size prior to the development in Subsection 4.3 of a descriptive summary of surface water and ice-motion

---

*One micron (μ) is equal to 10^{-6} m.
**Very High Resolution Radiometer

details. A final summary and discussion of all foregoing results is given in Section 5 along with a consideration of their implications for resource development planning and future environmental research.

3. CANADA BASIN OBSERVATIONS

3.1 Annual Variability and the Spring Break-up Process

Satellite observations of the Beaufort Sea during daylight April to October periods suggest that 1973 and 1975 on one hand, and 1974 on the other, could be classified respectively as extremal "open" and "closed" navigation years. The differences in the corresponding open water distributions are illustrated in Figure 1 where the amount of ice-free surface, determined from each year's NOAA imagery by mechanical planimetry, is plotted as a function of time. These estimates apply to the Beaufort Sea as geographically defined in the Canadian Arctic Pilot and neglect the open waters in those areas in which the ice surface fraction exceeds approximately 5/10. The relatively small amounts of open water in the latter areas may be marginally navigable and often are critical wildfowl habitats. Estimates of their extents and variations have been made in connection with biological studies. The specific seasonal configurations observed will be considered in Section 4. The immediate significance of the open water extent data relates primarily to year-to-year variations in navigability and to radiative and convective energy exchange (with the atmosphere).

Nevertheless, the evolution of the ice surfaces proceeded along remarkably similar lines in each of the observed years. A summary of the surface evolution will be provided in the hope that, because of the constraints imposed by coastal configurations and topography, the underlying massive movements of ice will be restricted to a small number of general forms or modes. This hypothesis seems consistent with historical records of repetitive lead formation in certain areas and would be an important simplification in any future attempt to develop a predictive model of the central ice pack boundary movements.

The March portion of the 1973 ice "break-up" process is perhaps best portrayed in the sketches made by Ackley and Hibler (1974) on the basis of NOAA-2 satellite infrared band imagery. These are reproduced in Figure 2 with the first of the sketches showing leads which parallel the northwestern Alaska coast. On March 19, the most prominent of these leads (actually at that time, a polynya) defined the landfast-ice boundary and gave rise, at its eastern extremity, to a family of long, nearly north-south tendril leads. During the March 19-21 interval, another northeasterly-southwesterly lead with north-south tendrils appeared to the northeast of the earlier openings. By March 25, the eastern portion of the lead system had undergone further development at the expense of its more western elements. Finally on March 30, a new northeasterly-southwesterly lead and north-south tendril complex appeared, accompanied by the disappearance of the north-western Alaska coastal leads and a diminuition in
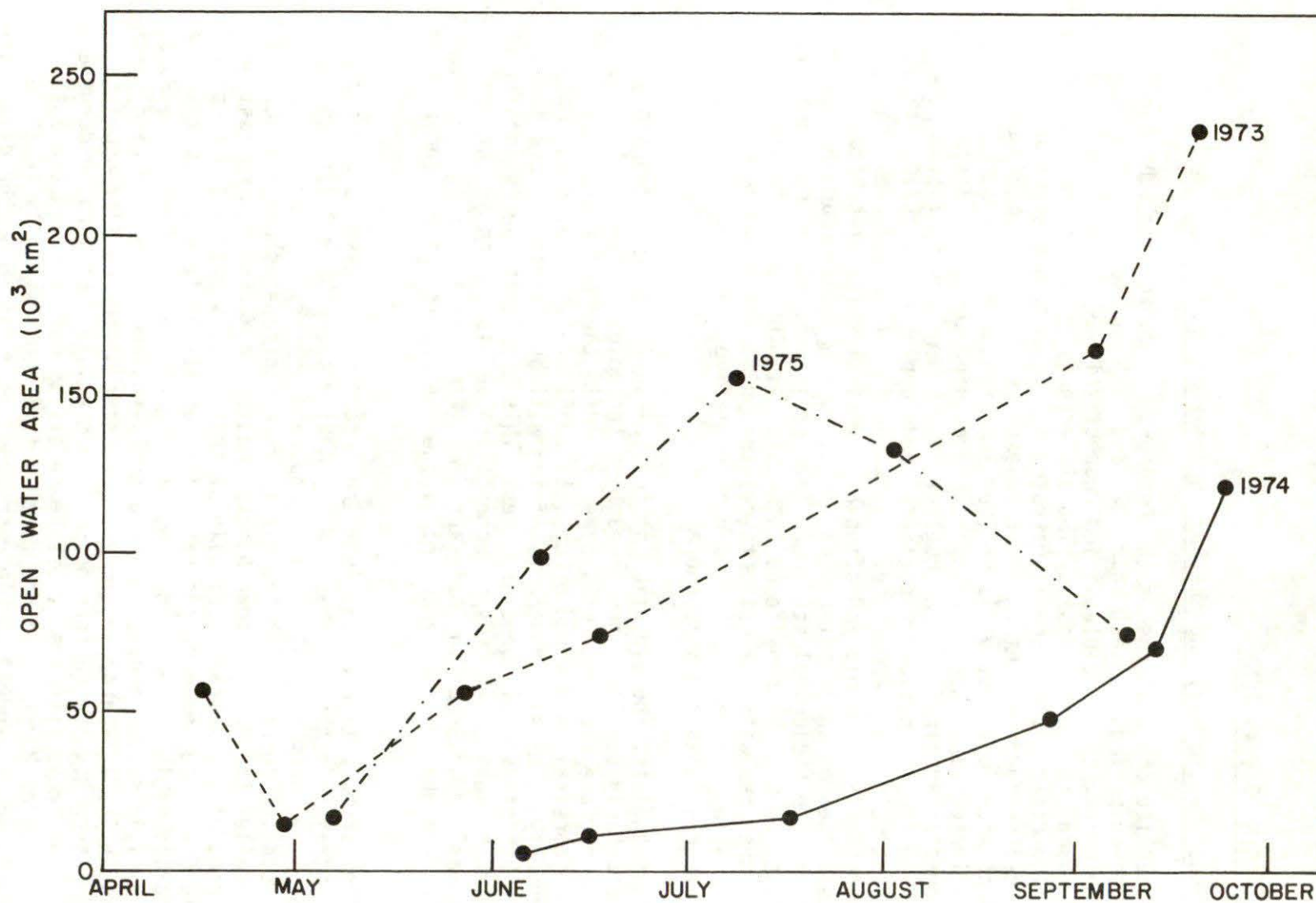
Figure 1. A plot of the open water area in the Beaufort Sea in 1973 (————), 1974 (——————) and 1975 (—·——·—).
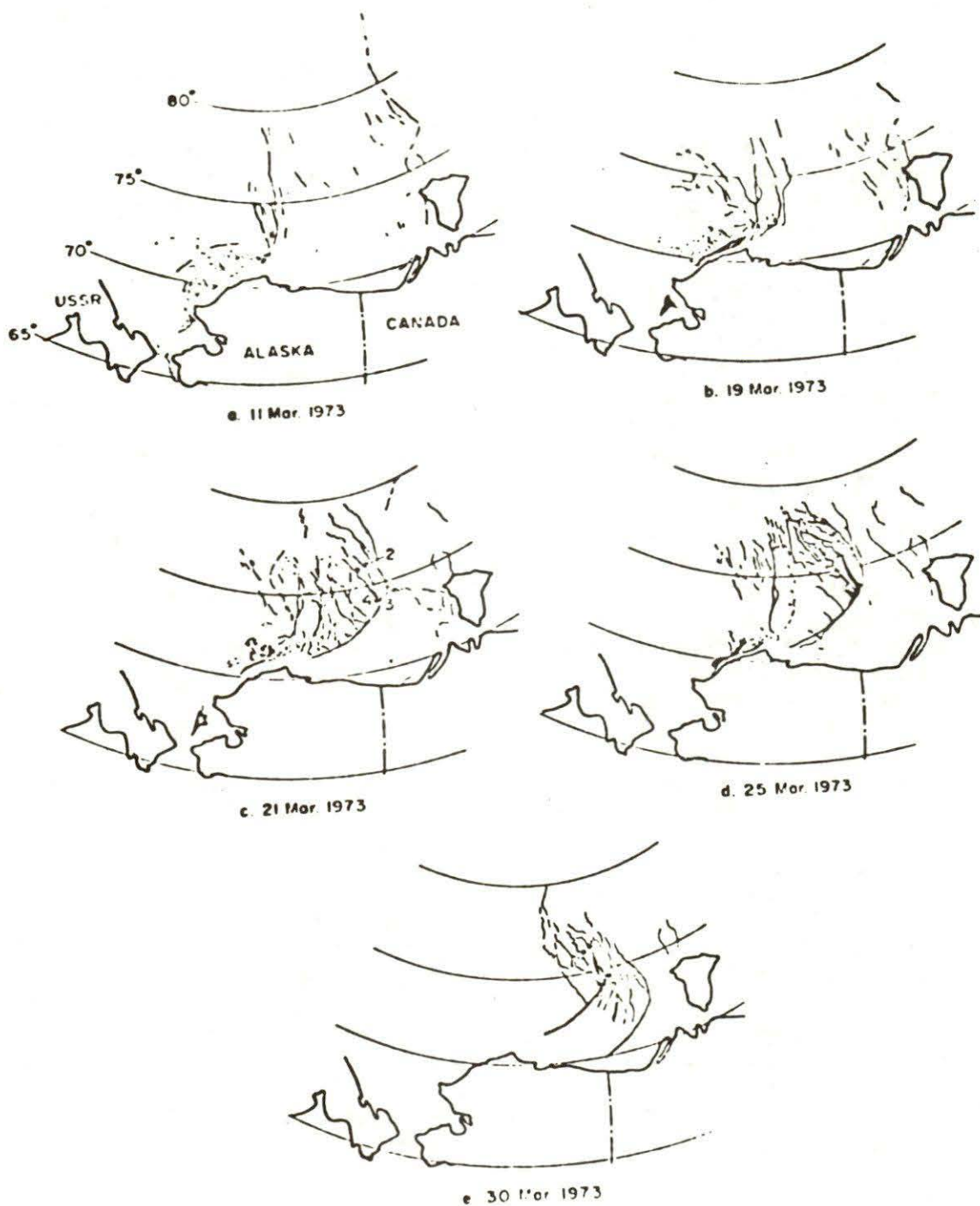
Figure 2.   The major lead configurations of March, 1973 in and near the
Canada Basin of the Arctic Ocean.

the amount of other western open water. Two more additional lead and tendril systems appeared on April 2 and April 7 (see Figure 3) successively to the east of the March 30 complex. The second of these opened with impressive rapidity and after a late April period of refreezing and near-closing, developed into a vast open water area abutting the landfast-ice along the edge of the Canadian Arctic Archipelago (Figure 4). This feature dominated the spring 1973 imagery of the Beaufort Sea and contained most of the open water area plotted in Figure 1.

The available early April 1974 imagery (see Figure 5) displays a lead pattern which developed eastwardly in a manner similar to that of the March 1973 process. During the two week period subsequent to April 7 a slowing and apparent retreat of this development occurred (see Figure 6). The eastward migration of lead complexes resumed sometime after April 24 and on May 9 began to approach the position of the April 1973 eastern landfast-ice boundary (see Figure 7). The 1973 pattern was generally repeated whereby new eastern leads appeared accompanied by the closing of earlier, more western leads and polynyas, although a subsequent fragmentation of the pack still left extensive open water in the west. This fragmentation, which is particularly prominent in the May 16 image (Figure 8), was not visible at a comparable (early April) stage in 1973. The vast open water region which eventually developed from the terminal 1973 eastern lead did *not* have a comparable 1974 counterpart and the eastern end of the Beaufort Sea remained heavily ice-bound throughout the latter year.

Much of the spring behaviour is explicable if one makes the assumption that the directions of large-scale, cooperative ice movements are restricted by adjoining land masses and the locations of open water areas capable of accepting the divergence of the disintegrating ice sheet. The dynamics of ice in coastal regions are often quite distinct from those in areas well removed from land. In the latter case, the ice constitutive parameters are assumed to be invariant under horizontal translation; hence lead generation may be expected to be driven by spatial gradients in the geostrophic wind. Thus, as anticipated by Crowder *et al.* (1974), a correlation should exist between the divergence of the ice velocity and the Laplacian of the surface atmospheric pressure. In the coastal zone, however, the ice properties lose their translational invariance and relative internal ice motion can be produced by a divergenceless wind-field.

Analysis of the satellite imagery suggests that the early season ice motion can be categorized into two closely related phases: (1) There is an initial southwestward movement of the sea ice which lies off the northwestern Alaska coast. Because of the enhanced shear resistance of the landfast-ice, this motion can result in coast-paralleling leads which appear in this area during March. (2) There is a general westward drift of that portion of the Beaufort Sea ice pack which lies to the west of the existing, most-eastern north-south lead complex. Such a movement would be consistent with the observation that the opening of new leads in the east was generally accompanied by the closing of existing western lead systems. The

Figure 3.   An April 10, 1973 NOAA satellite image of the Beaufort Sea. Point Barrow is in the lower left-hand corner. Re-frozen remnants of the leads and polynyas of March and early April may be seen to the left of center along with the huge terminal north-south lead at the edge of the landfast ice in the eastern Sea.

Figure 4.   A June 6, 1973 NOAA satellite image of the Beaufort Sea. Banks
             Island and Cape Bathurst are seen in the lower right-hand corner
             on the eastern boundary of the huge 1973 open water area.
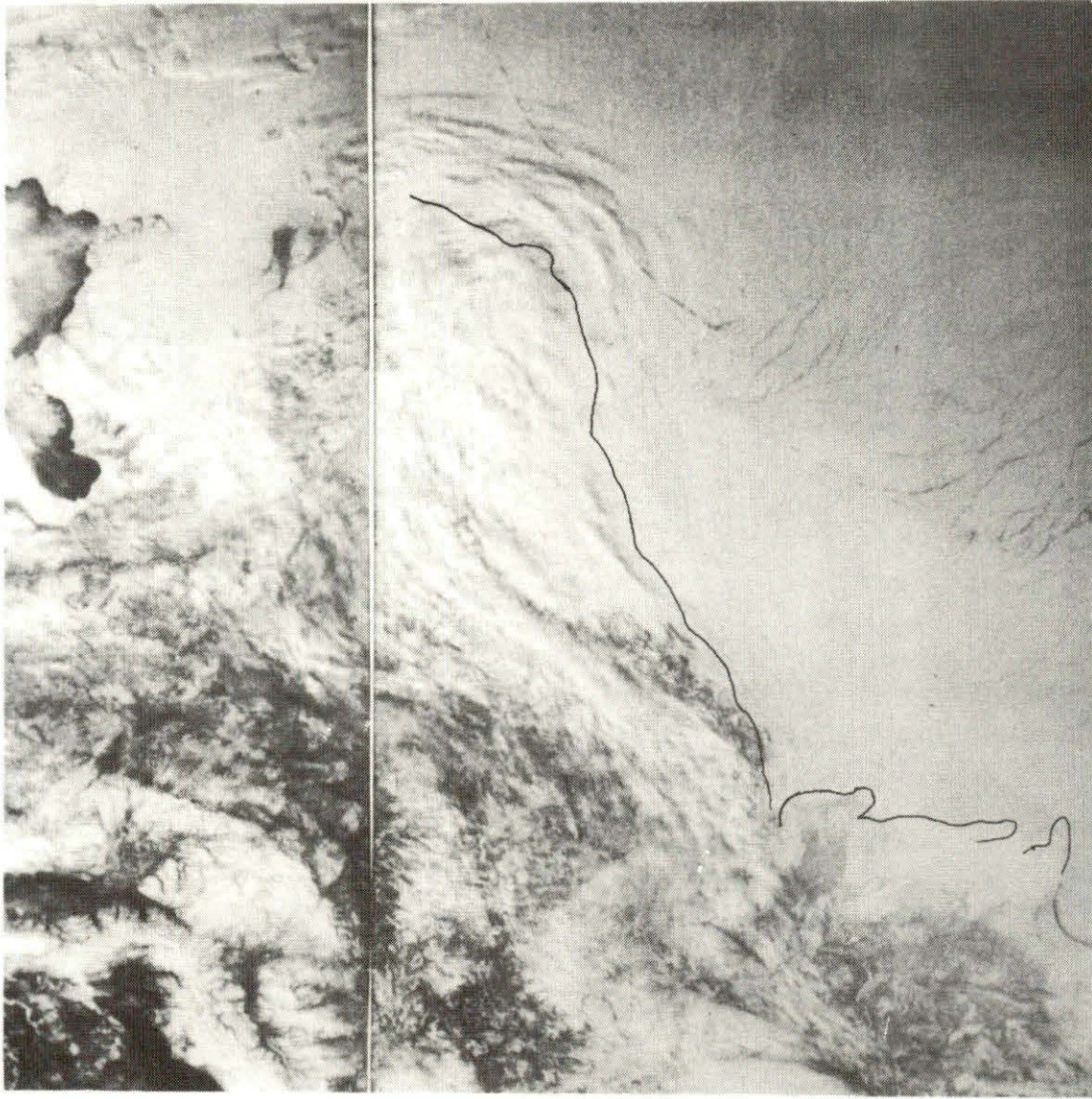
Figure 5.   An April 7, 1974 NOAA satellite image of the Beaufort Sea. Cape
Bathurst is again in the lower right-hand corner while Point
Barrow, Alaska lies under cloud in the upper center. The success-
ively eastward-migrating lead formations are evident.
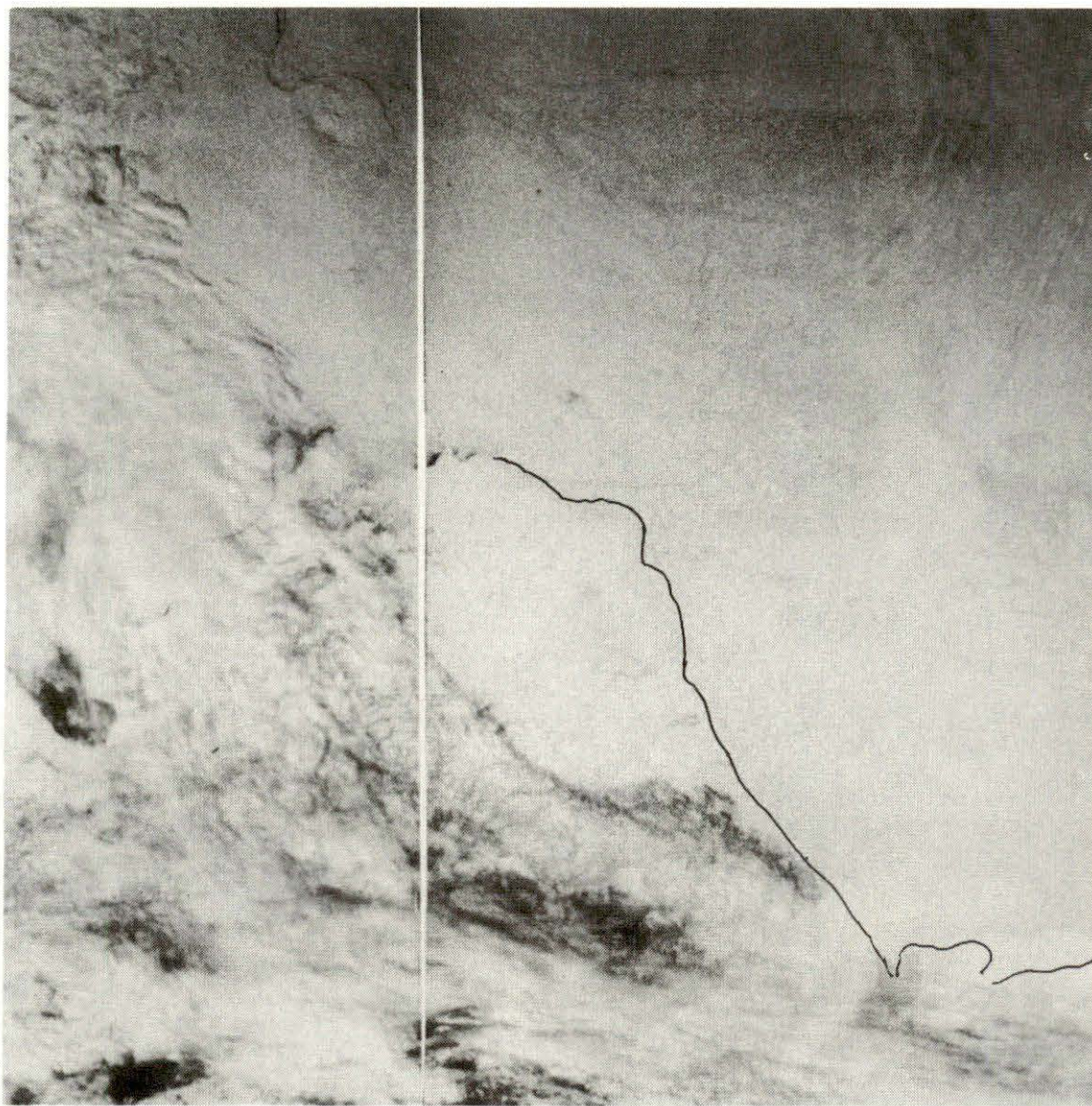
Figure 6.   An April 24, 1974 NOAA satellite image of the Beaufort Sea. The lead structures of Figure 5 can be seen to have vanished without the appearance of more eastward openings.
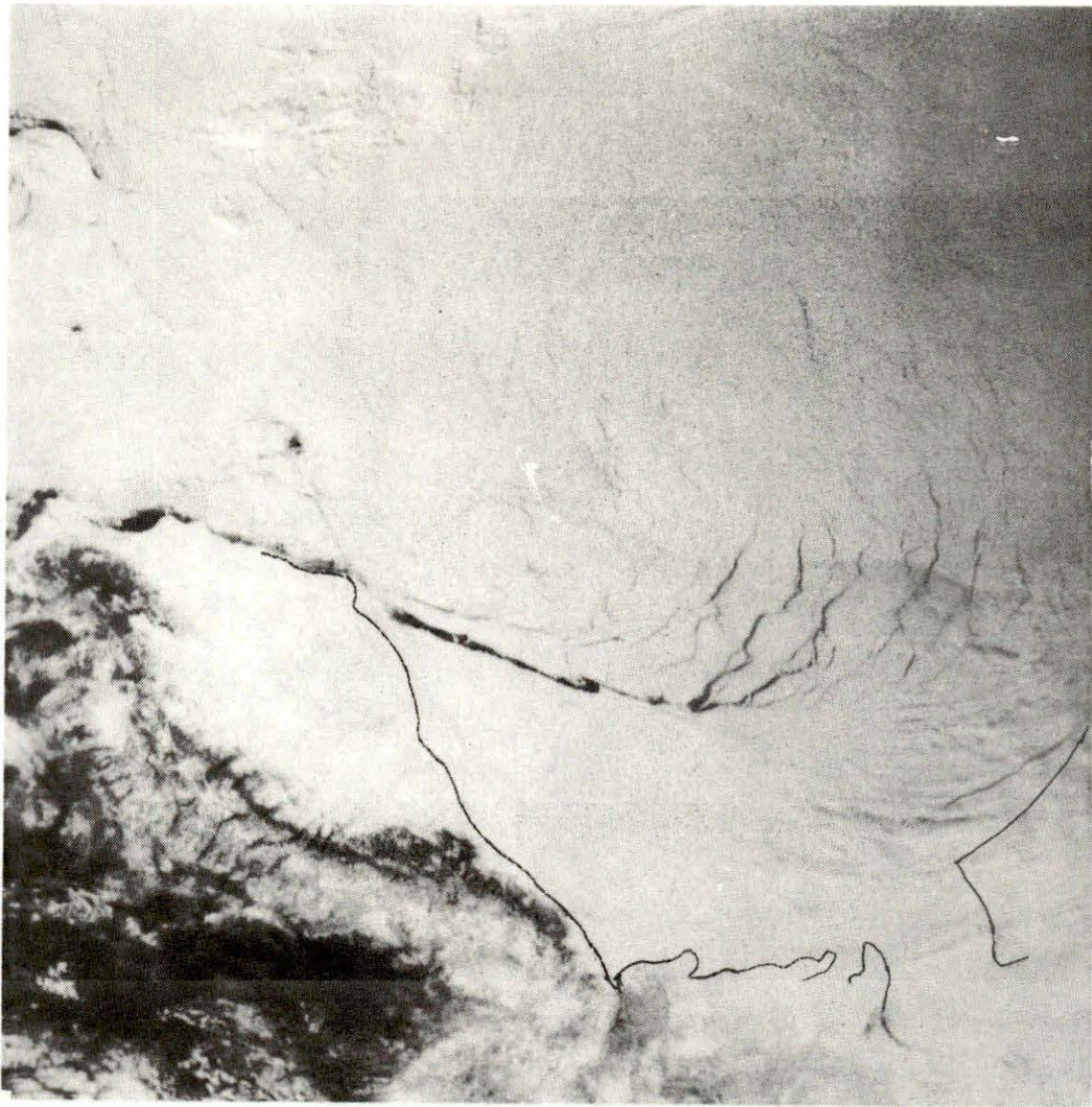
Figure 7.   A May 9, 1974 NOAA satellite image of the Beaufort Sea. The eastward lead migration pictured in Figure 5 has resumed and north-south oriented openings have appeared near the eastern boundary of the Sea.
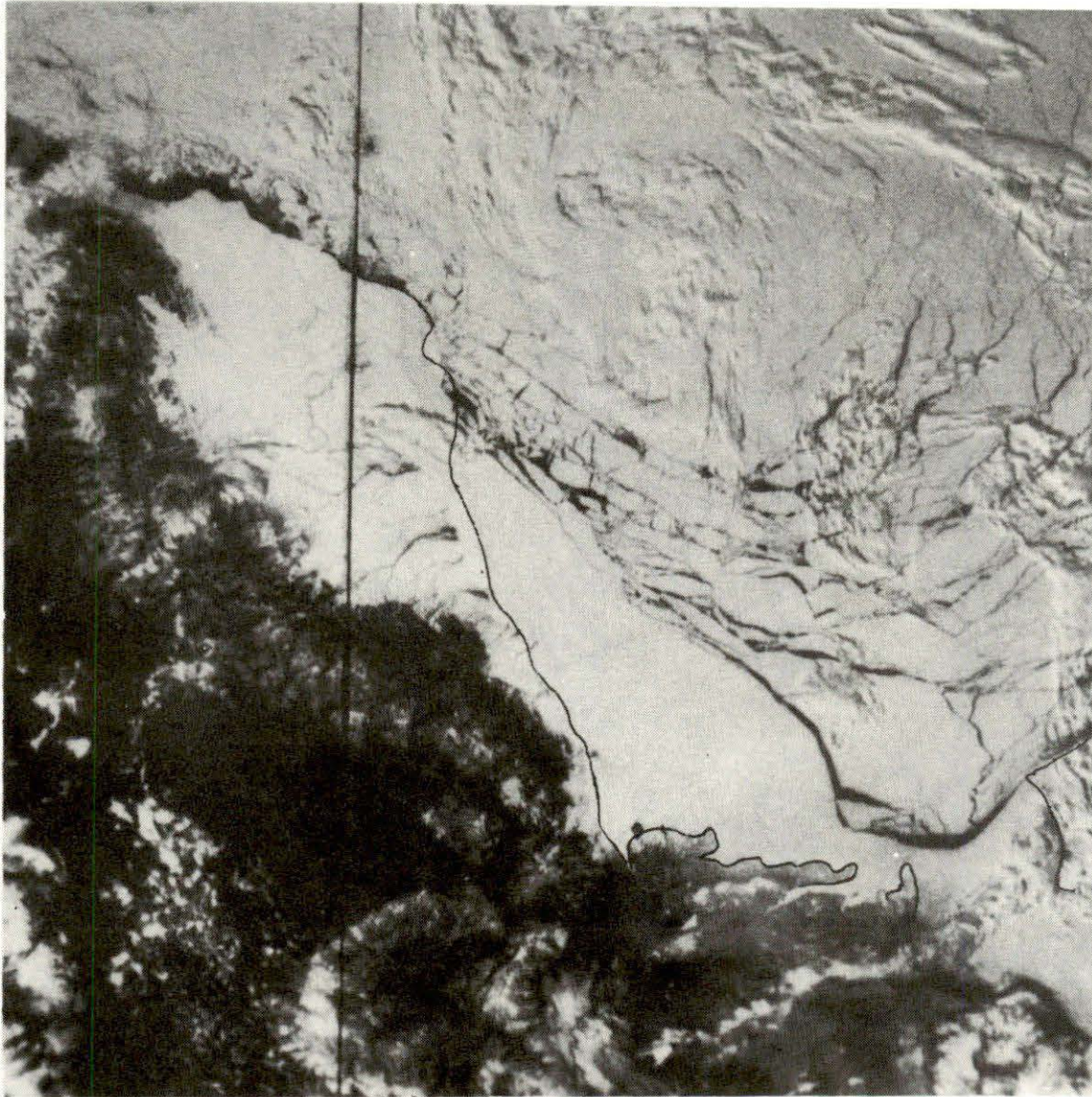
Figure 8. A May 16, 1974 NOAA satellite image of the Beaufort Sea. A general large-scale fragmentation has occurred and large leads are well off-shore in the Mackenzie Bay and Tuktoyaktuk Peninsula regions.

motion is that expected if huge segments are successively detached and moved away from the western edge of a rigid ice sheet anchored in the eastern Beaufort Sea.

An examination of wind data from the northwestern Alaska coastal and central Beaufort Sea regions indicates an excellent correlation between the ice movements described and wind components parallel to the "preferred" westward direction of ice drift. To illustrate, Figure 9 shows the east-west wind component in the central Beaufort Sea (at 134°W, 73°N) for the March 1 to April 30 periods of 1973 and 1974. The plotted winds were obtained from the Canadian Meteorological Service barometric charts by making the geostrophic assumption and including a 20° leftward rotation due to surface friction (Carstensen, 1967). It can be seen that the major lead developments of 1973, as detailed in Figures 2 and 3, invariably coincide with times when the wind has a strong easterly component. The previously-noted mid-April refreezing and near closing of the eastern lead system occurred during a period of negligible easterly winds.

It follows that the later start of the 1974 eastward lead migration resulted from the nearly continuous westerly orientation of the early March winds. Easterly winds finally appeared near the end of the month and evidently resulted in the development of the northwestern Alaska coastal open water region and the initial eastward lead migration shown in Figure 5. The slowing down of this process (Figure 6), on the other hand, was presumably due to the prevalence of westerly mid-April winds. Still yet another wind reversal was responsible for the early May resumption of the eastward lead migration (Figure 7).

Inspection of the ice and wind data shows that similar correlations extend into the summer period. Nevertheless, on a more exacting scale, the weakness of this interpretative approach lies in its failure to account for the dependence of the ice constitutive properties upon time and previous history. For example, no simple reason exists whereby the easterly winds of the May 9-16, 1974 interval produced a general fragmentation of the pack and widely distributed open water areas (see Figure 8) rather than the more localized lead widening occasioned by similar winds in 1973. The relative solidity of the western pack observed in the latter case could have been due to compaction by the previously steady easterly winds, however, it is likely that account must be taken also of the effects of windfield gradients, melting and lead production by the mechanisms to be discussed in 3.3.

Sometime before March 15, 1975, the earliest yet satellite-observed appearance of the eastern Beaufort Sea terminal lead and polynya occurred. The NOAA image of that date (Figure 10) shows this feature as well as a high density of leads to the west. The terminal polynya underwent a near-closing and freezing-over cycle in April but then reopened to give rise to the largest ice-free area observed in the Beaufort Sea during the three years of our study. The rectilinearity and spatial periodicity in the western lead systems evident in Figure 10 will be discussed later in Subsection 3.3.
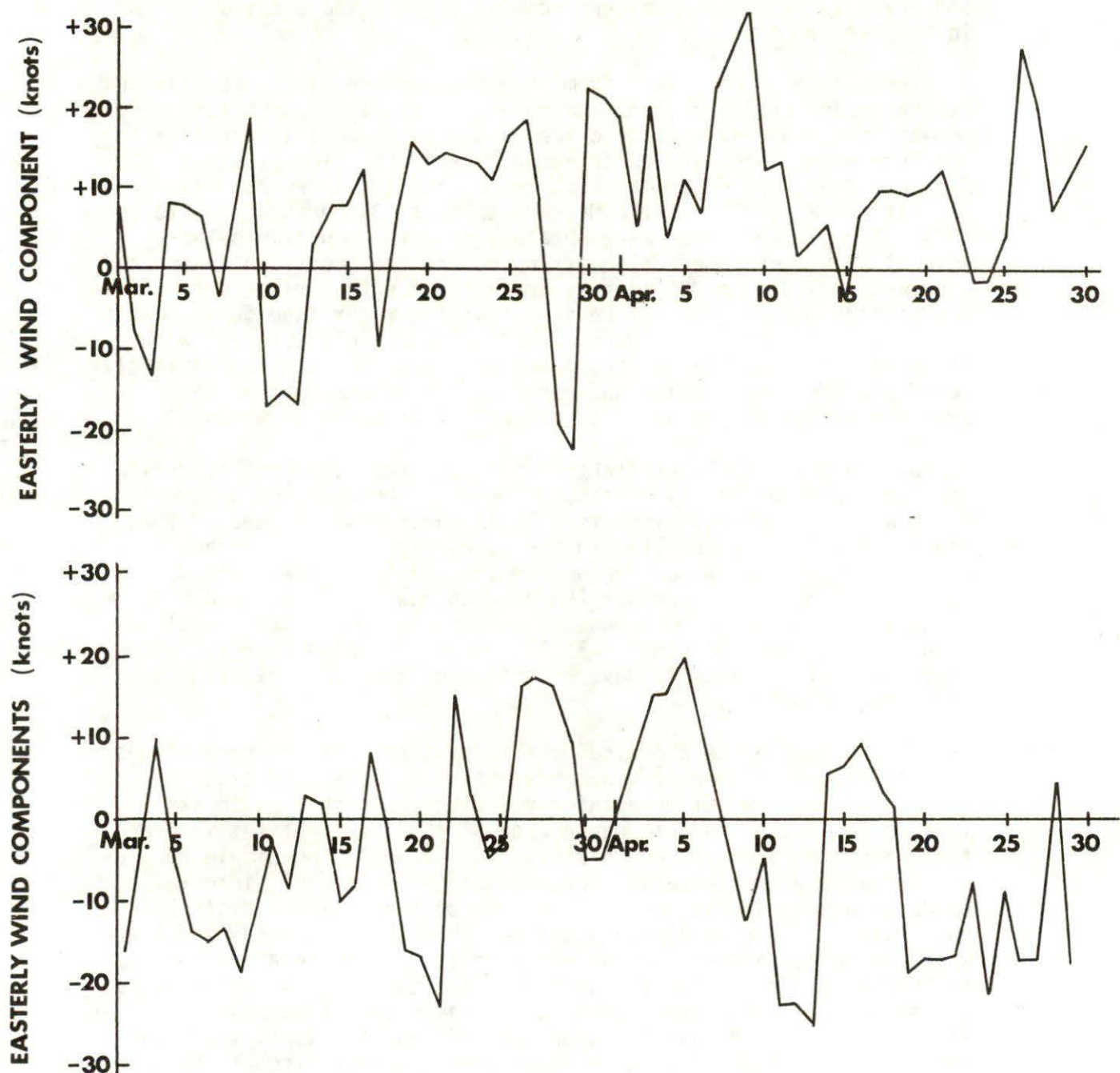
Figure 9 a,b   A plot of the easterly, blowing from the east (+) and westerly, blowing from the west (−), wind components for the March and April periods of 1973 (a) and 1974 (b). The plotted values were calculated for the point (134°W, 73°N) from the surface air pressure chart data using the geostrophic assumption and allowing for a 20° leftward wind rotation due to surface air friction.
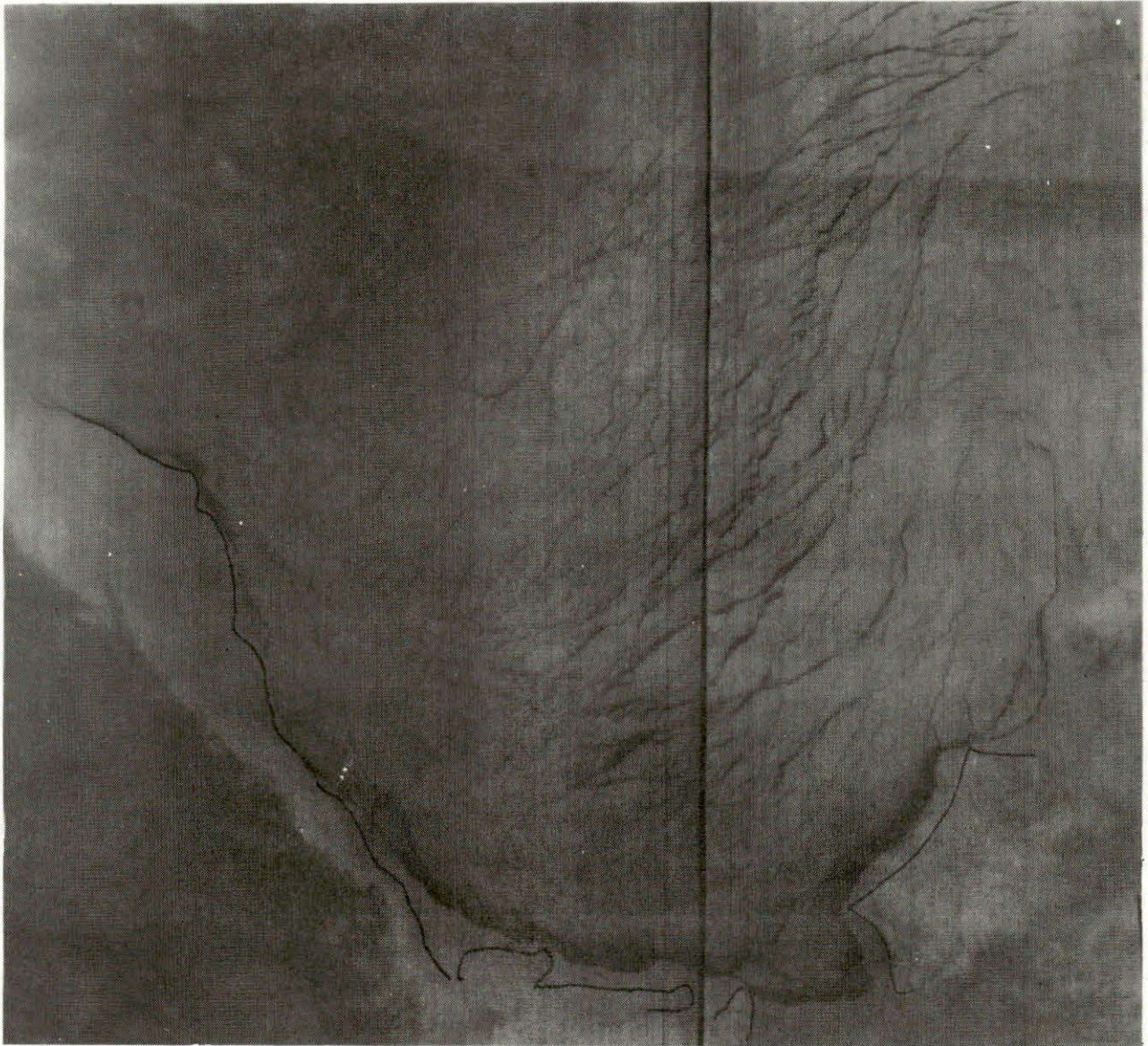
Figure 10. A March 15, 1975 NOAA satellite (infrared band) image of the Beaufort Sea. The eastern terminal polynya and Banks Island are in the lower right-hand corner. A pronounced lead rectilinearity in two nearly north-south directions may be noted along with an eastward-directed curvature in the sections of these leads which extend to the landfast ice edge off the mainland coast (see the lower central portion of the image).

The given interpretation of the evolving ice cover assumed rapid
fracturing of ice under certain wind stresses. This approach differs
considerably from that of Markham (1976) which predicted summer
season navigational conditions on the basis of the net value of a sum
of air pressure differentials taken over the previous months of
January, February and March. The geographic locations of points in
the pressure net were specifically chosen so that the corresponding
spatial differentials would give a measure of the magnitude and dir-
ection of wind-driven ice transport across the principal boundaries
of the Beaufort Sea and Canada Basin regions. These criteria resul-
ted in a reasonably high success rate. In view of the very short
response times observed in our work between favourable wind re-
orientations and steps in the break-up process, it seems that a
better prediction scheme could be based solely upon March, or even
April, atmospheric data. From satellite observations, it is hard to
believe that atmospheric conditions in January and February can ever
counter-balance favourable wind fields in March and April to the
extent that poor early summer navigation results. Consequently, it
would seem that winter winds are of secondary importance to the
spring and summer open-water configurations which correlate closely
with the contemporary and recent wind fields.

3.2 Ice Movement Details

Ocean current measurements and geostrophic calculations based upon
density profiles obtained over many years have established the details
of a long-term, mean gyral ice circulation in the Canada Basin. The
latest calculations are presented in the dynamic height contours of
Figure 11 (Newton, 1973). The largest current velocities are found
to the southwest of the gyral center (which lies at roughly 76°N,
145°W) while the slowest flow occurs to its north-northwest over the
northern Chukchi Province and the northwest arm of the Basin.

The general character of the seasonal movements of ice has been
examined by measuring the displacements of several widely spaced ice
floes over simultaneous intervals of time using 1975 NOAA imagery
(Figures 12-29). The displacement vectors are sketched for success-
ive and sometimes slightly overlapping intervals of roughly one or
two weeks duration. Before discussing details, note should be taken
of the paucity of ice drift data in the southern Beaufort Sea which
results from frequent obstruction by cloud and fog and the rapidly
changing shapes and sizes of floes in this area. Some southern ice
drift measurements obtained near the edge of the ice pack will be
shown in Subsection 4.3.

The resulting ice drifts shown in Figures 12-29 only rarely followed
the gyre-like pattern shown in Figure 11. Instead, over a given
interval, there was usually a common direction to the motion at
different points, although there were distinct differences in speed.
The general trend of the drifts can be seen in Table 1 in which is
contained the average speeds and directions as deduced over each
interval in the immediate vicinity of point "A" in Figure 12. Point
A was chosen for particular attention because of the continuity of
its ice displacement data. Early in the season (through May), major
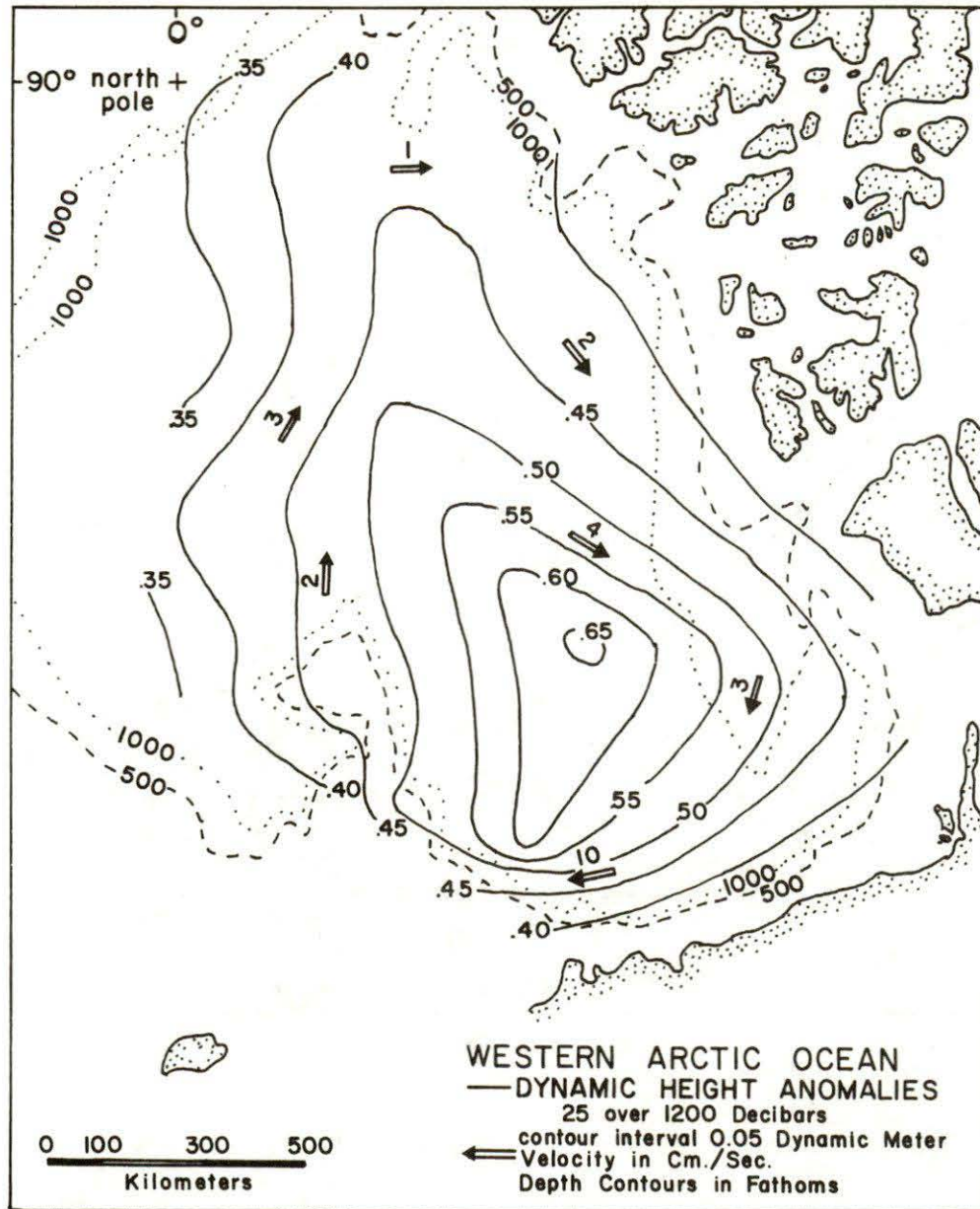
Figure 11. A compilation by Newton (1974) of dynamic height anomaly data for the Canada Basin of the Arctic Ocean. The corresponding near geostrophic velocities are indicated by the labelled arrows.
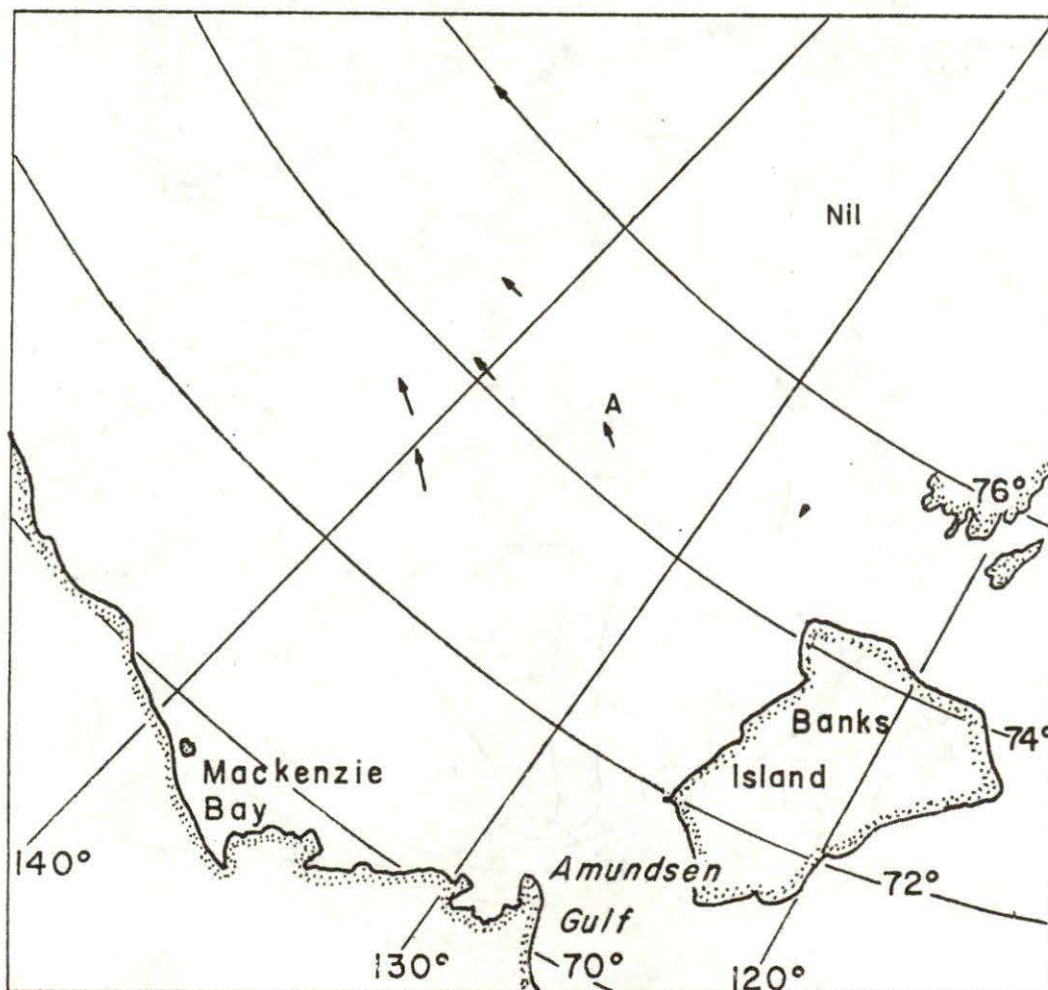
Figure 12.   Ice displacement vectors in the Canada Basin for the March 28, 1975 to April 3, 1975 interval.   Because of the corresponding high frequency of observations, a compilation of the velocities at or near point A is presented in Table I.
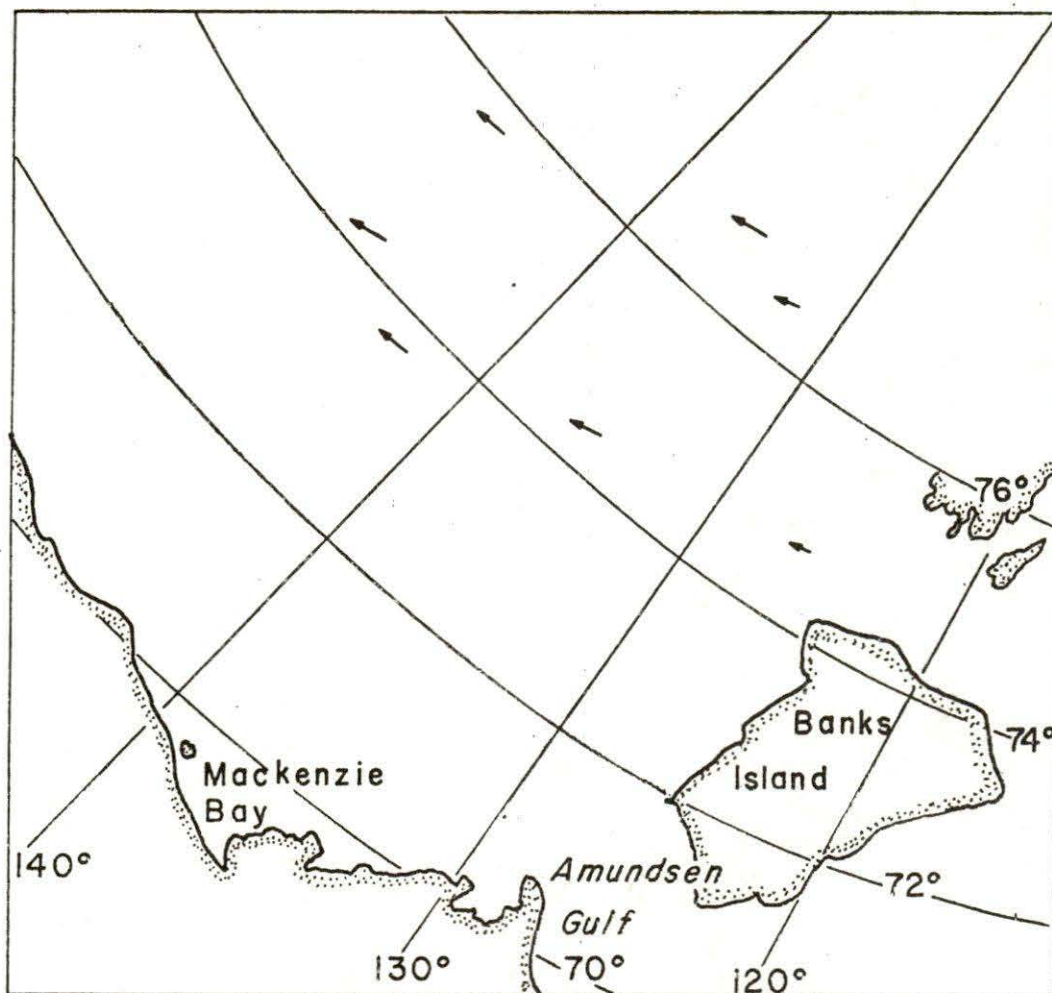
Figure 13. Ice displacement vectors in the Canada Basin for the April 3, 1975 to April 9, 1975 interval.
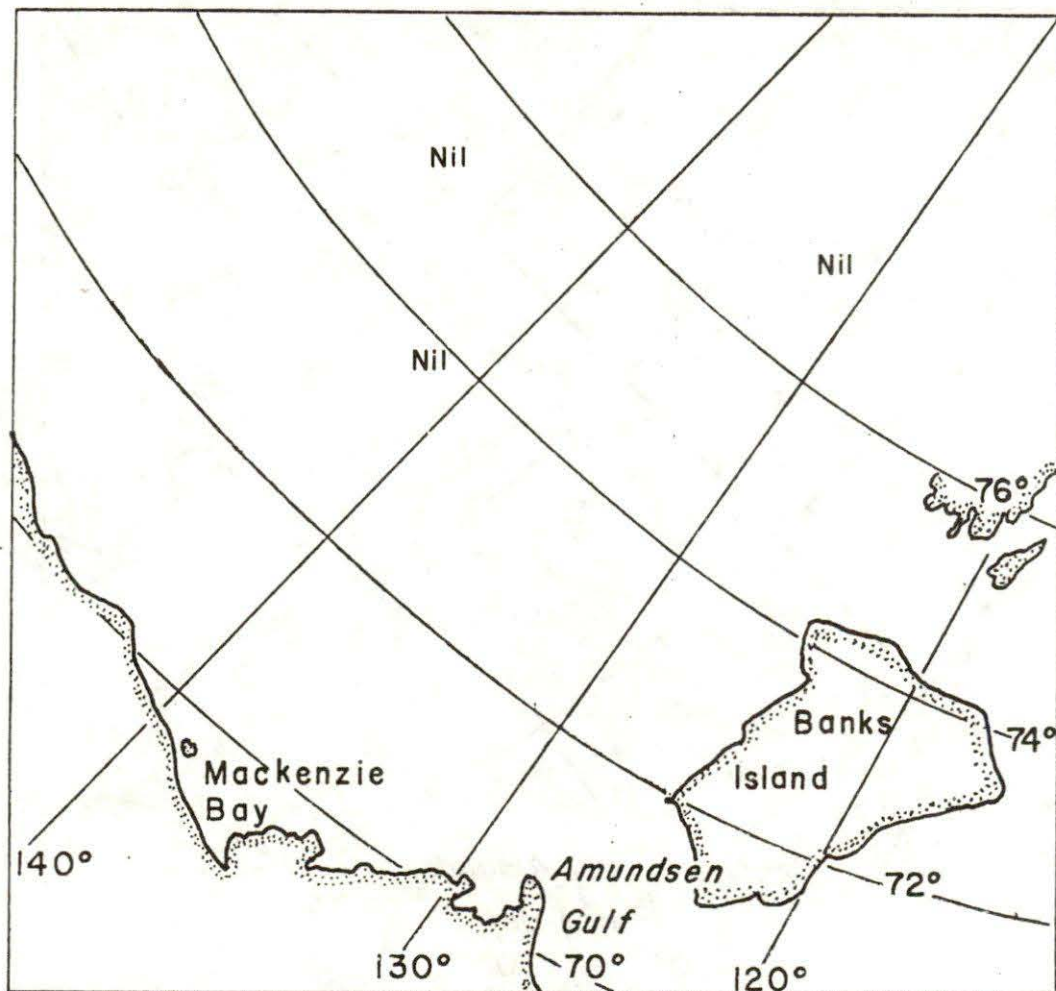
Figure 14. Ice displacement vectors in the Canada Basin for the April 9, 1975 to April 15, 1975 interval.
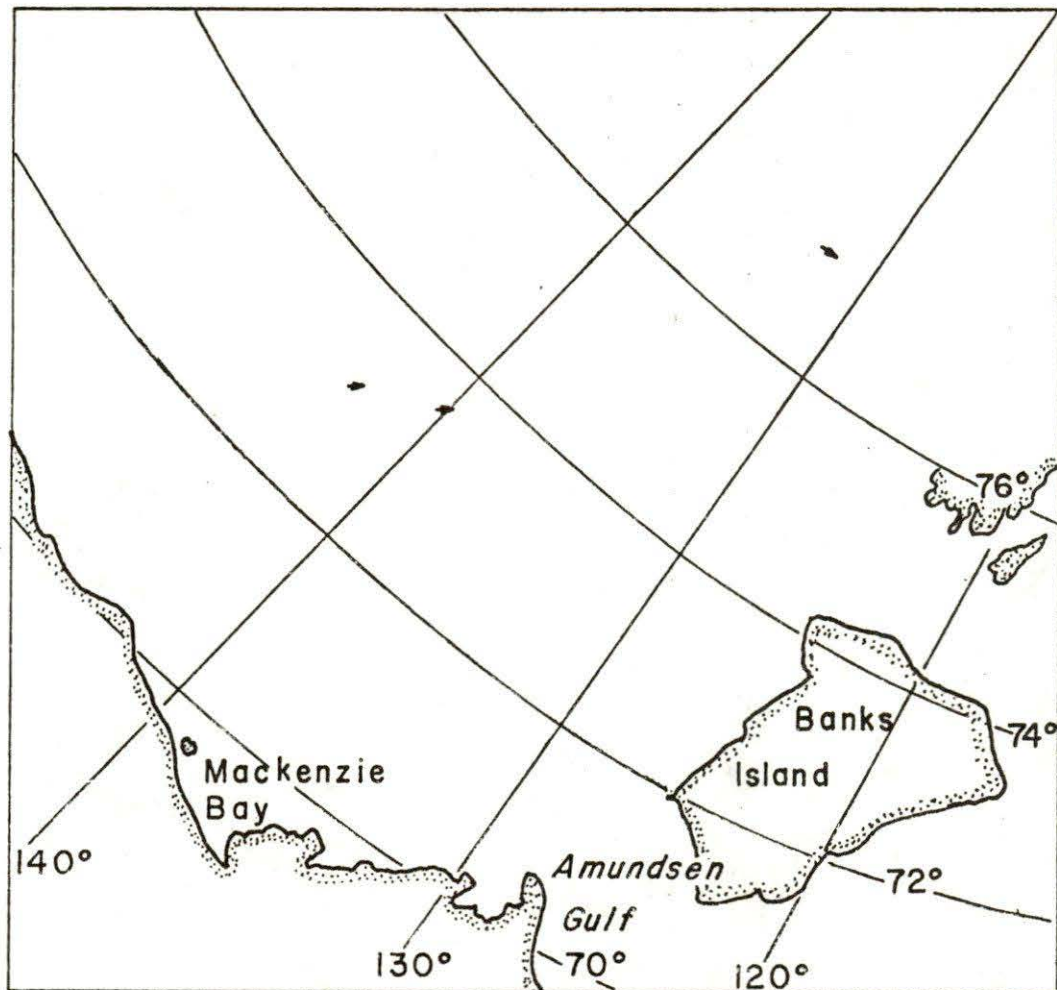
Figure 15.   Ice displacement vectors in the Canada Basin for the April 15, 1975 to April 25, 1975 interval.
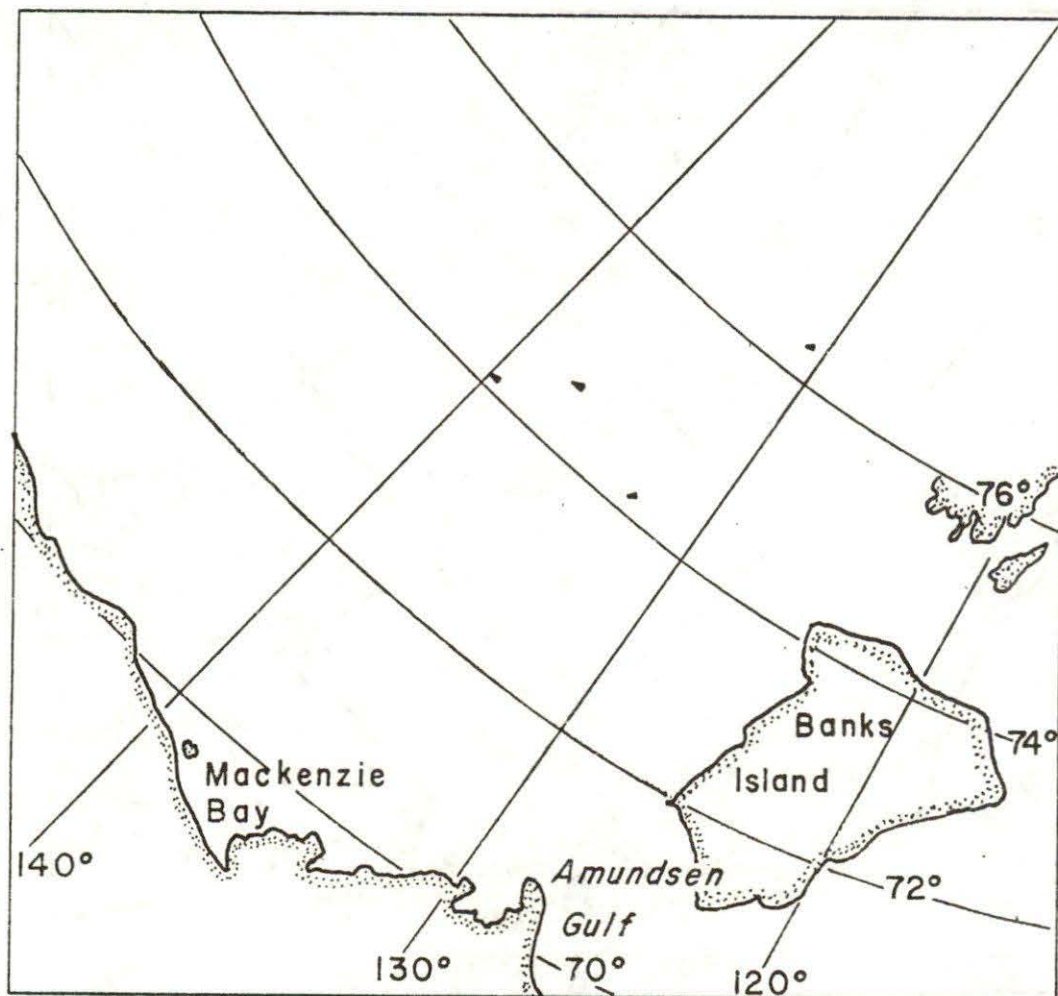
Figure 16.   Ice displacement vectors in the Canada Basin for the April 26, 1975 to May 2, 1975 interval.
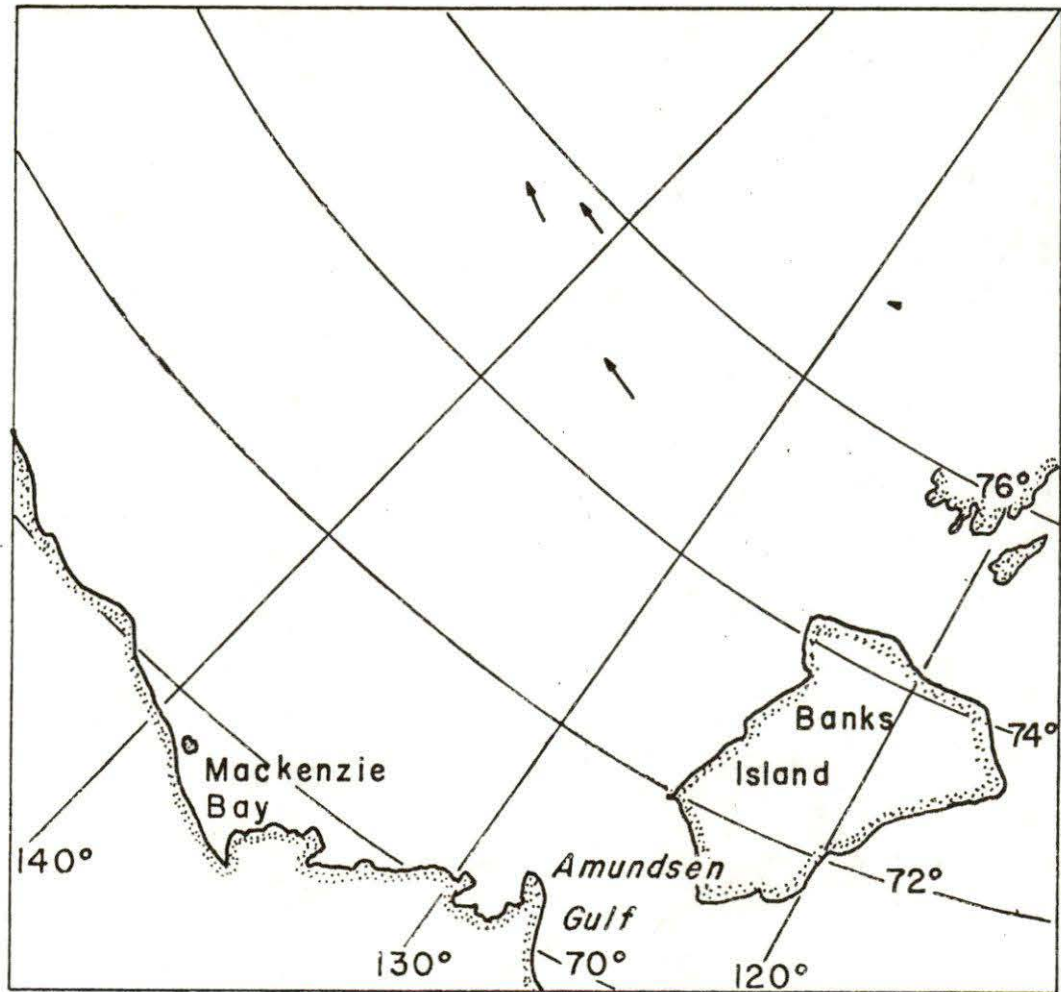
Figure 17.   Ice displacement vectors in the Canada Basin for the May 1, 1975
to May 7, 1975 interval.
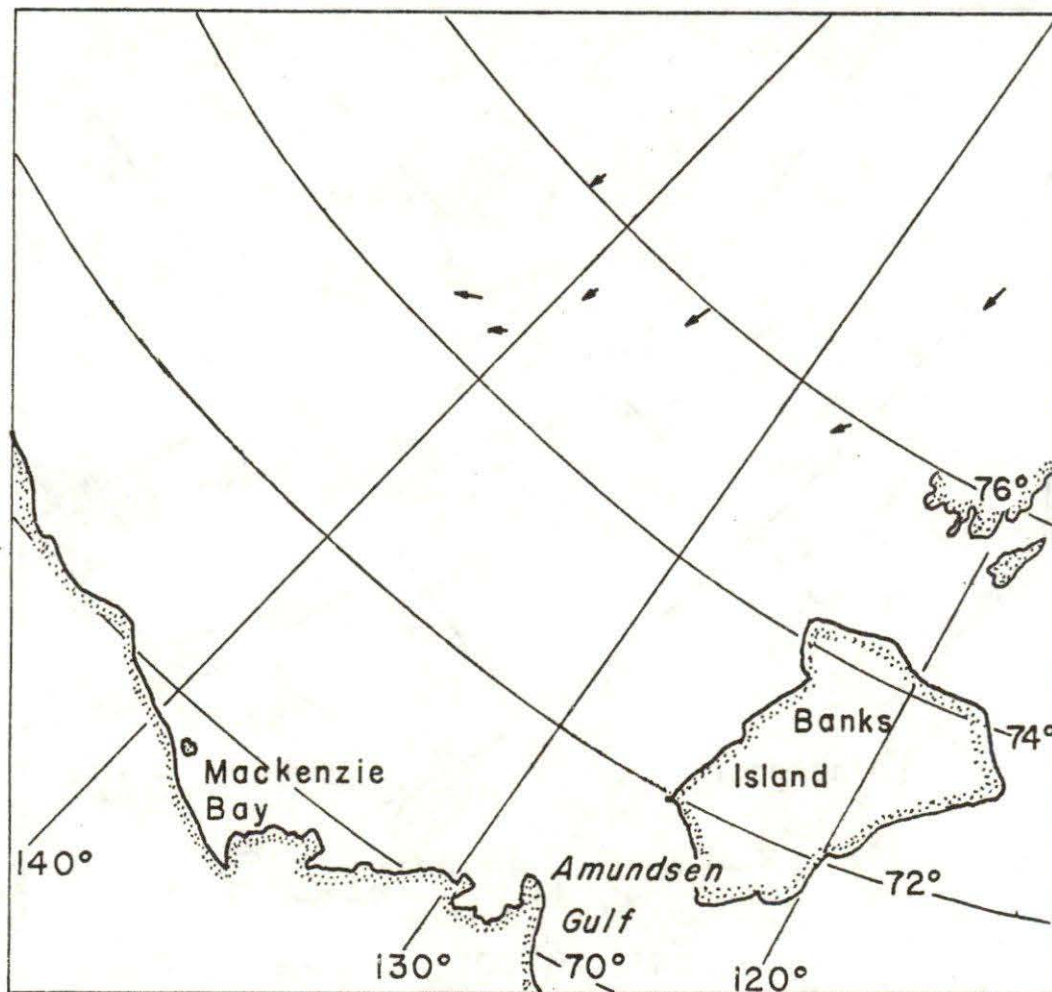
Figure 18.   Ice displacement vectors in the Canada Basin for the May 7, 1975 to May 13, 1975 interval.
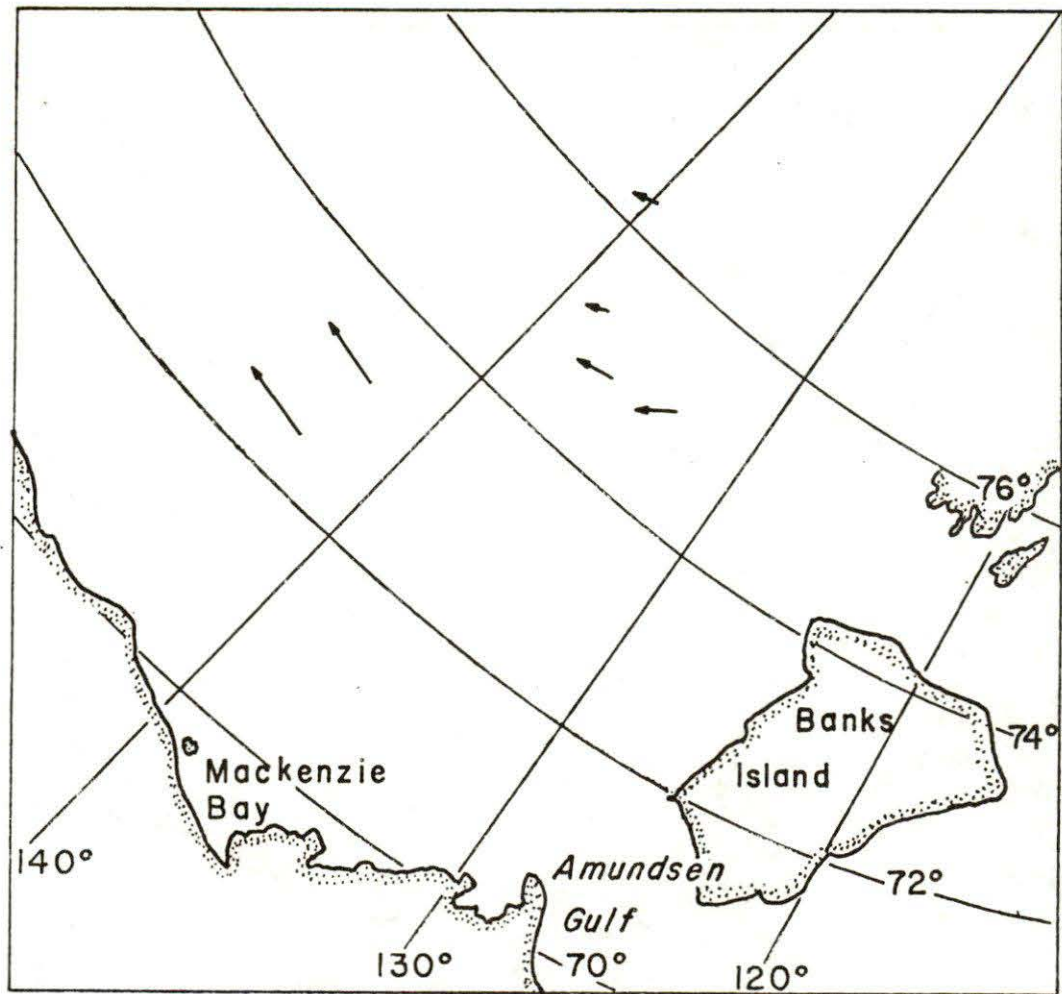
Figure 19. Ice displacement vectors in the Canada Basin for the May 15, 1975 to May 30, 1975 interval.
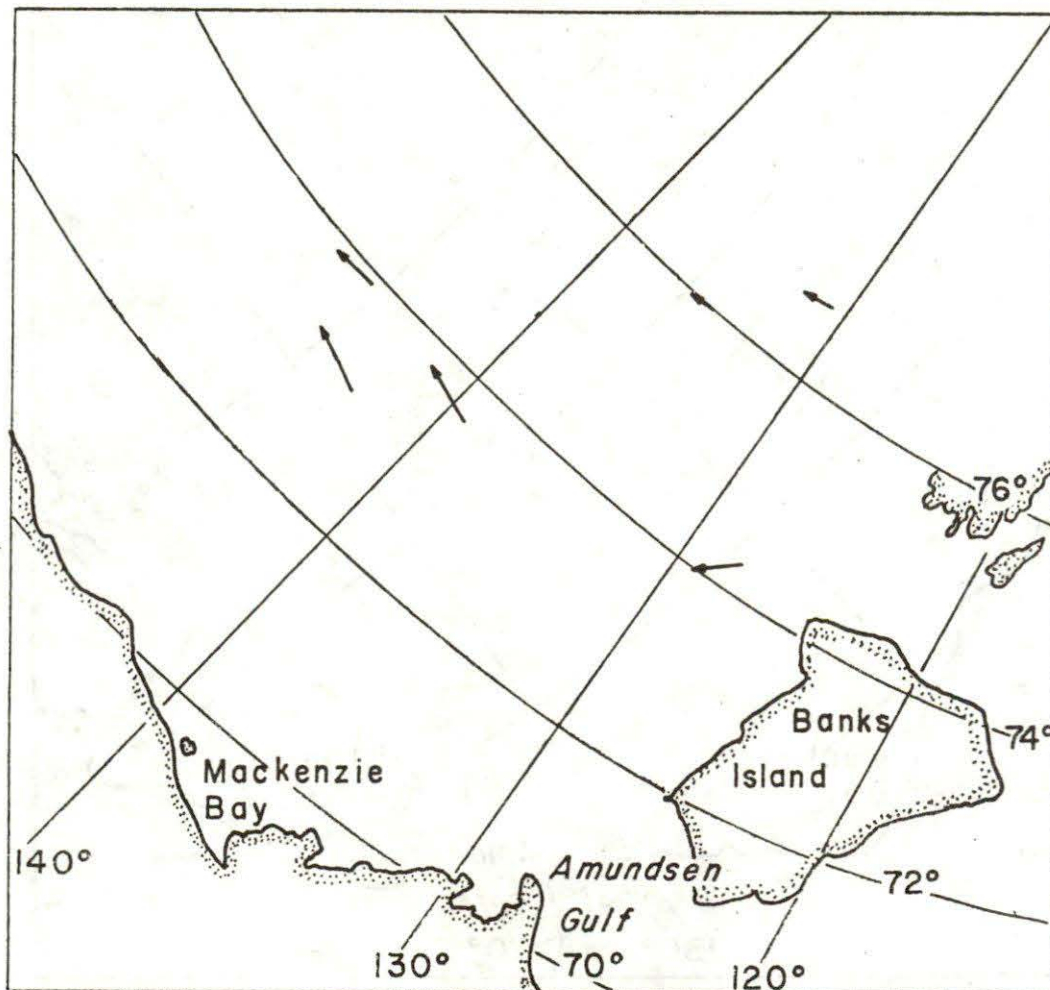
Figure 20.   Ice displacement vectors in the Canada Basin for the May 27, 1975 to June 6, 1975 interval.
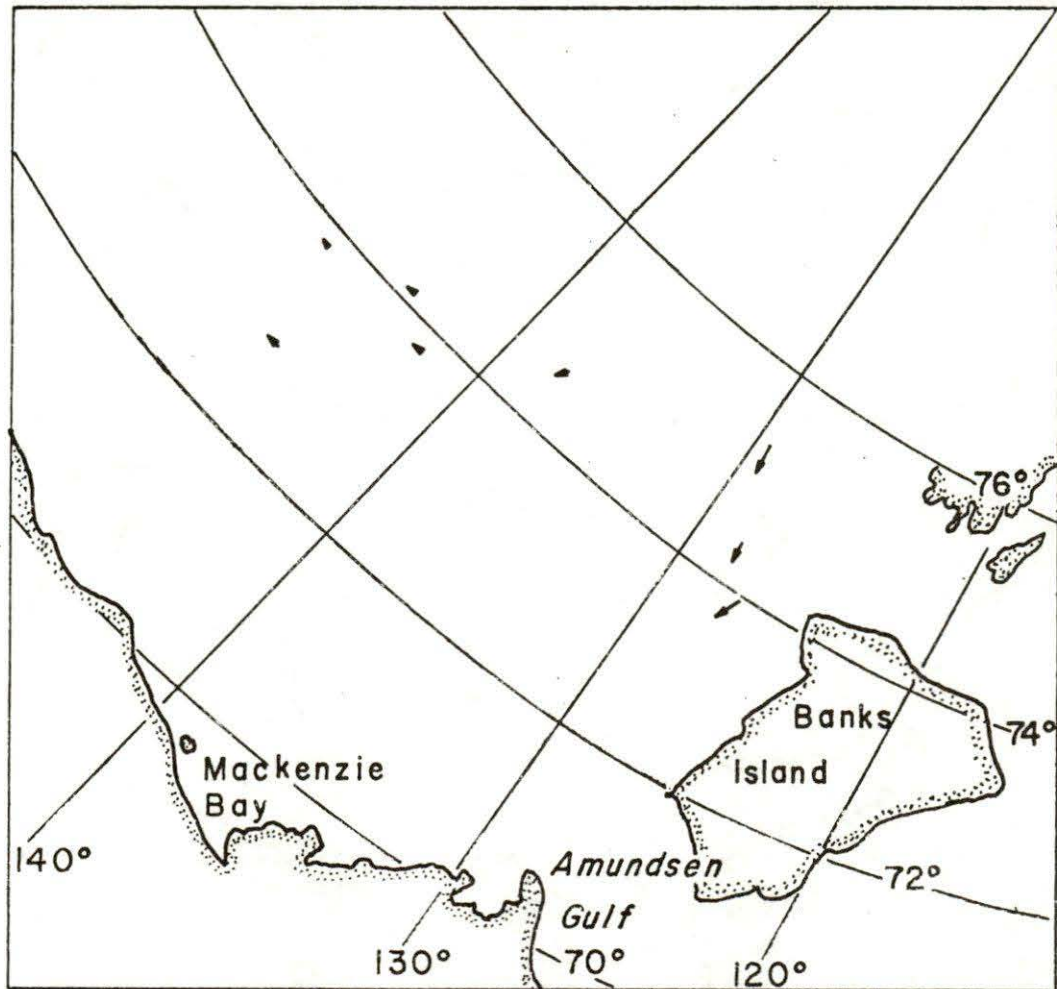
Figure 21.   Ice displacement vectors in the Canada Basin for the June 6, 1975
to June 12, 1975 interval.
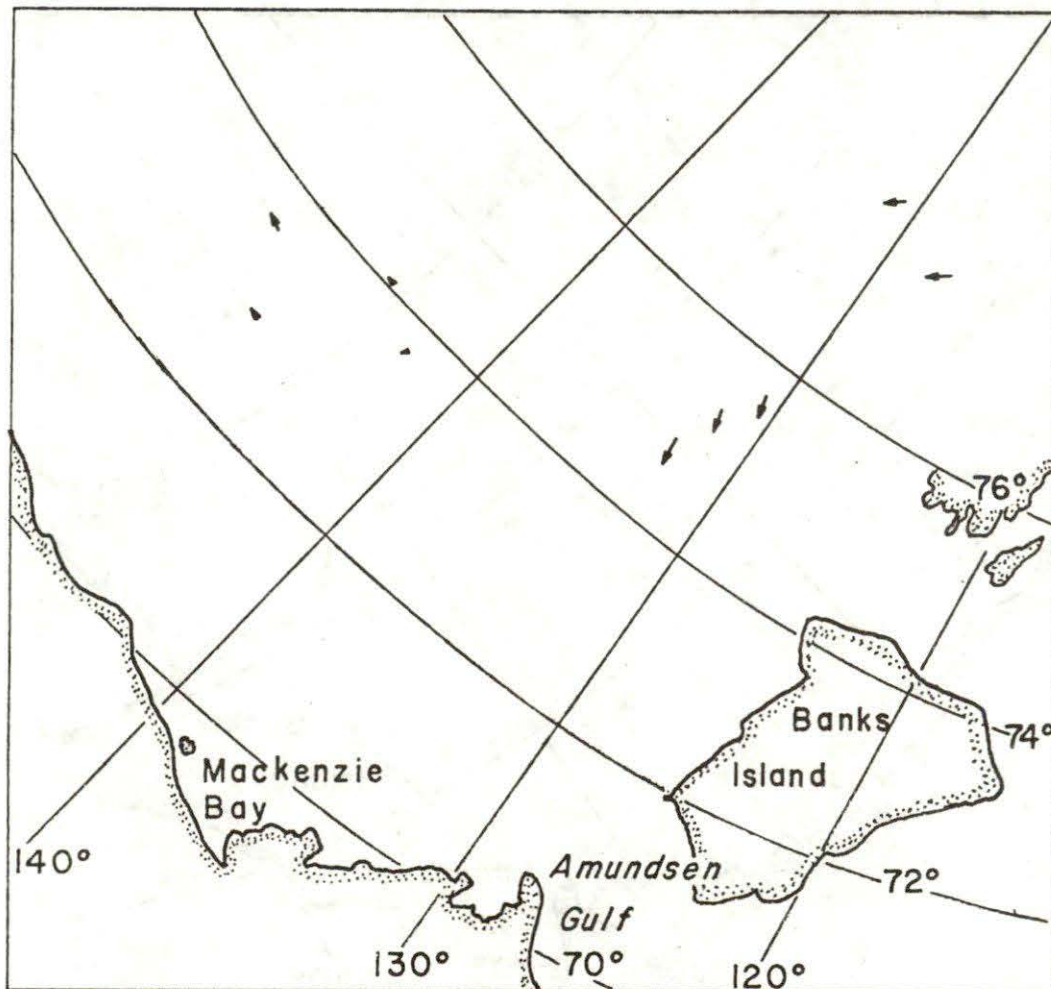
Figure 22. Ice displacement vectors in the Canada Basin for the June 12, 1975 to June 19, 1975 interval.
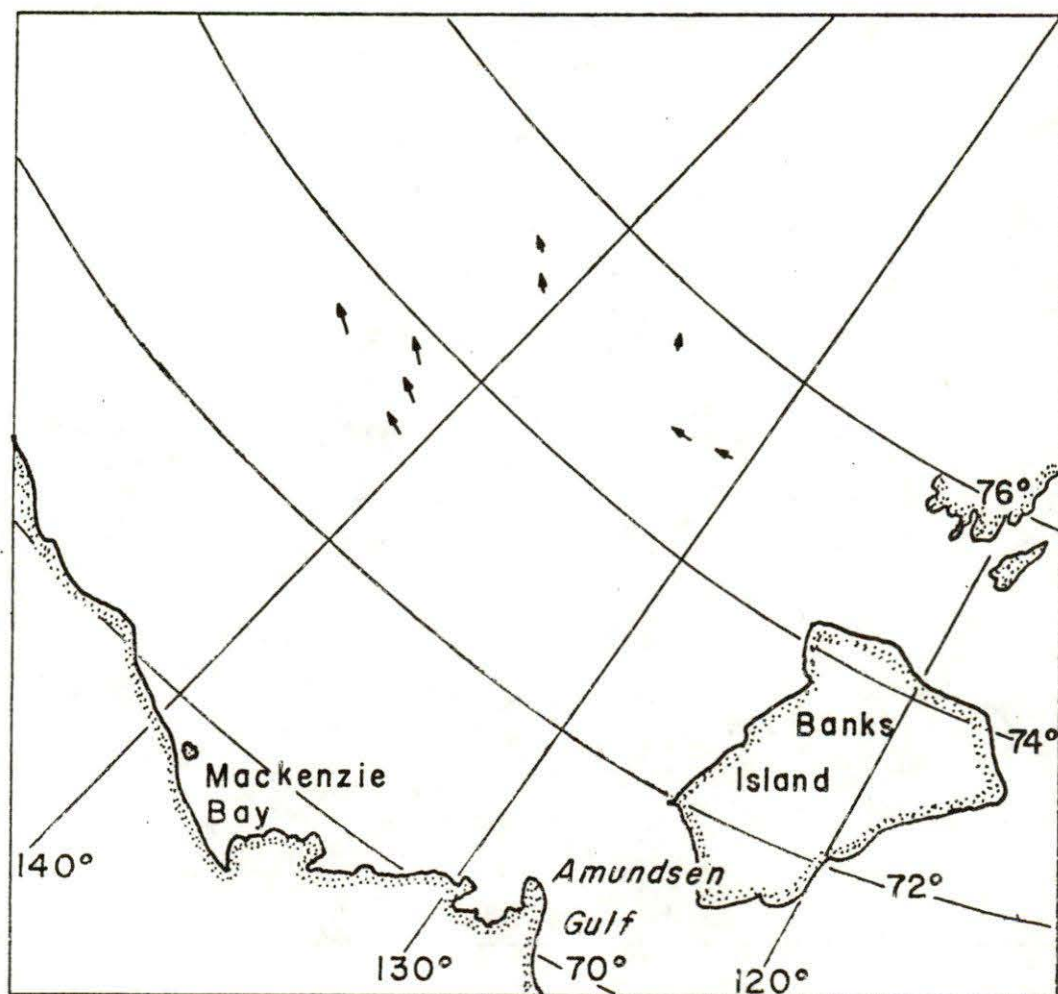
Figure 23. Ice displacement vectors in the Canada Basin for the June 19, 1975 to June 27, 1975 interval.
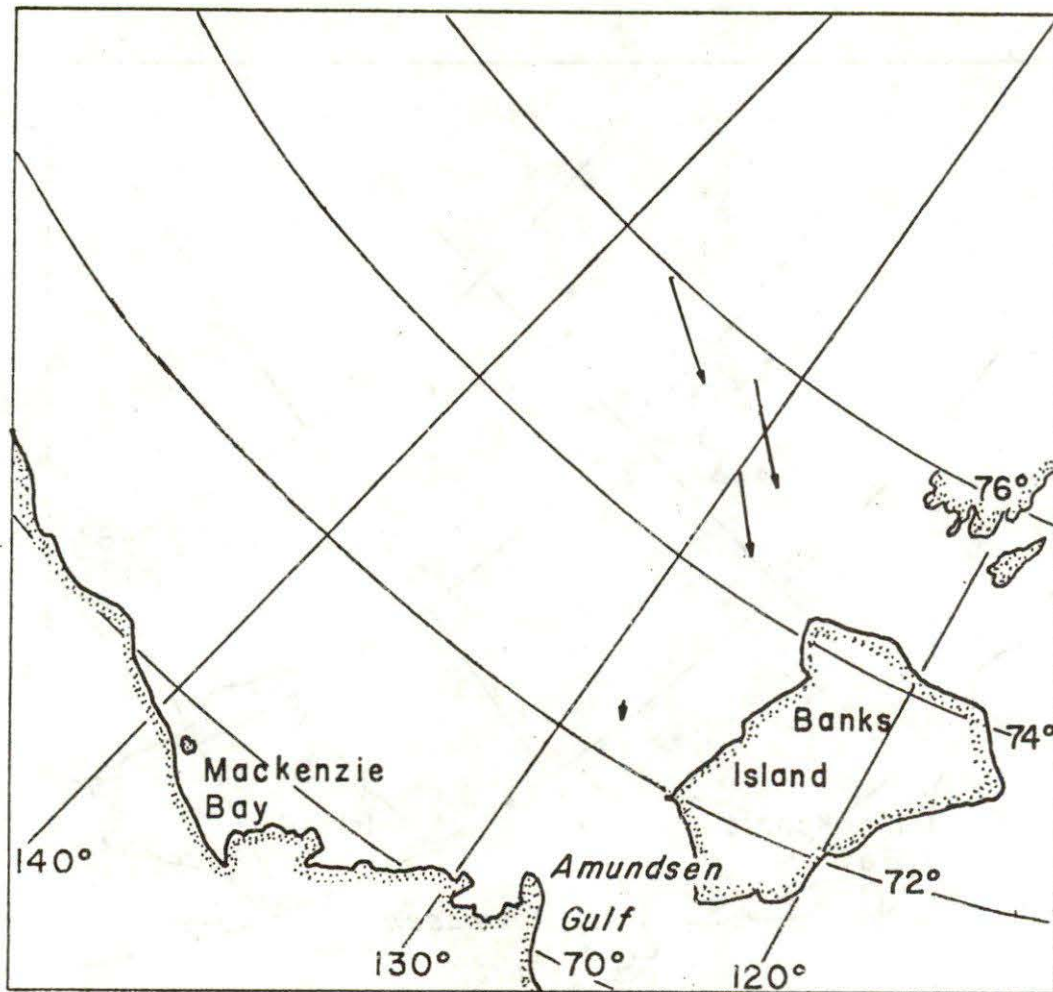
Figure 24.   Ice displacement vectors in the Canada Basin for the June 26, 1975 to July 14, 1975 interval.
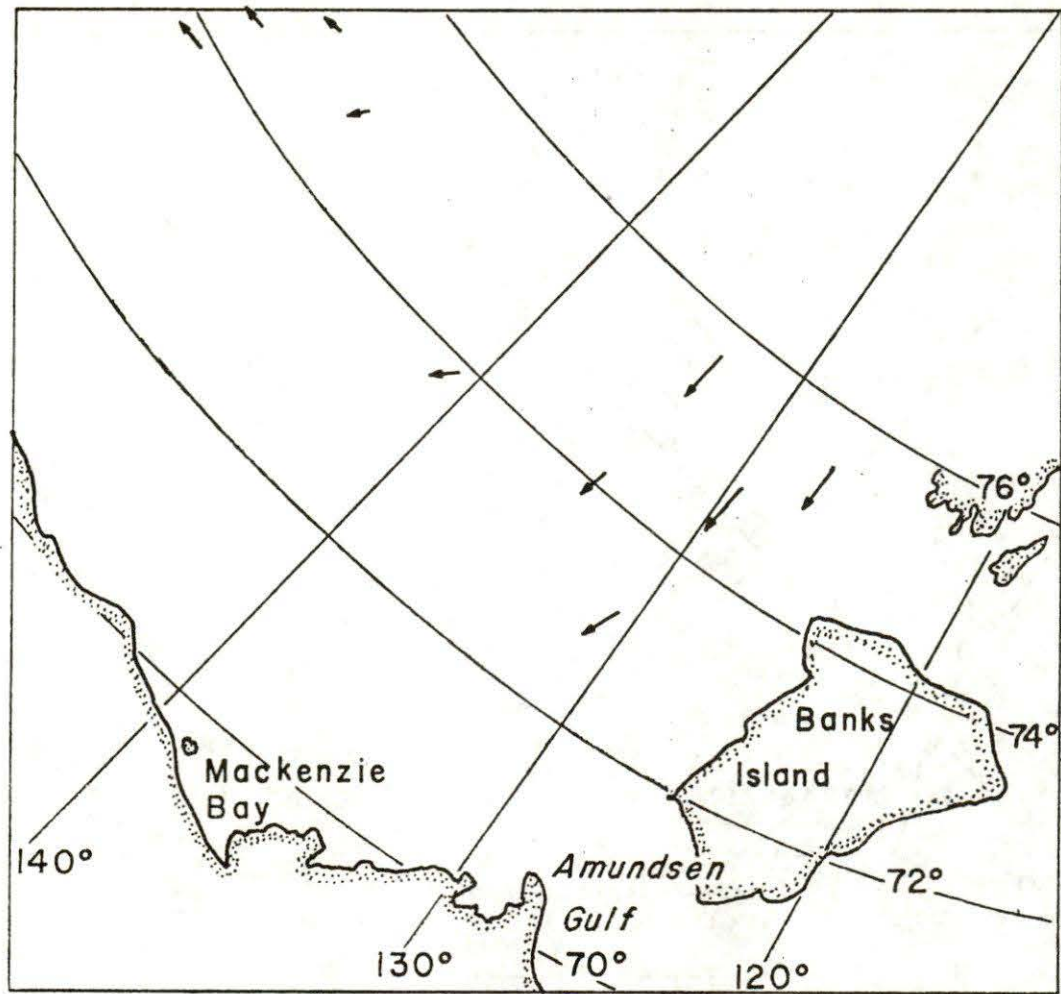
Figure 25. Ice displacement vectors in the Canada Basin for the July 14, 1975 to July 21, 1975 interval.
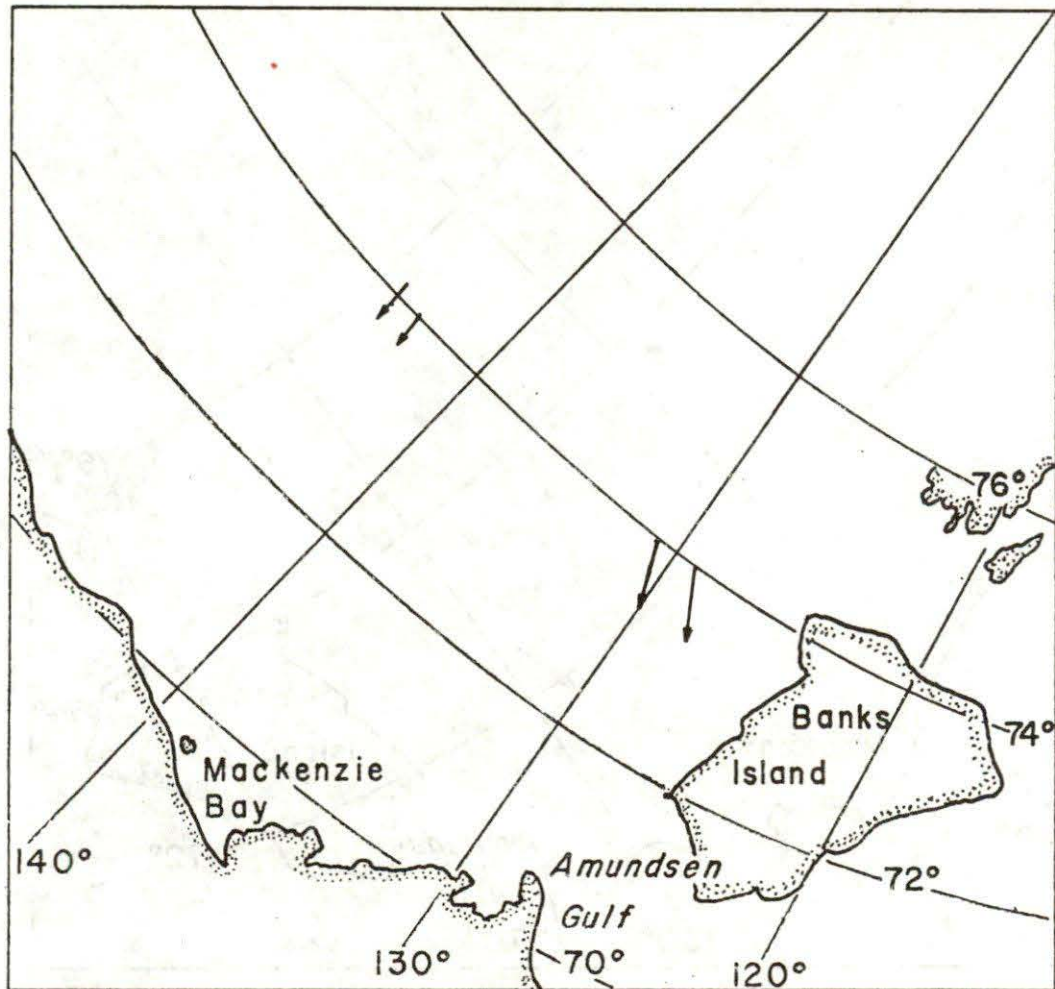
Figure 26.   Ice displacement vectors in the Canada Basin for the July 21, 1975
to July 31, 1975 interval.
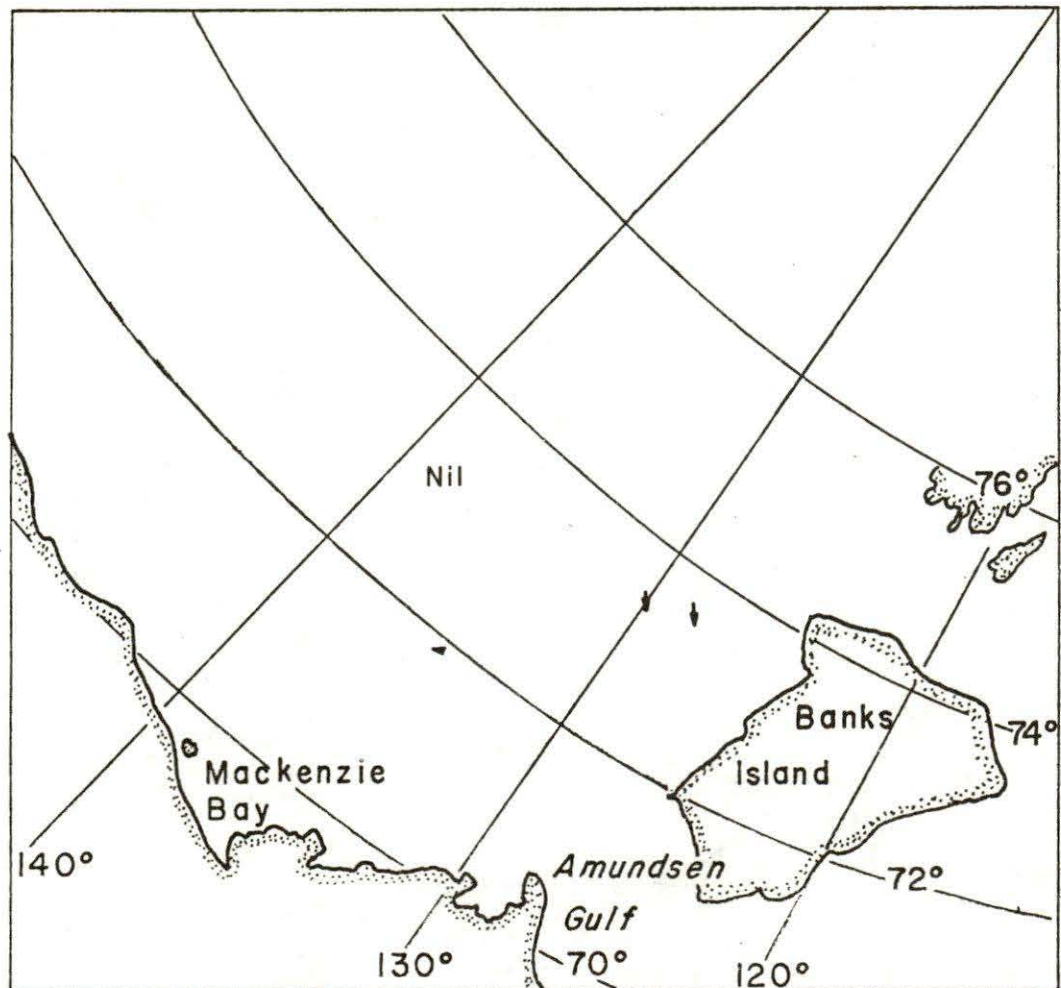
Figure 27.   Ice displacement vectors in the Canada Basin for the July 31, 1975
to August 6, 1975 interval.
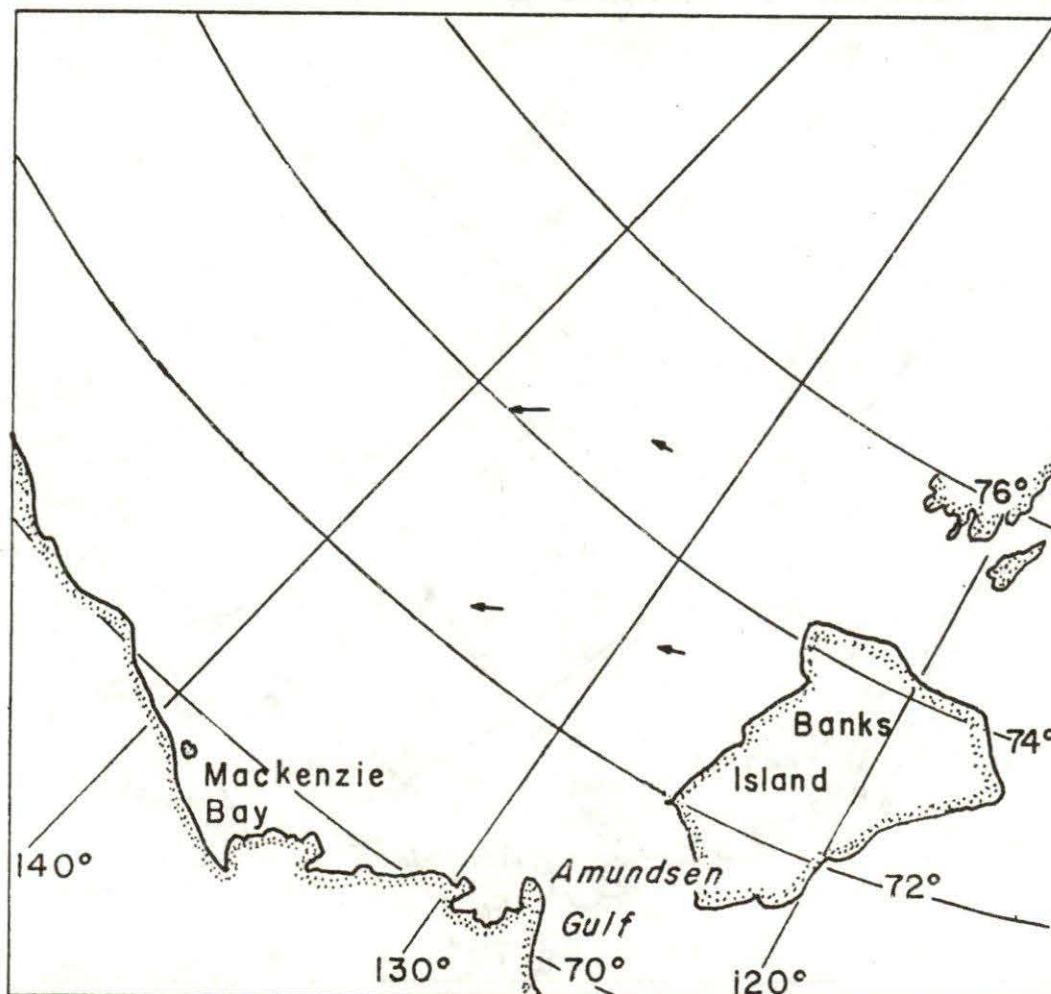
Figure 28.   Ice displacement vectors in the Canada Basin for the August 16, 1975 to August 21, 1975 interval.
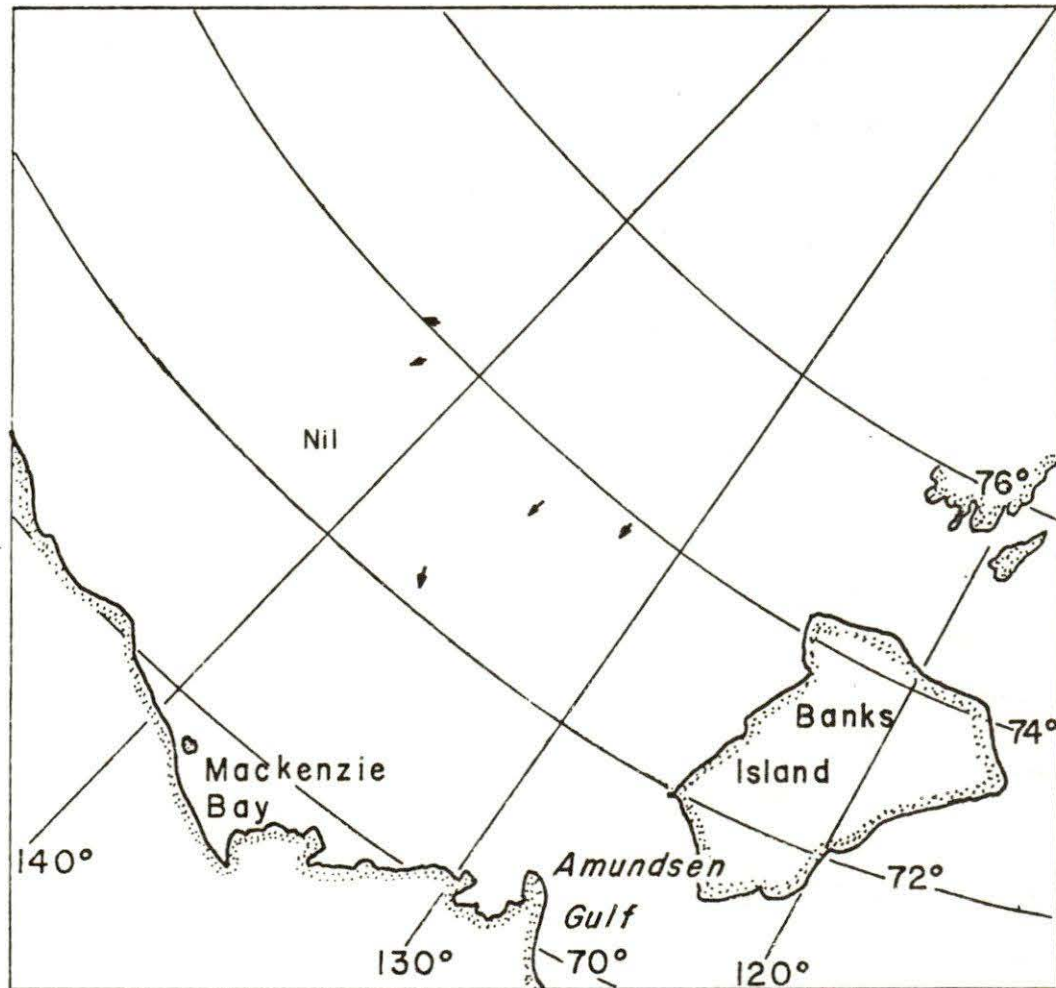
Figure 29.   Ice displacement vectors in the Canada Basin for the August 30, 1975 to September 6, 1975 interval.

TABLE 1.

Interval	Net Daily Displacement in Region A
March 28 - April 5	5 km/day, W
April 3 - 9	6 km/day, W
April 9 - 15	0
April 15 - 25	1.2 km/day, NE
April 26 - May 2	1.4 km/day, SW
May 1 - 7	8 km/day, W
May 7 - 13	3.1 km/day, S-SW
May 15 - 20	3.0 km/day, W-SW
May 29 - June 6	1 km/day, W
June 6 - 12	2.5 km/day, S
June 12 - 19	3.5 km/day, S
June 19 - 27	2.6 km/day, W
June 26 - July 14	6.5 km/day, E-SE
July 14 - 21	7 km/day, S
July 21 - 31	11.5 km/day, SE
July 31 - August 6	5 km/day, SE
August 16 - 21	10 km/day, SW
August 30 - September 6	4 km/day, S

displacements, having mean speeds in excess of 5 km/day, were in-variably to the west in accord with predominant movements in the early 1973 and 1974 break-up processes. Movement in a westerly direction was encouraged by the existence of open water expansion areas in the Bering Strait and in the Siberian shelf. Motion in other directions was generally inhibited by coastal resistance. This anisotropy disappeared during the summer months when large areas of open water existed along several boundaries of the Arctic Ocean and an apparent decrease occurred in the internal pack forces with the result that the ice motions more or less followed the direction of the local wind. At point "A", a predominantly south-southeastward motion ensued that gradually closed the open water area of the eastern Beaufort Sea. The average ice motion near Point A over the March through September interval followed the southwestward trend predicted by the gyral plot of Figure 11. This motion appeared to proceed in two distinct steps corresponding to early season westward-and mid-to-late summer south-southeastward drifts. These seasonal trends, followed here only at one point, appear to be essential to an understanding of the ice and surface water movements.

Models of ice drift in the Canada Basin which have been developed to date have been directed mainly toward the reproduction of a pattern of surface water- and ice-flow similar to that shown in Figure 11. Here, long-term mean ice flow has been observed to deviate to a negligible extent from the oceanic current flow at depths above 30 m (Newton and Coachman, 1973). These models have considered several different rheologies for the "ice fluid" and have assumed a primal driving force derived from the 15-year average of atmospheric pressure distributions. The inherent flexibility in analytical boundary conditions has been such that roughly equivalent results have been obtained, assuming that the sea ice is a viscous fluid (Campbell, 1965) or an inviscid fluid (Rothrock, 1973). A better model may now be possible through the availability of NOAA imagery and short-term ice displacement data of the kind plotted in Figures 12-29. The availability of displacement data for intervals as short as three or four days permits a great reduction in the averaging time over which ice currents are measured and allows a given atmospheric pressure configuration to be directly related to a measured ice response. Mappings for approximately one week intervals in 1974 are shown in Figures 30-33, together with the corresponding average atmospheric pressure patterns (provided by W. Markham of Ice Fore-casting Central, Ottawa). The correlation between ice motions and the atmospheric pressure distribution were generally not in agreement with simple expectations. One might expect a paralleling of ice displacement and air pressure contours because of the near cancelling effects of a leftward surface friction-induced rotation of the geostrophic wind and the tendency of ice to move to the right of the surface wind. This expectation was not consistently fulfilled and a poor correlation was noted between the magnitudes of the ice dis-placements and those of the corresponding geostrophic winds. In Figure 31, for example, the maximum ice displacements actually occurred in the northeastern corner of the Beaufort Sea while the largest winds, on the basis of the average pressure contours, appeared near Point Barrow. Similarly anomalous results are evident
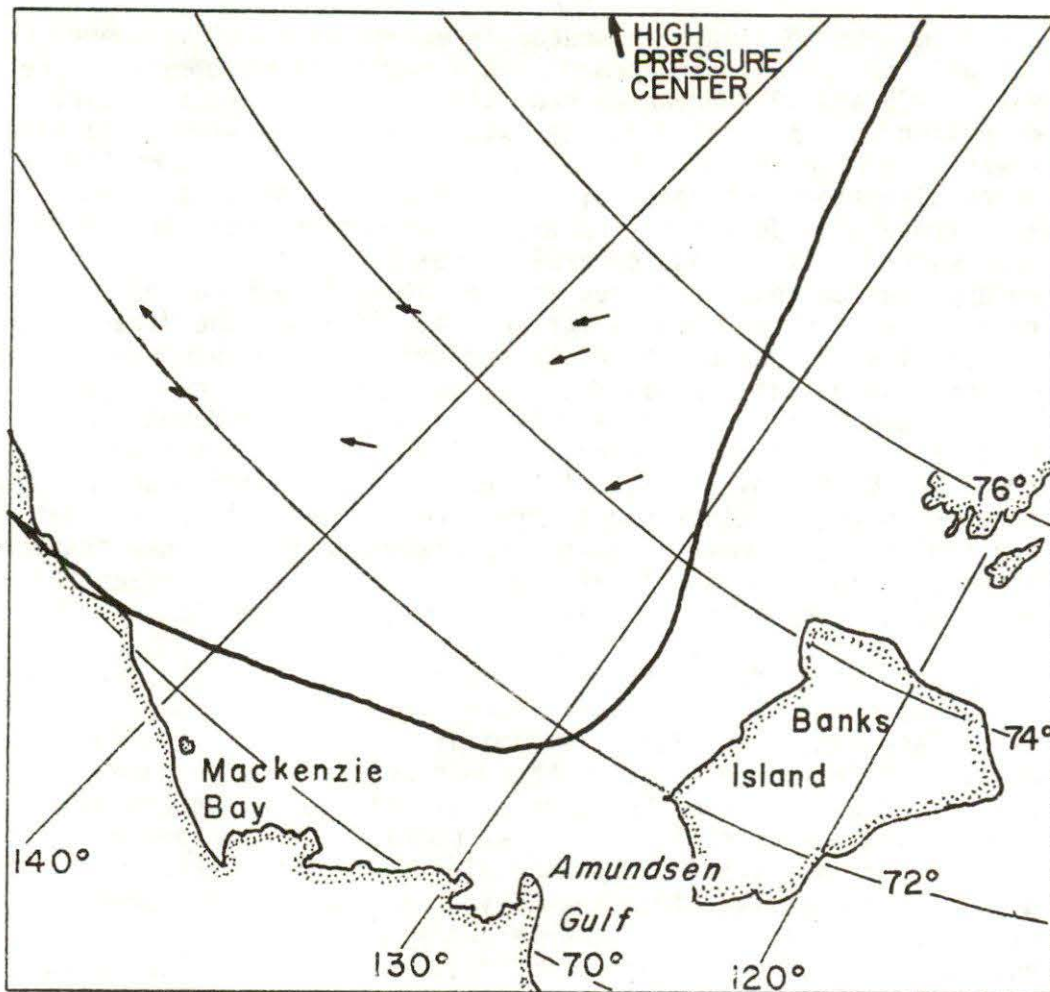
Figure 30. Ice displacement vectors in the Canada Basin for the May 16, 1974 to May 22, 1974 interval. The average atmospheric pressure configuration over this interval is represented by the plotted contours of the height of the 1000 mb level. Adjoining contours correspond to a height difference of 30 m.
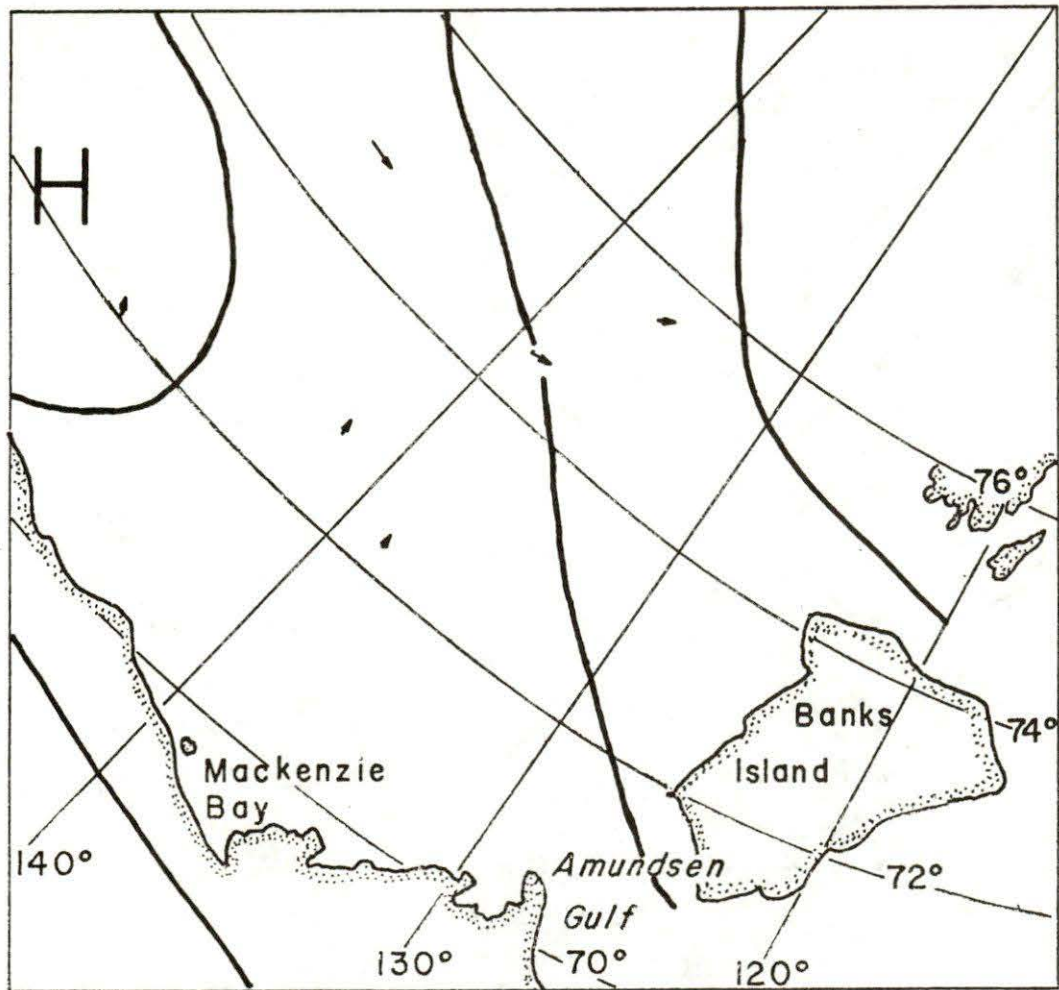
Figure 31. Ice displacement vectors and average 1000 mb height contours in the Canada Basin over the May 22, 1974 to May 29, 1974 interval.
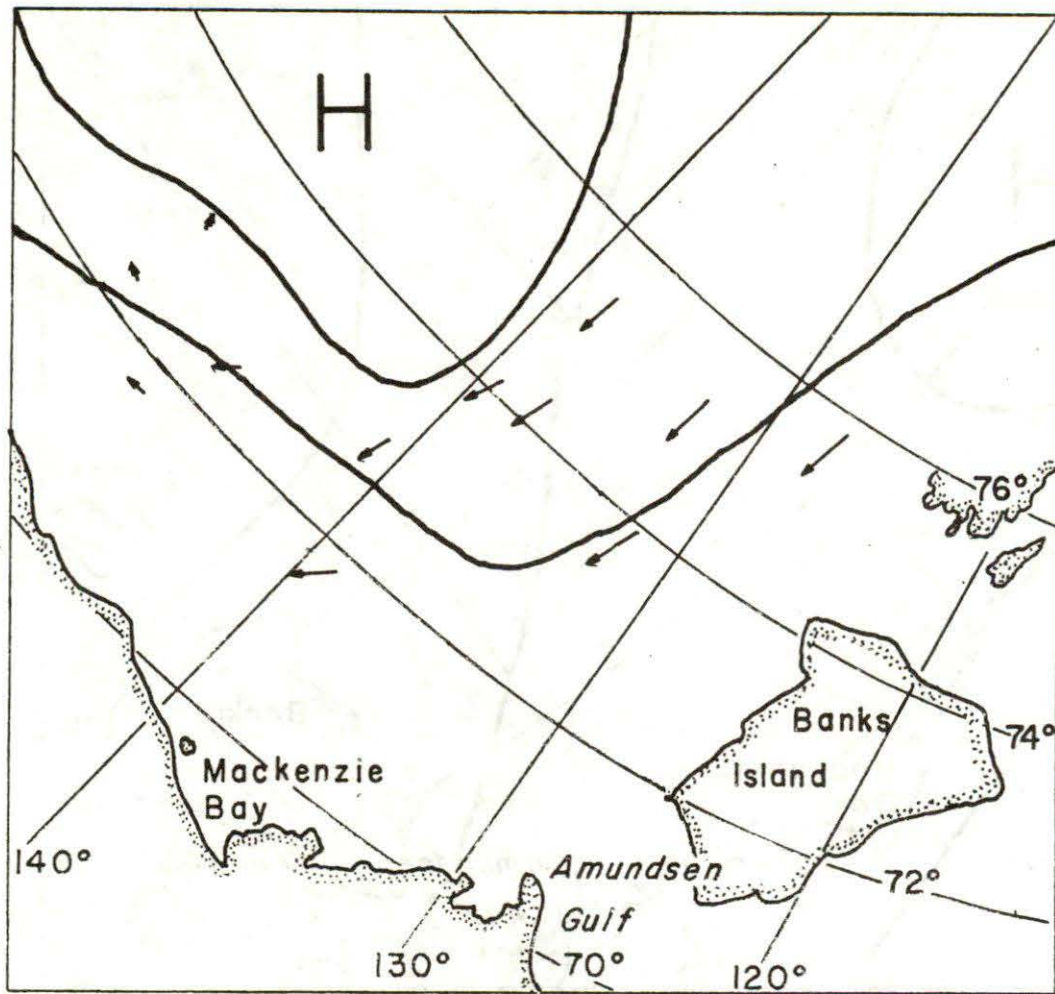
Figure 32. Ice displacement vectors and average 1000 mb height contours in the Canada Basin over the June 20, 1974 to June 26, 1974 interval.
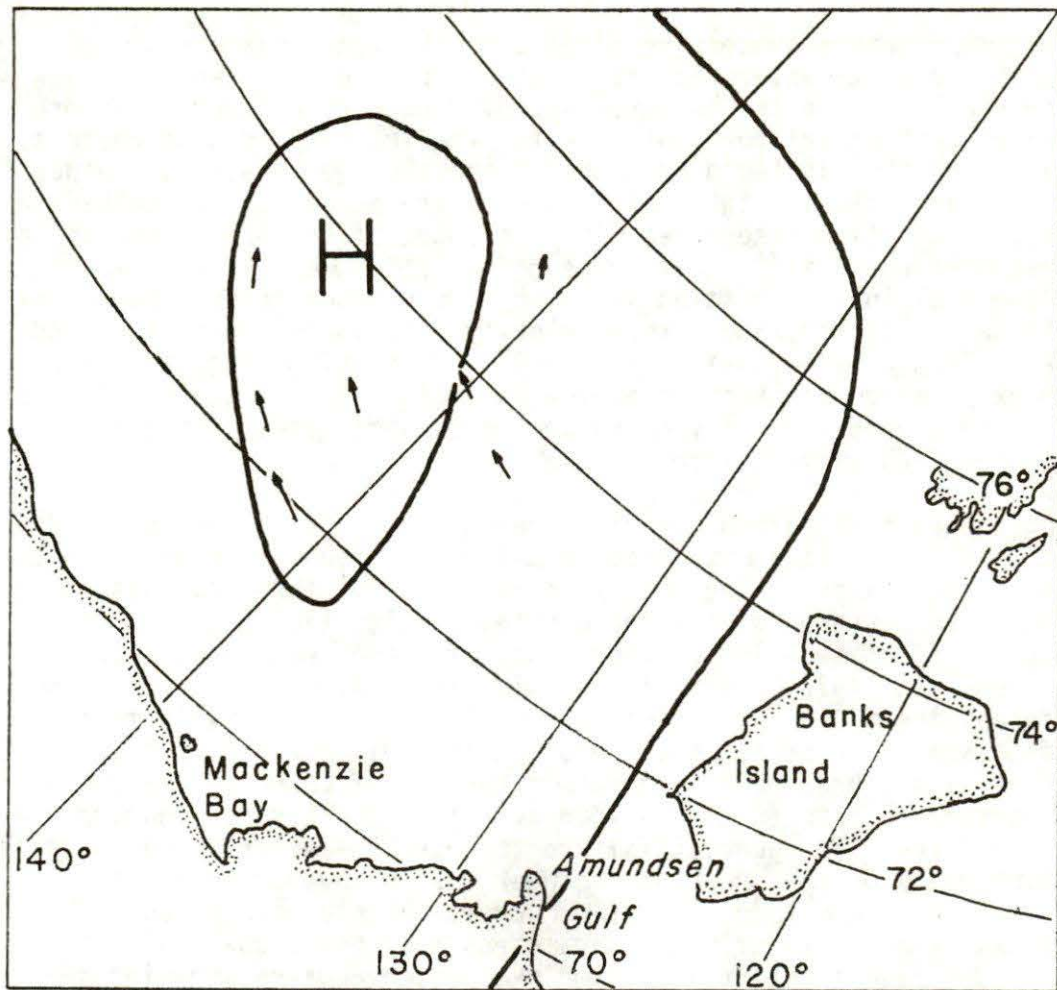
Figure 33.   Ice displacement vectors and average 1000 mb height contours in the Canada Basin over the September 23, 1974 to October 1, 1974 interval.

in Figure 34 where successive displacements of a single large ice floe in the northeastern Beaufort Sea are plotted over an extended period in 1973. In the latter case, over each time interval, there was a consistent *leftward* rotation for the ice displacement vectors relative to the plotted directions of the average geostrophic winds. The displacements in Figure 34 also show the previously described increase in motion associated with the onset of summer. There is, of course, the possibility that these difficulties were introduced in the average wind calculation in which, among other things, the quadratic nature of the wind stress-velocity relationship was neglected. Nevertheless, the deviations from drift expectations suggest a more complex problem, inherent to an ice pack with strong internal forces and acted upon by the varying force fields associated with the atmosphere and landfast-ice.

Using satellite-obtained ice displacement data for intervals having particularly stable atmospheric conditions, it should be possible to directly test alternative models on the basis of their calculated response to correspondingly representative wind fields. Theoretical calculations of such ice responses have already been made by Campbell and Rasmussen (1972) for typical anticyclonic atmospheric gyres and different ice-fluid rheologies. As noted above, the development of a large scale ice drift model requires careful consideration of the time-averaging process to understand the significance of the close correspondence between the 15 year average air pressure- and surface current-gyres. The general failure to observe similar correspondences for intervals on the order of one week must be accounted for if shorter term ice motion prediction schemes are to be derived. Seasonal dependences of model parameters must be deduced and estimates made of the interval of time over which a given ice-wind relationship retains its validity. For example, it would be of interest to know whether the net ice displacements during May 16-29, 1974 can be related to the average atmospheric pressure pattern in a manner which is consistent with the ice-wind relationships operative in the May 16-22 and May 22-29 periods (Figures 30 and 31). This information would help to establish the time scales appropriate to realistic modelling of Arctic Ocean ice and water motion.

3.3 Spatial Variations in the Ice Cover and Rectilinear Lead Patterns

Earlier observations of the summer ice pack by ERTS satellite (Campbell *et al.*, 1973) show a roughly monotonic east to west decline in floe size in the Canada Basin. This effect has been attributed to a tendency for the gyral flow to collect older and stronger multi-year ice in eastern regions. The NOAA satellite observations, for example Figures 35 and 36, support this ice distribution asymmetry. The very largest floes were generally found on or near the eastern continental shelf off Banks Island while much more finely divided, loosely packed ice appeared in the central and western portions of the gyre (see Figure 37). An alternative explanation can be devised either in terms of the pressure distribution inherent to the numerically modelled "ice fluid" (Rothrock, 1973) or as evidence of a spatial asymmetry in the distribution of
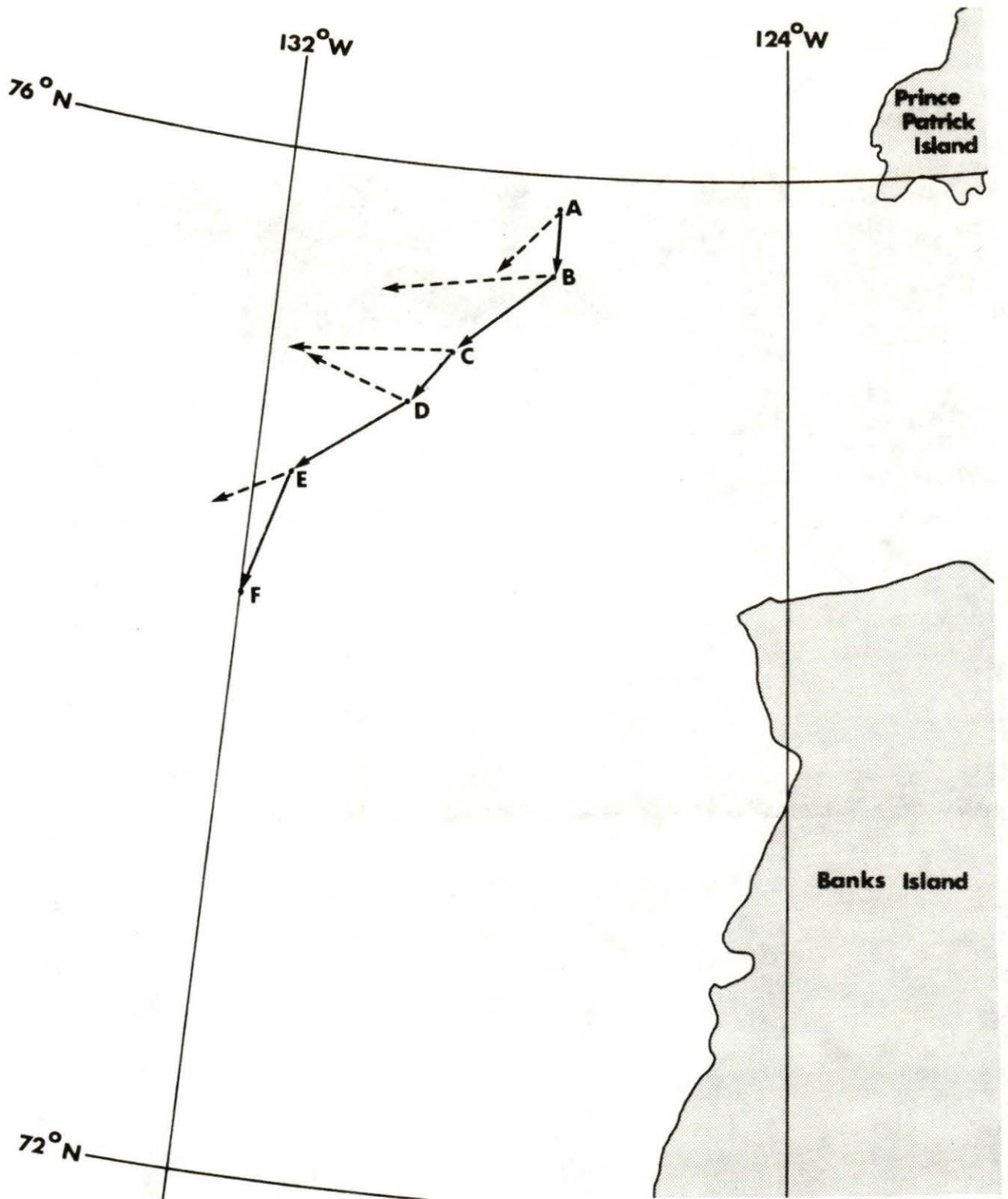
Figure 34. The displacements of a vast ice floe in the northeastern Beaufort Sea during a portion of 1973. The labelled points give the floe position on: A - April 12; B - April 26; C - May 16; D - June 7; E - June 17; and F - June 29. The average speeds over the successive intervals are respectively 2.0 km/day, 2.8 km/day, 1.3 km/day, 5.9 km/day and 4.9 km/day. The calculated mean winds over these same periods are represented at each starting point by broken-line vectors (scale 1 cm = 4 knots = 7.4 km/hr).
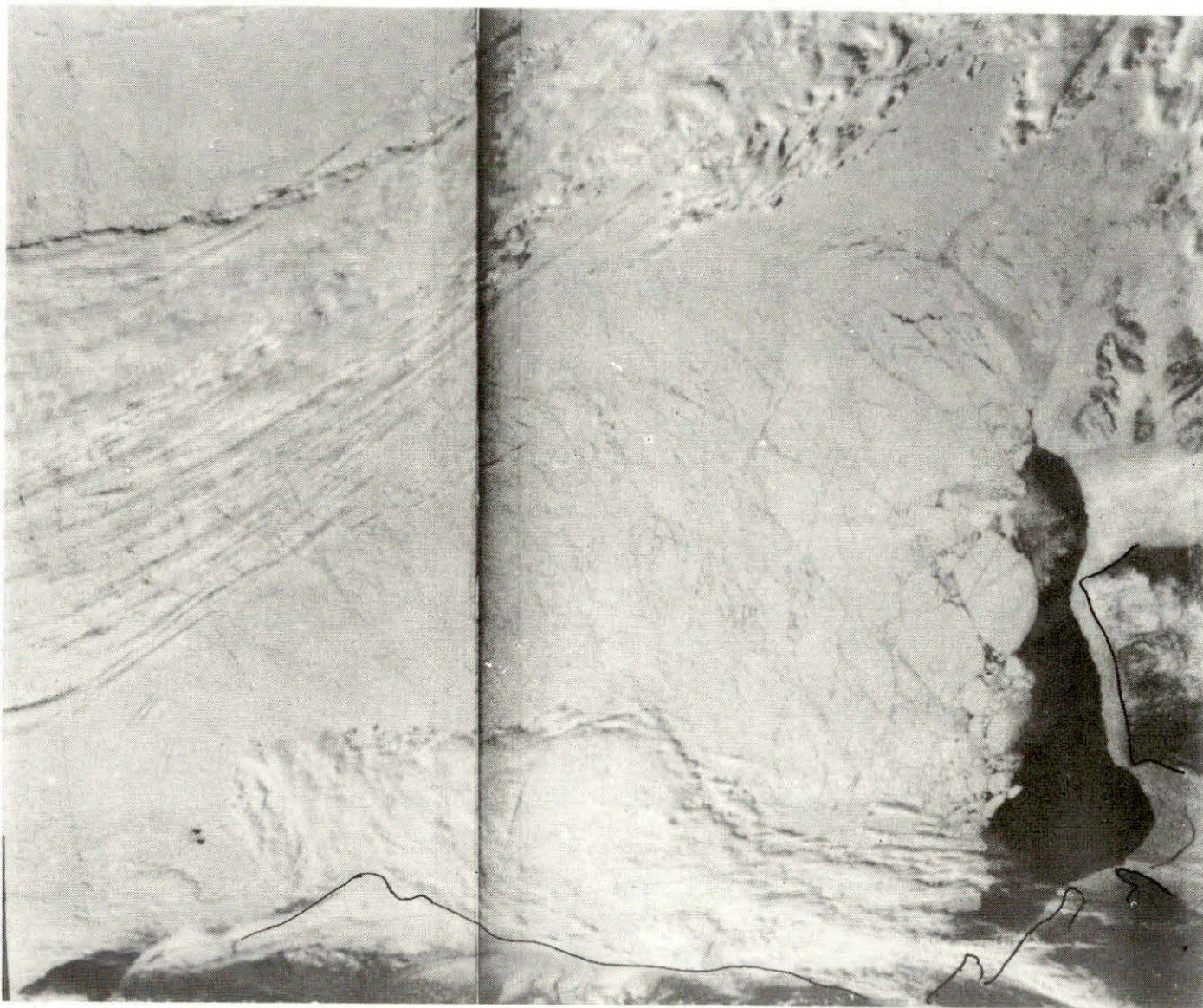
Figure 35.   A June 5, 1973 NOAA satellite image of the Canada Basin. The larger floes are seen primarily in the eastern portion of the Beaufort Sea.
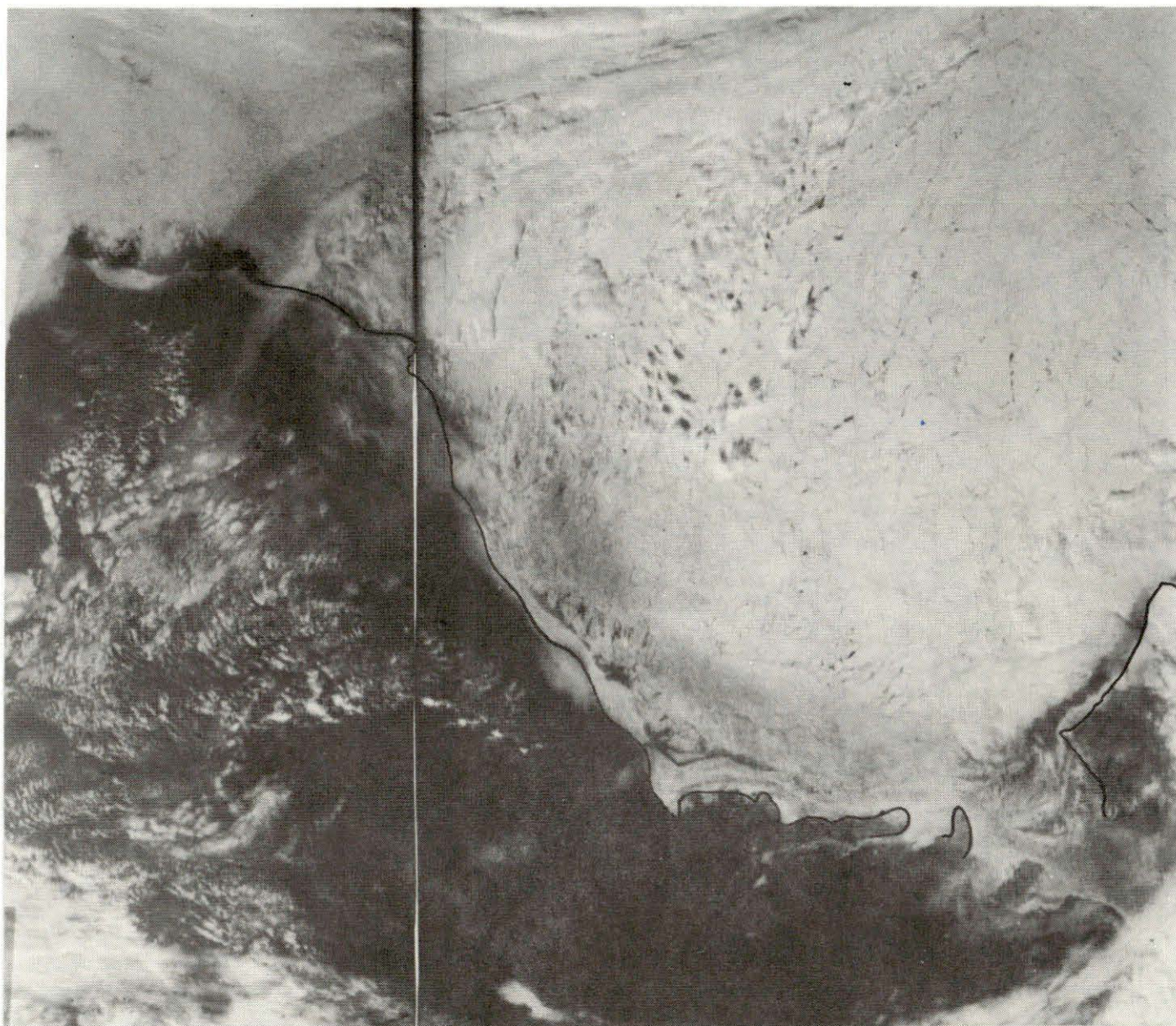
Figure 36. A June 20, 1974 NOAA satellite image of the Canada Basin.
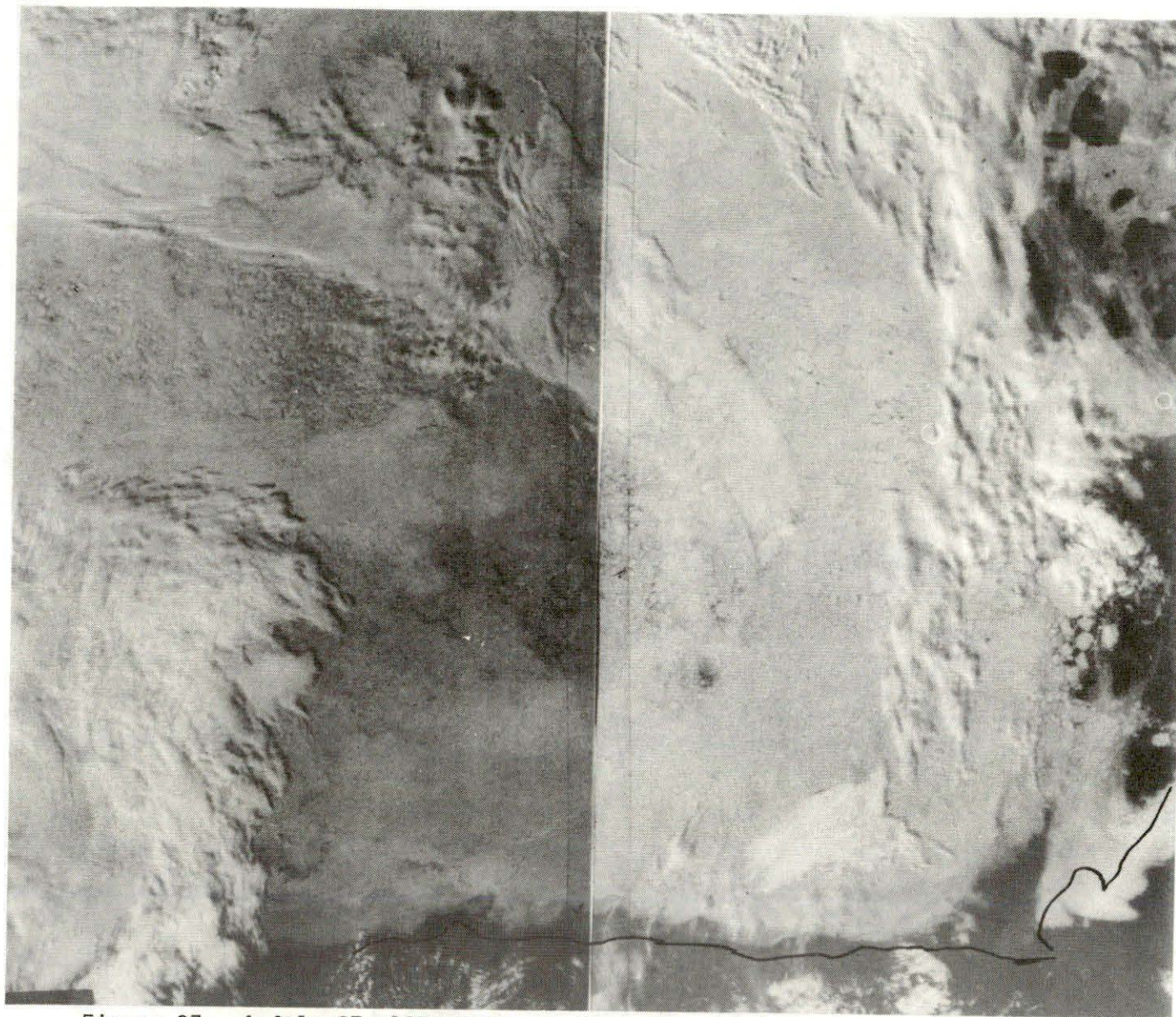
Figure 37. A July 27, 1973 NOAA satellite image of the Canada Basin. Mackenzie Bay is seen in the lower right-hand corner. A very loosely packed area of relatively small floes occupies the center of the image, north of Point Barrow, Alaska.

intermediate scale ocean surface currents which may influence ice fracturing.

The latter possibility arises from an analysis of the origin of long, narrow rectilinear leads which, according to our NOAA satellite observations, are common in the Arctic pack ice (see, for example, Figure 35). It was originally believed that these leads could easily be distinguished from the long leads associated with the spring break-up by their rectilinearity, slow formation rates and their limitation to widths less than 5 km. However, the 1975 NOAA imagery (to be discussed below) suggests that this distinction is not always possible since the rectilinear lead system appears to play a role in the evolution of the spring ice cover. To my knowledge, the rectilinear leads were first faintly visible, but not specifically documented in the 1972 ERTS imagery studied by Campbell *et al*. (1973). In my NOAA satellite observations, they were first evident during the advent of the summer season in May 1973, primarily in western Canada Basin and in the relatively shallow adjoining Chukchi Province (see the map in Figure 38 and Figure 39). Characteristic criss-cross leads later developed to form two intersecting sets of parallel, equidistant lines on the imagery. The related phenomena of the 1974 season were even more distinct and widespread. As a result, my discussion will concentrate on the chronological evolution and other details of 1974's ice surface. Similarities as well as novel aspects of the 1973 and 1975 seasons will then be described prior to a discussion of possible mechanisms for the production of these leads.

The early-summer ice-surface of 1974 can be seen in the May 22 image of Figure 40. The criss-cross leads in the upper left hand corner of the figure lie at and beyond the northern end of the Chukchi Province and in the northwest arm of the Canada Basin. The separations between adjoining parallel leads are approximately 60 kilometres. In more eastern areas a rectilinear lead system is also faintly observable. After a mid-summer absence of imagery due to cloud and fog and technical interruptions of satellite coverage, a large scale pattern was subsequently observed on August 23 extending into the southern Basin. After August 25, a fading of this pattern was noted which, south of 72°N, could be partly attributed to increased atmospheric opacity. Thus ERTS-1 satellite close-ups early in September do not show a rectilinear lead system in the southern Basin. Instead, a loosely packed collection of moderately-sized and small floes was observed, having interstitial open and/or lightly ice covered water. A closer look at images (such as Figure 41), however, revealed the presence of several rectilinear concentrations of dark open water (see the upper right hand corner of the Figure). Plotting on successive days of the indicated fixed ice points identified these open-water concentrations as loci of localized shearing motion between adjoining rigid ice fields. The relative motions of the fields paralleled the rectilinear features and were unidirectional in that no reversal of sense was observed. The displacement speeds ranged from 1 to 5 cm/sec.

Continued ERTS and NOAA observation indicated that a progressive solidification of the pack occurred from late August through
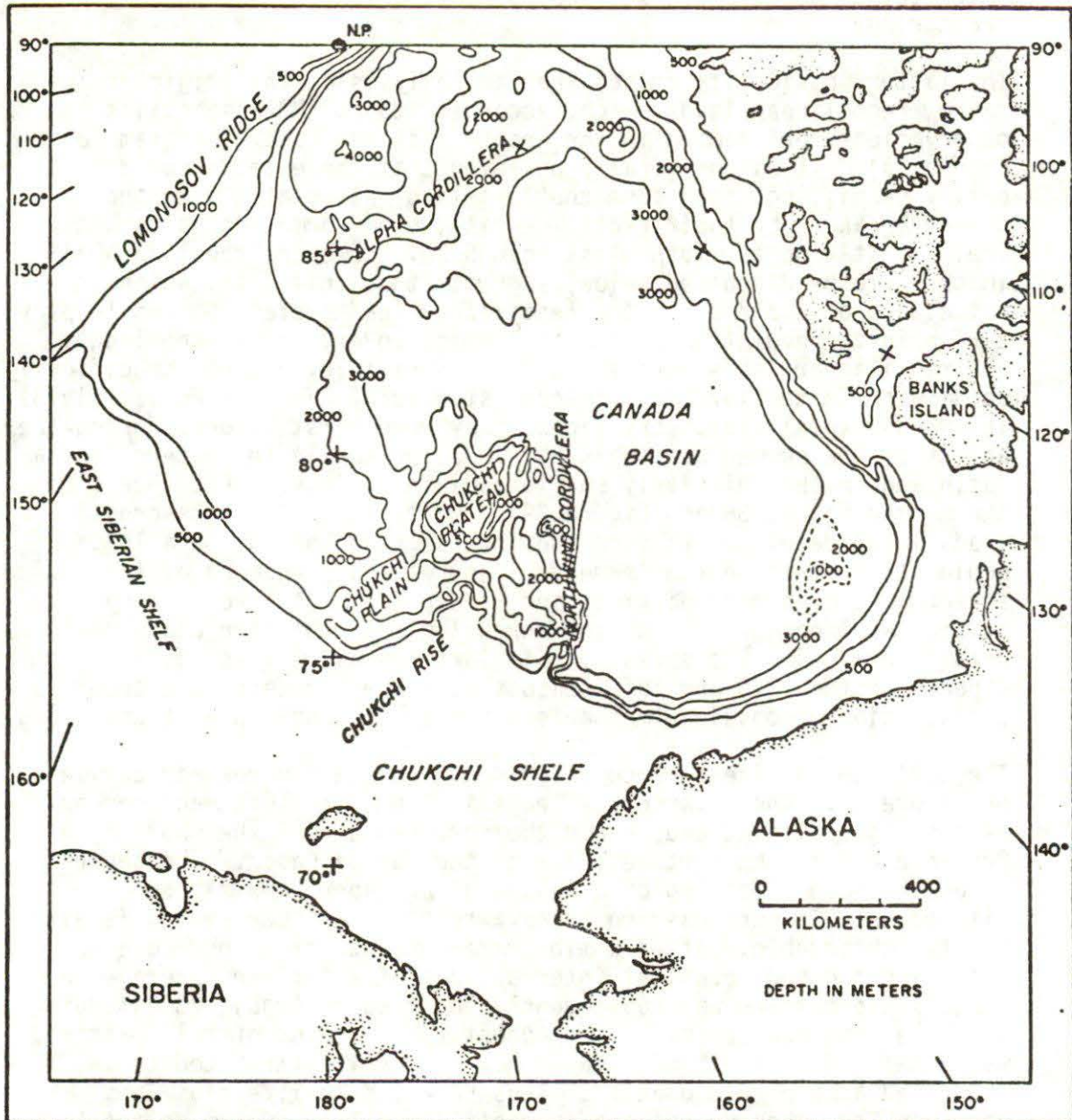
Figure 38. Bathymetry of the Canada Basin.
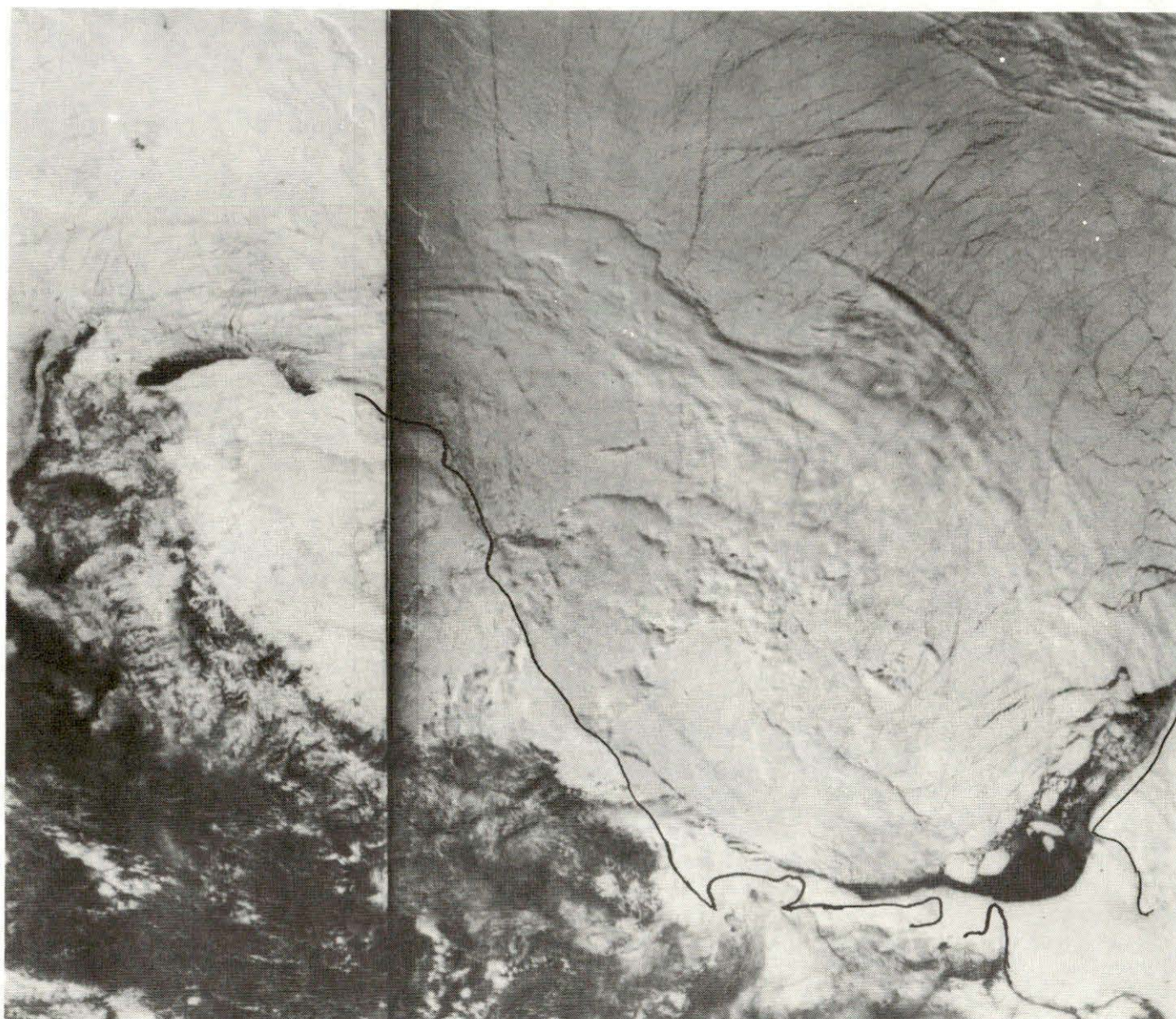
Figure 39. A May 20, 1973 NOAA satellite image of the Canada Basin. Rectilinear leads are prominent features of the ice surface.
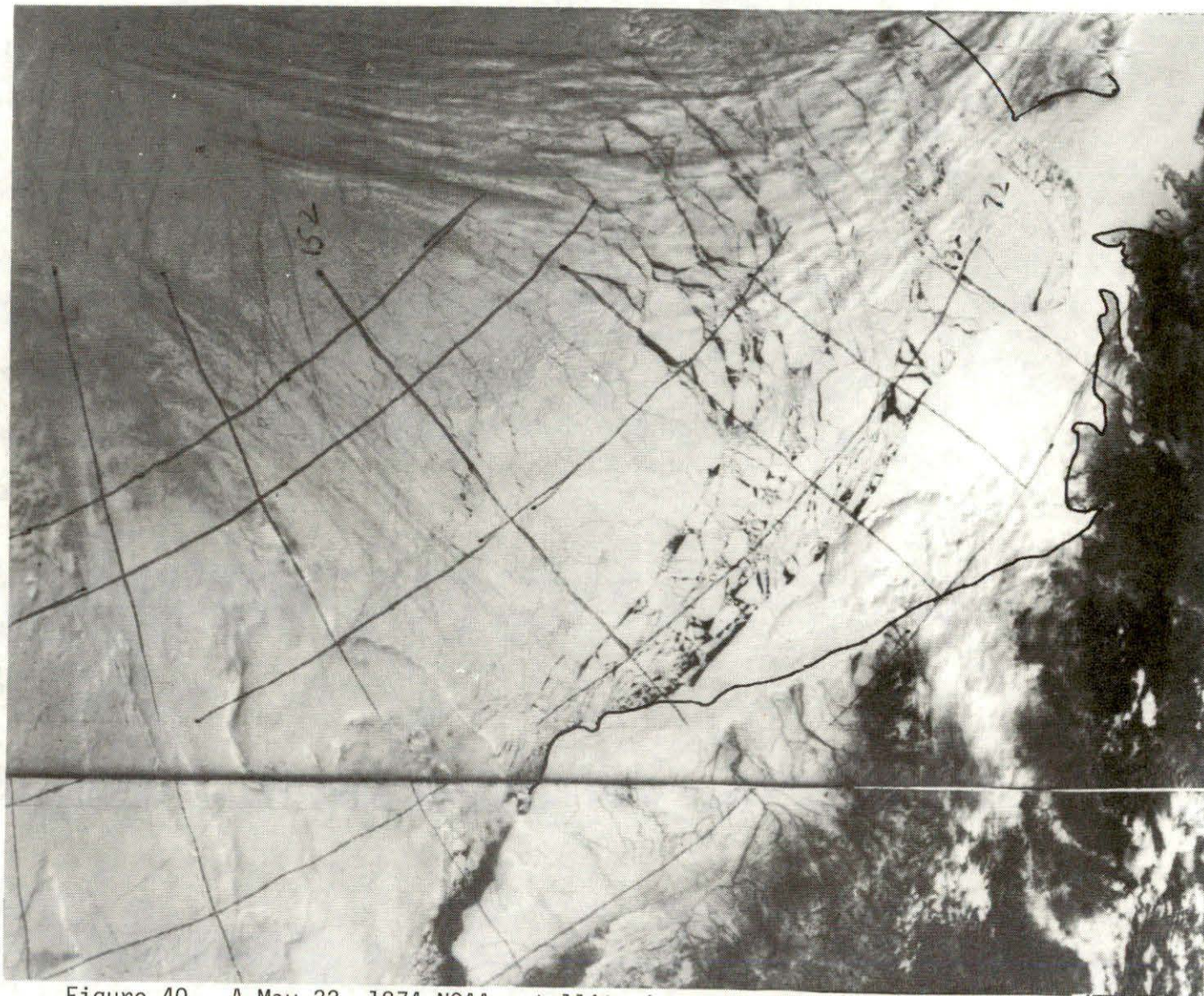
Figure 40. A May 22, 1974 NOAA satellite image of the Canada Basin. Two paths of apparently equally-spaced rectilinear intersecting leads can be seen in the upper right-hand corner.
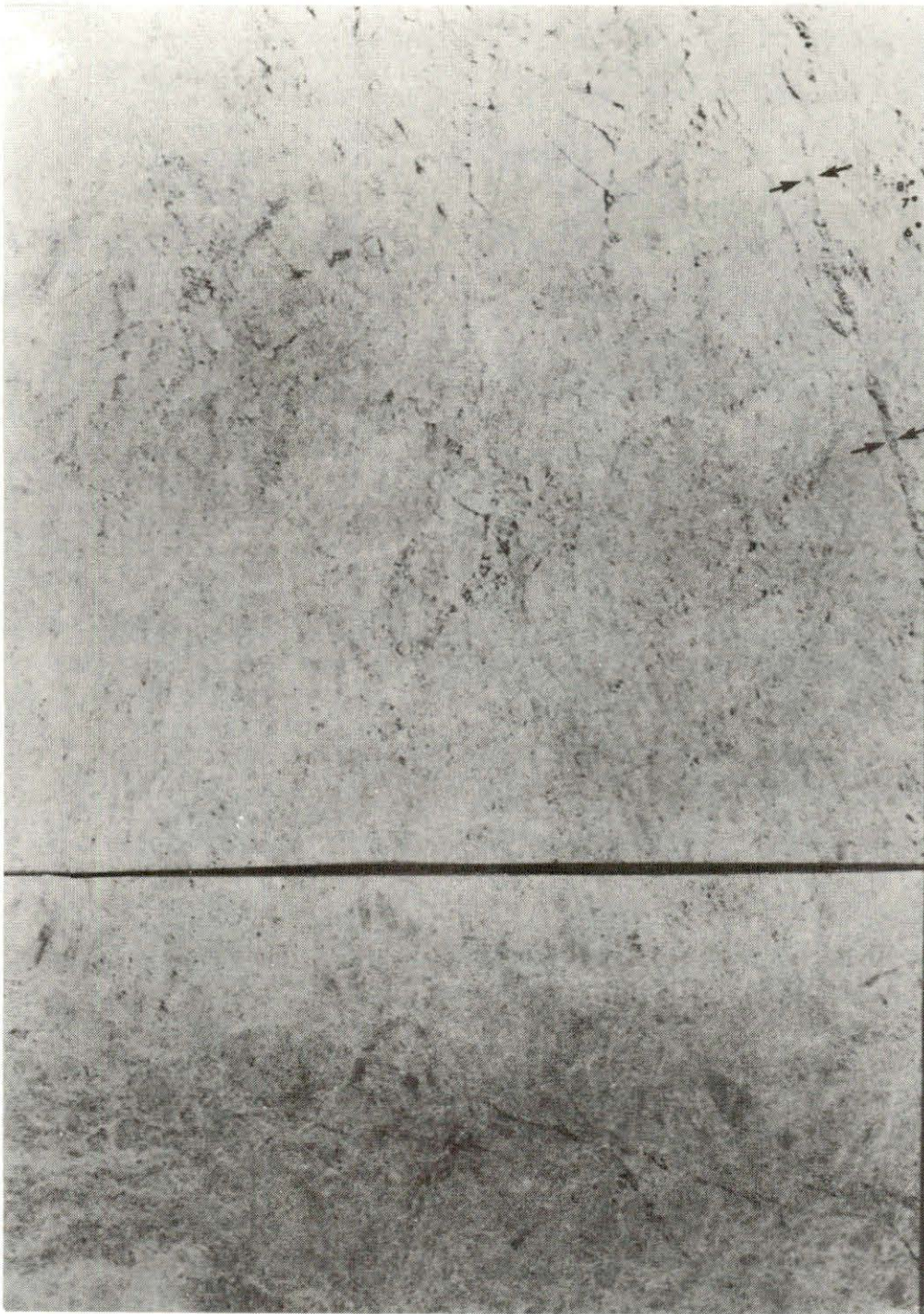
Figure 41. A September 8, 1974 ERTS satellite image of an area near the southern edge of the ice pack at 73°N, 146°W. The width of the image corresponds to 185 km and a relative shearing displacement occurred across the linear feature visible in the upper right-hand corner. Relative to the ice pack on the left side of this feature, the positions of a distinguishable ice floe are given on the September dates.

September which coincided with the development of recognizable leads from the previously faintly discernable rectilinear features. The gradual process of lead extension and development eventually gave rise to the spectacular pattern shown in the September 26 image of Figure 42. This pattern is decomposable into two sets of parallel north-south tending leads with individual separations of approximately 100 km. An ERTS-1 close-up of the pack-edge northwest of the Alaska-N.W.T. border in Figure 43 shows the solid, snow-covered state of the ice and the irregular, often ice-clogged, leads. This figure also includes the successive-day position plots of ice features relative to the rigid bulk of the adjoining diamond-shaped ice fields. Deviations from rigid body relative motion were observed only near the vertices of these fields and the motions themselves paralleled the common boundaries with unidirectional velocities similar to those noted earlier in the month. These motions can be resolved into progressive sliding along each of two sets of inter-secting leads as indicated in Figure 44.

The late September lead pattern is still visible, although somewhat degraded on the last observation date of 1974, October 15 (see Figure 45). During the period September to October, the pattern in the southern Basin was observed to be rigidly advected with the Beaufort Sea Gyre at approximately the 3 cm/sec mean speed.

Lead patterns in 1973, relative to 1974, were generally less prominent. Their occurrences were confined to the months of May and June. The patterns observed in the Canada Basin itself were in-distinct but were characterized by lead orientations and spacings similar to those of the following year. Sharp, well-defined leads and criss-cross patterns were confined to western regions, mainly in the Chukchi Province. In the northern sections of this Province the roughly northeast-southwest lead orientations and their spacings again resembled the 1974 observations (compare Figures 39 and 40). In the southern Chukchi Province, however, a persistent set of basically east-west leads appeared (see Figures 35 and 46), which were not observed in 1974, possibly because of cloud opacity.

Observations made during the few breaks in the cloud-cover of August and September 1975 indicated the frequent presence of late season lead patterns similar to those of 1974 (see Figure 47). The 1975 results of most interest were the similarities evident between the orientations and spacings of the spring leads and those characteriz-ing the fall 1974 patterns. The resemblance could be seen in the March 15 image of Figure 10 and became clearer shortly thereafter when many of the smaller leads had closed (see Figures 48-51). Through the sequence of images, the major leads of the original March 15 scene were observed to freeze while at the same time remaining fully visible until mid-June because of the contrasting darkness of the newly frozen surfaces. It is significant that, when lead and polynya refreezing occurred in more southern areas, the initial darker aspect of the new ice surface disappeared over a comparatively short, several day period. On the other hand, the new ice in the refrozen March 1975 leads remained darkened and observable for at least three months. Similar behaviour was noted in earlier years for
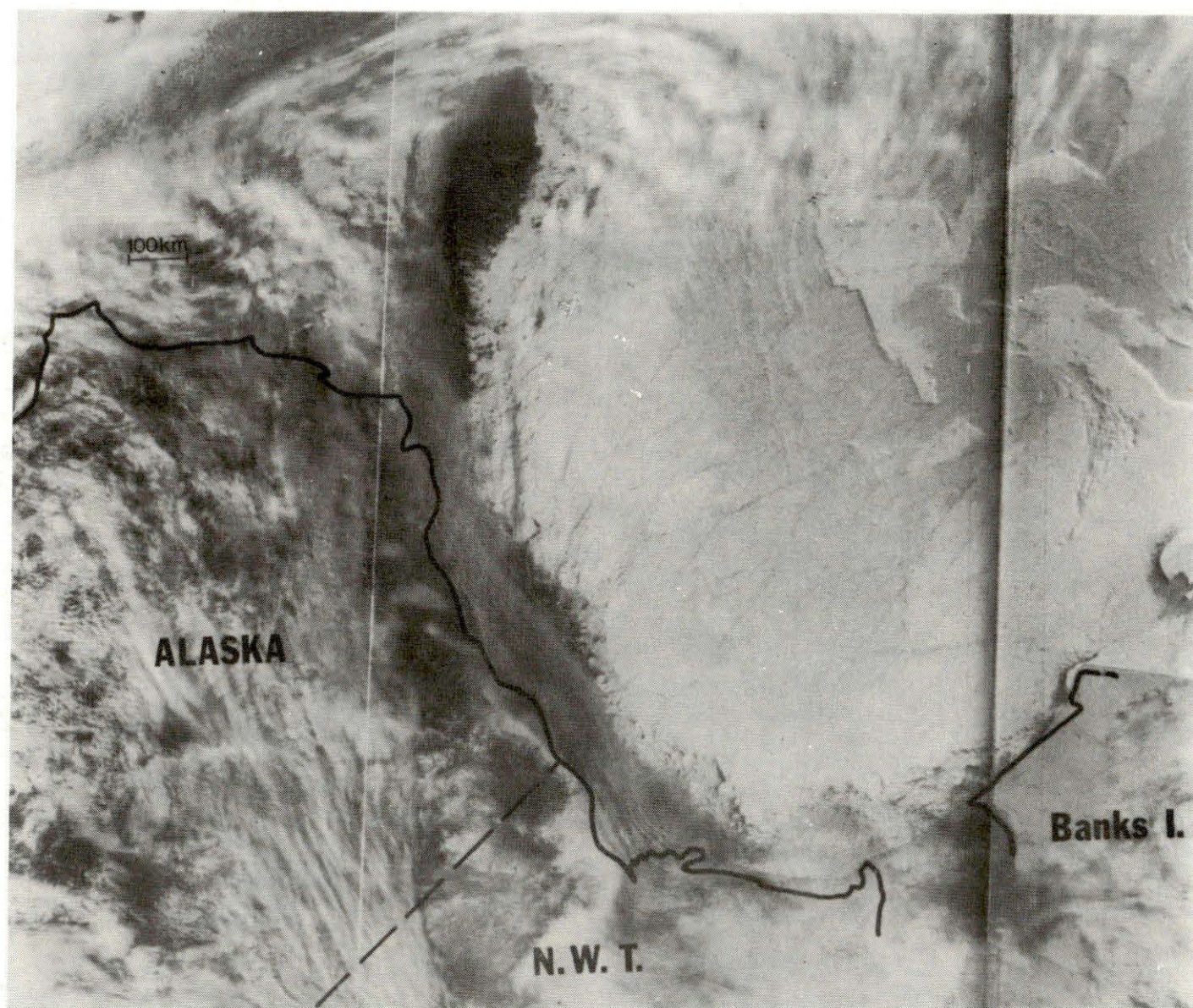
Figure 42.   A September 26, 1974 NOAA satellite image of the Canada Basin.
A pronounced lead pattern is visible in spite of intervening
cloud and fog formations.
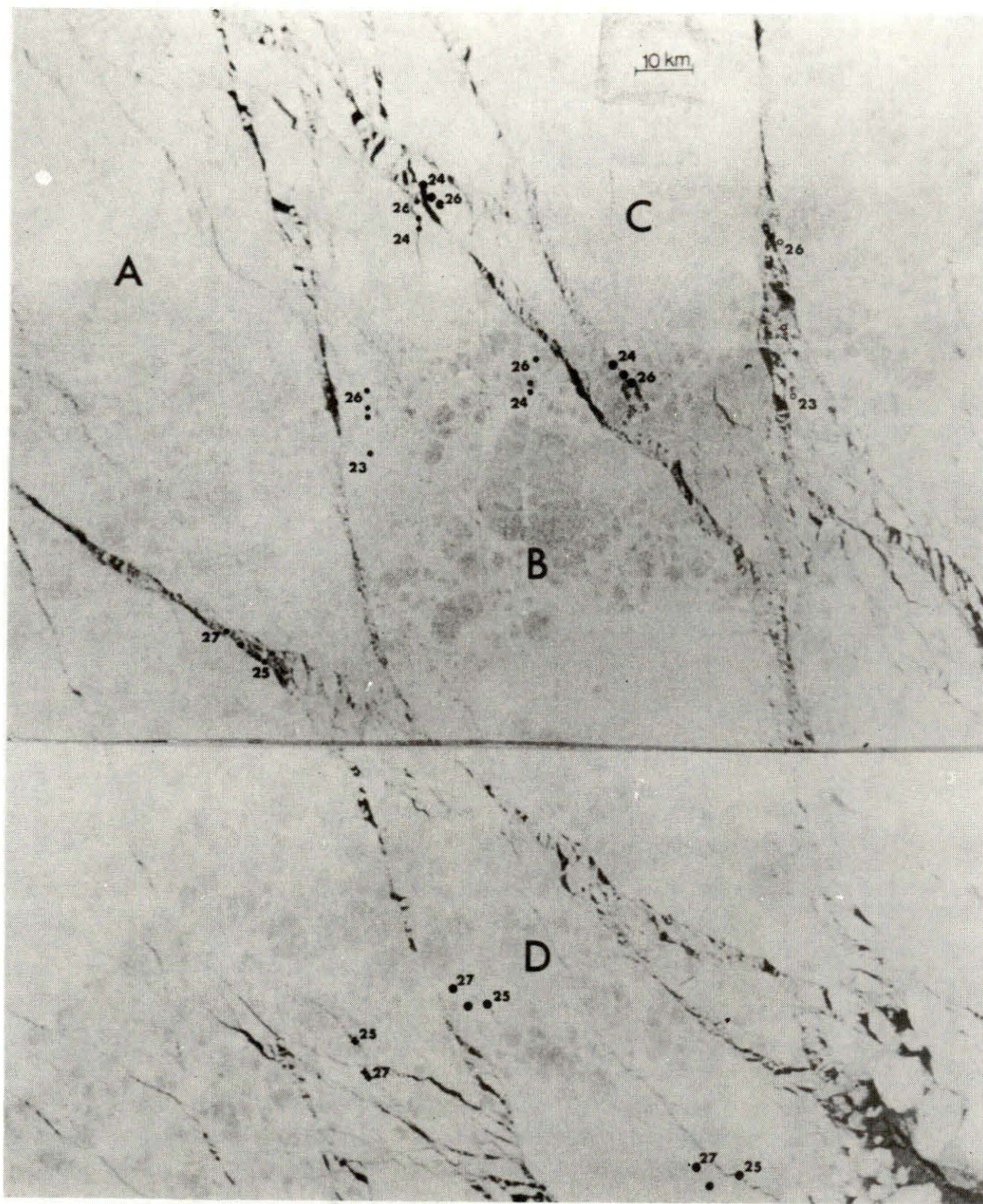
Figure 43. A September 25, 1974 ERTS satellite image of pack ice in the southern Canada Basin. The area covered is centered roughly at 73°N, 144°W. Positions on the appended September dates are given for surface features relative to the central portions of the lettered neighbouring ice fields according to the code: A - (.); B - (•); C - (o); and D - (+).
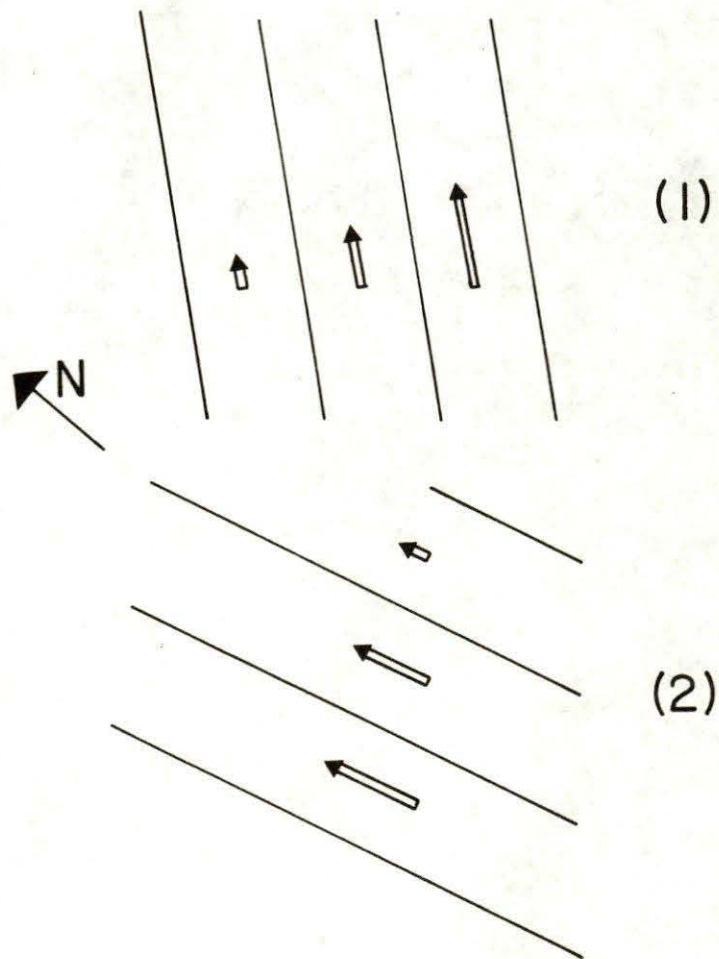
Figure 44.   A resolution of the relative ice field displacements of Figure 42
into progressively sliding bands bounded by lead sets (1) and (2).
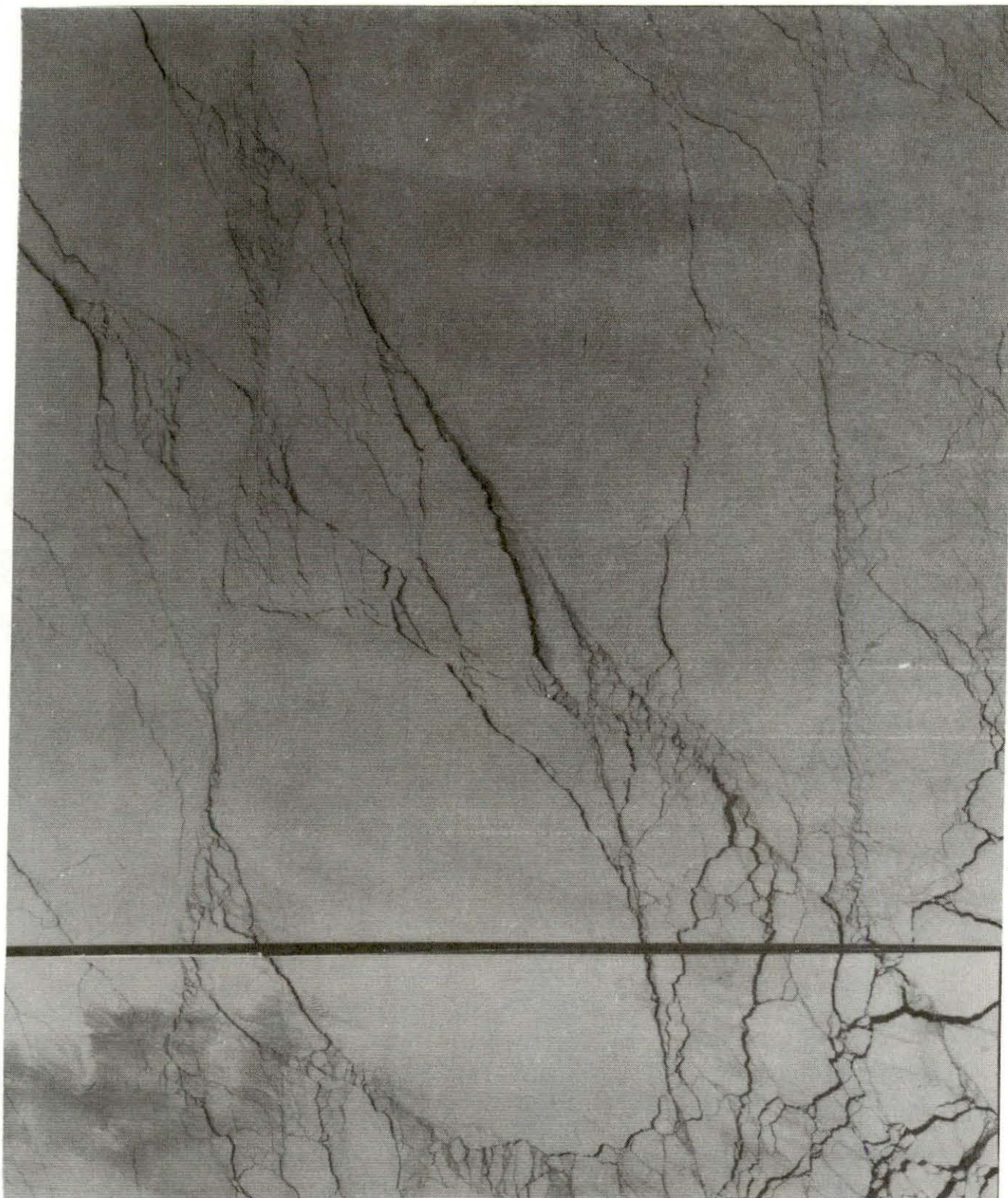
Figure 45. An October 11, 1974 ERTS satellite image of an area roughly centered at 73°N, 142°W.
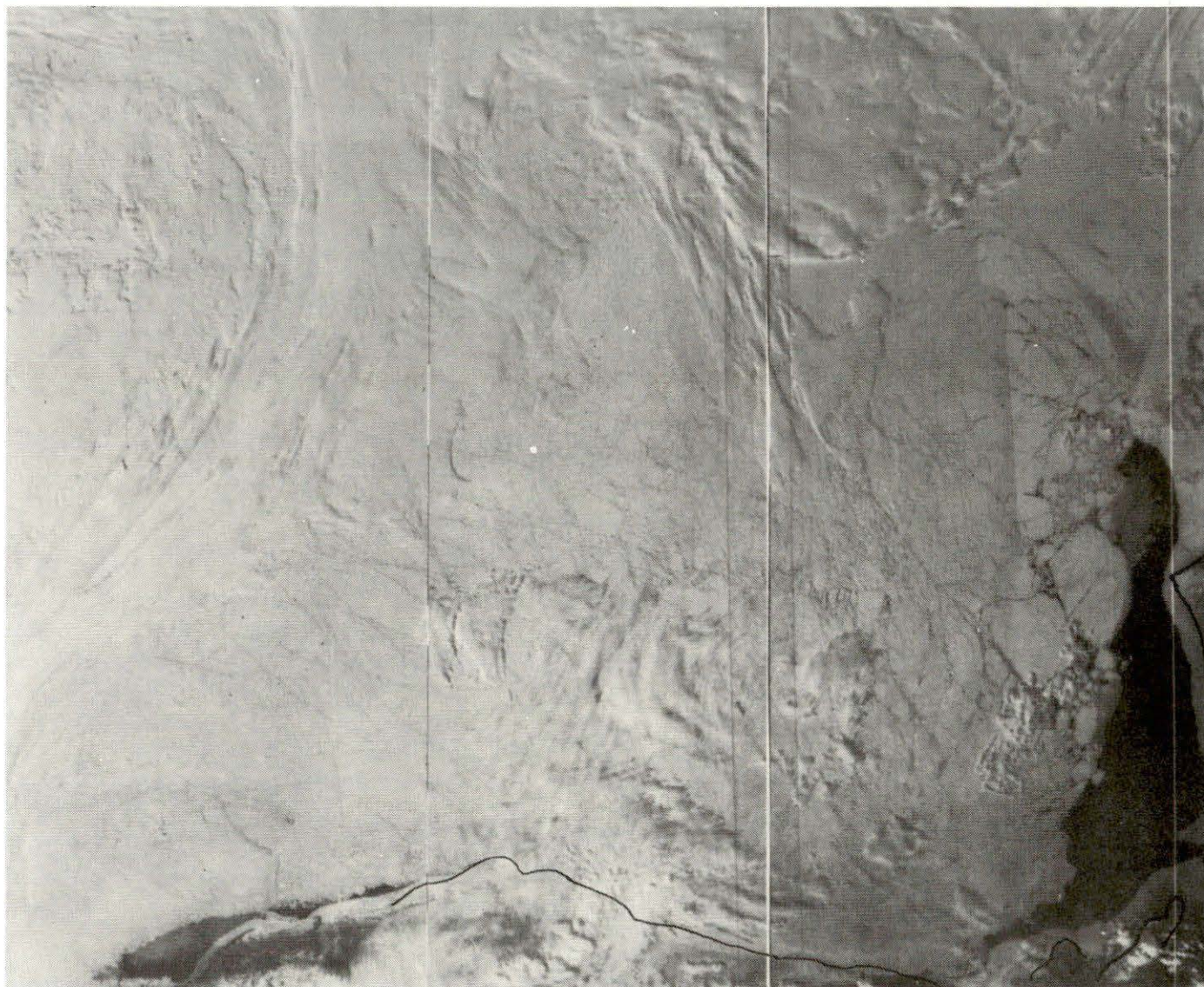
Figure 46. A June 7, 1973 NOAA satellite image of the Canada Basin. Banks
Island and the Tuktoyaktuk Peninsula lie respectively along the
right-hand and lower borders of the visible large open water area.
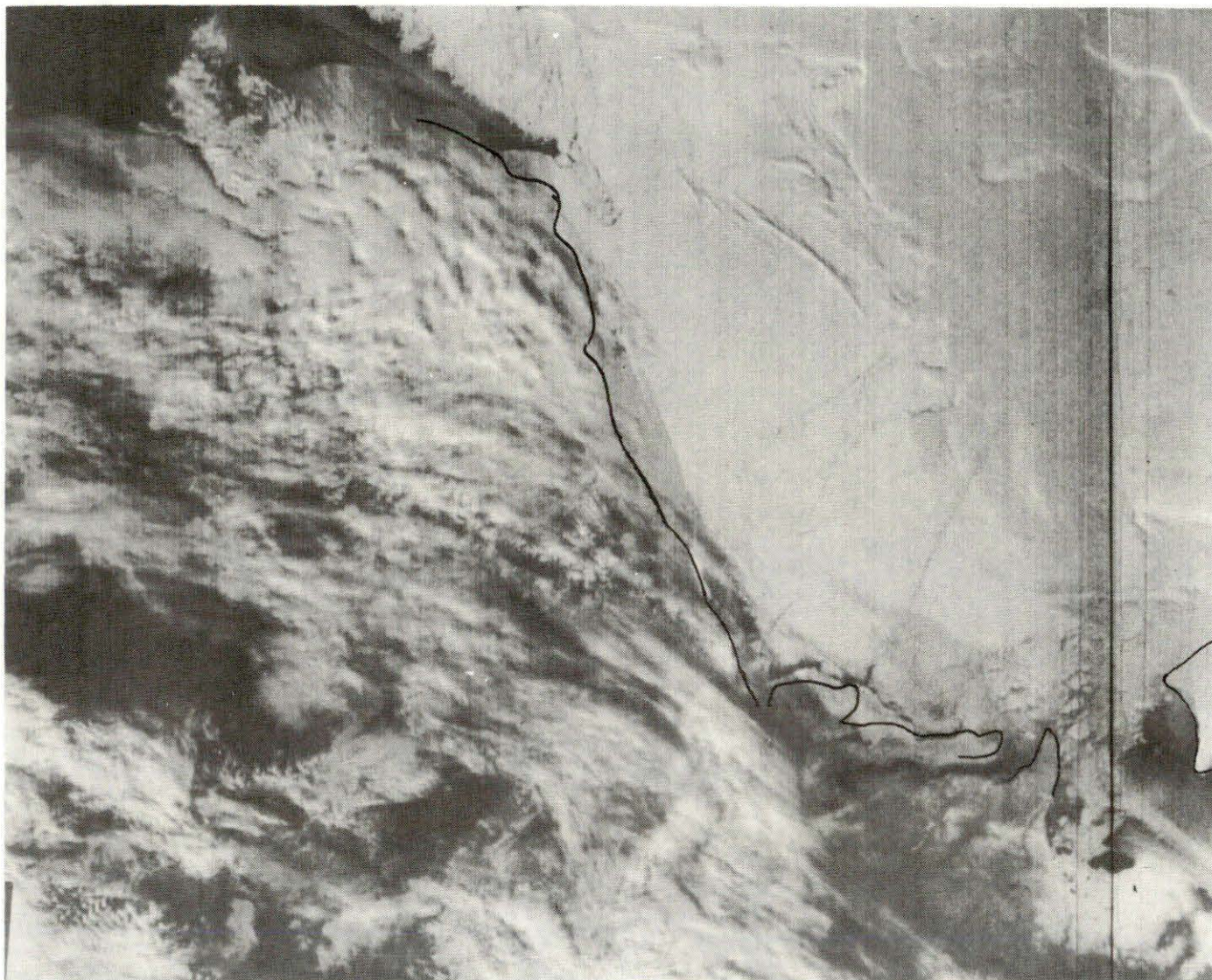
Figure 47. A September 29, 1975 NOAA satellite image of the Canada Basin.
Banks Island, Cape Bathurst and the Tuktoyaktuk Peninsula are all
visible in the lower right-hand corner. In spite of heavy cloud
cover, long rectilinear leads are visible to the north and west of
Mackenzie Bay.
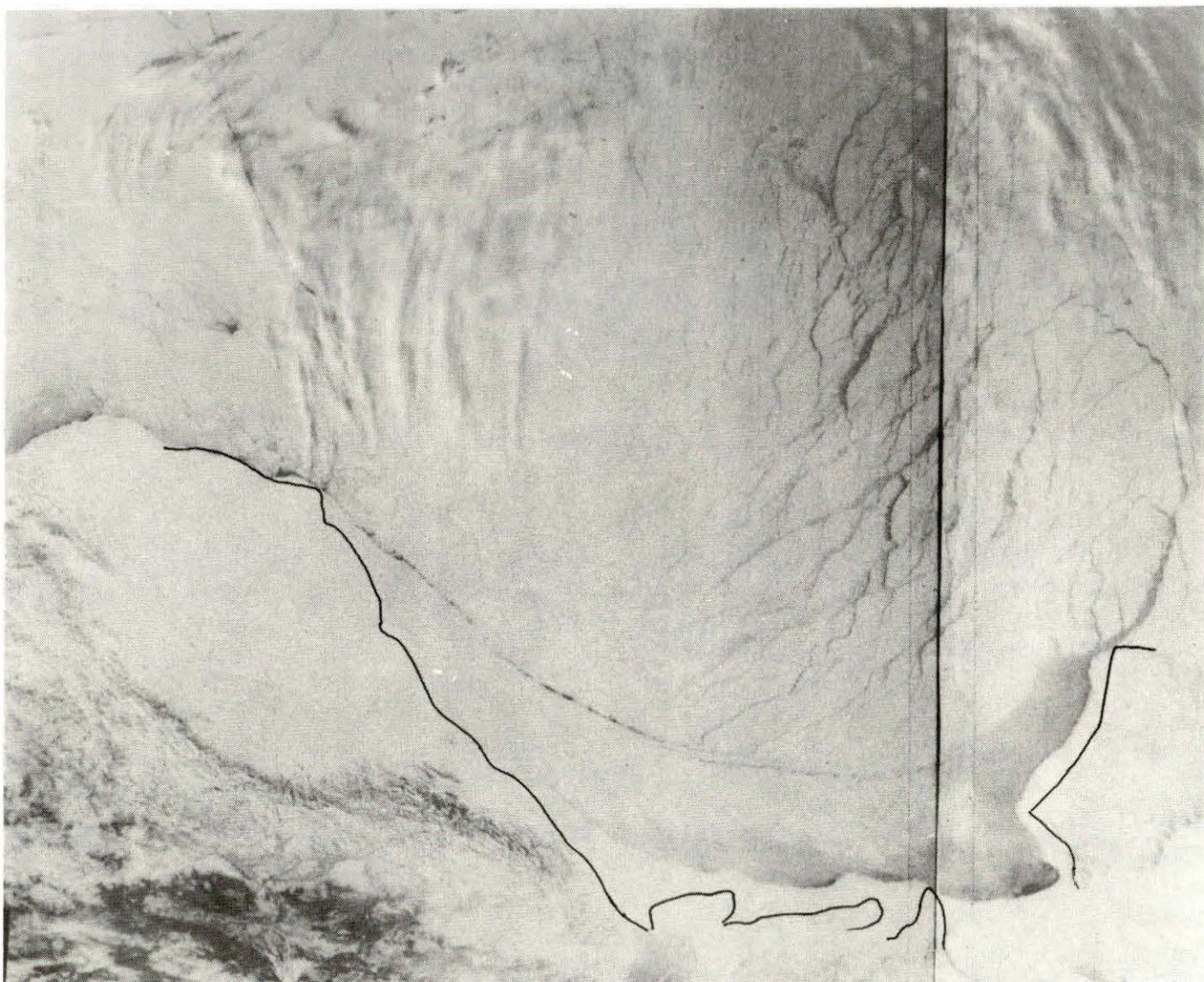
Figure 48. A March 26, 1975 NOAA image of the Canada Basin. Banks Island and the Bathurst Peninsula are again clearly visible in the lower right-hand corner. The northern "rectilinear" leads are seen not to extend south of the almost orthogonal major lead which reaches eastward from Point Barrow.
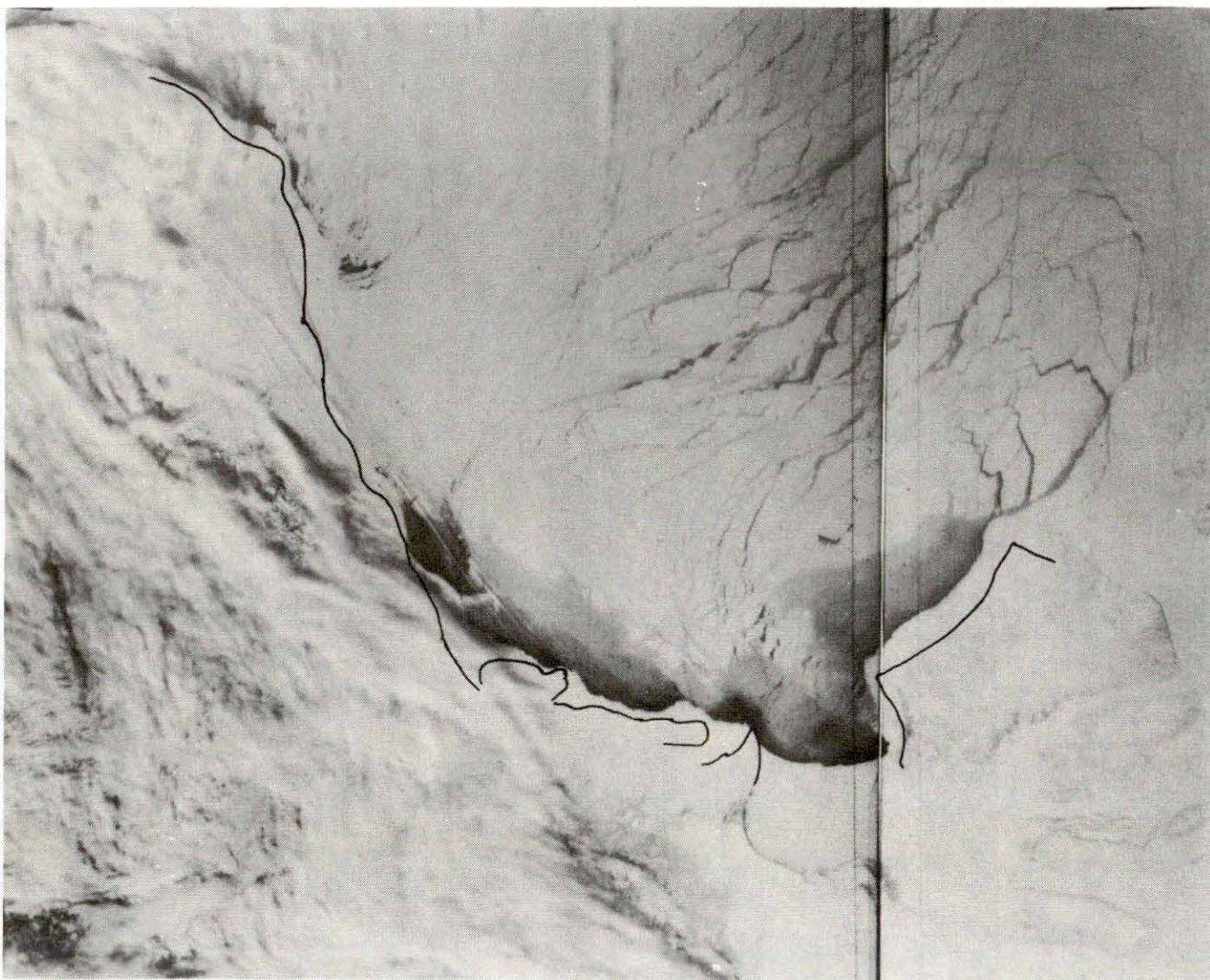
Figure 49. A March 29, 1975 NOAA satellite image of the Canada Basin. The east-west lead originating from Point Barrow in Figure 48 is barely visible and some northern leads can be seen to extend (with an eastward bending) to the southern edge of the ice pack.
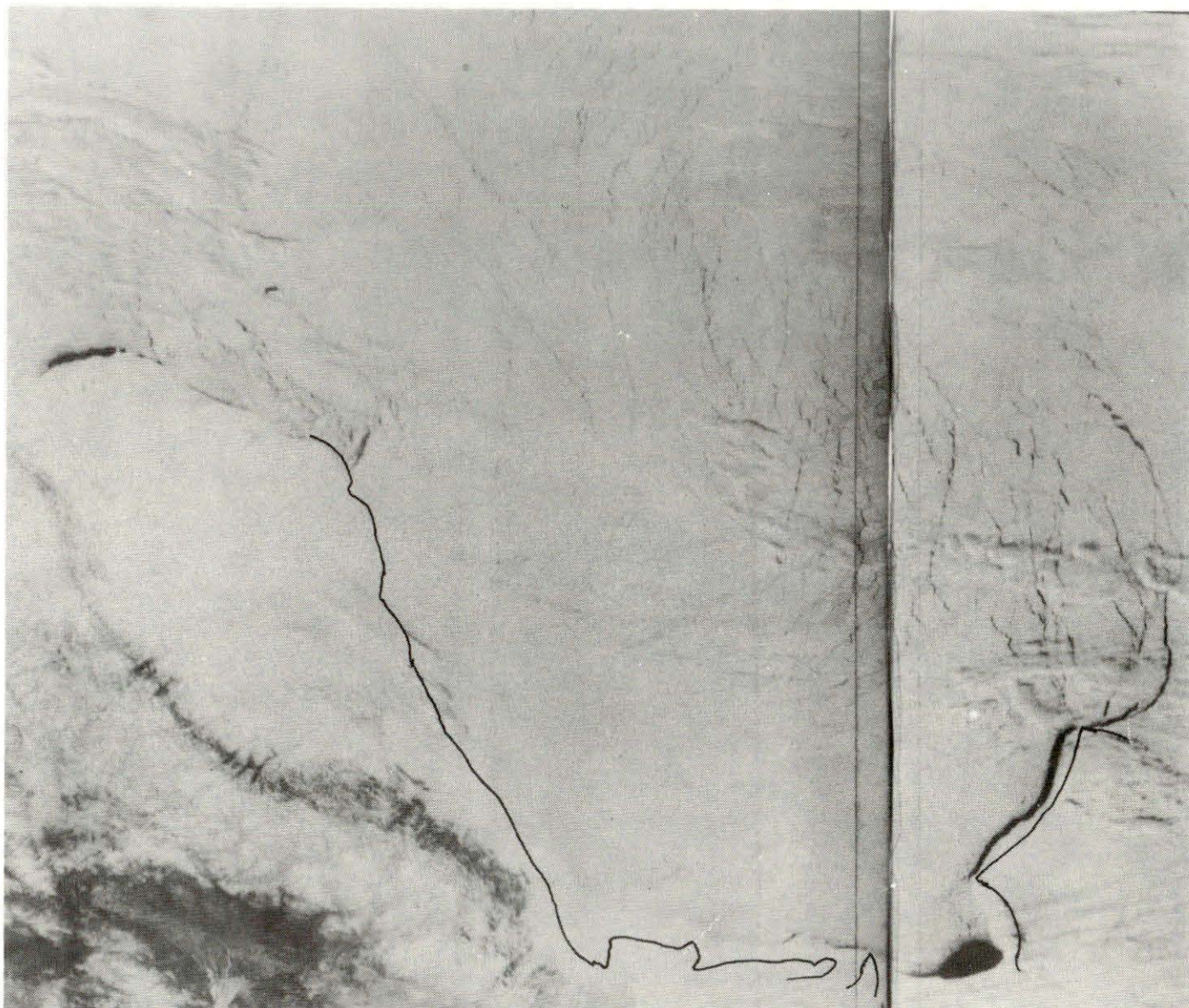
Figure 50. A May 2, 1975 NOAA satellite image of the Canada Basin. The re-
frozen March leads are seen just to the right of center and
several sets of new rectilinear leads are also visible.
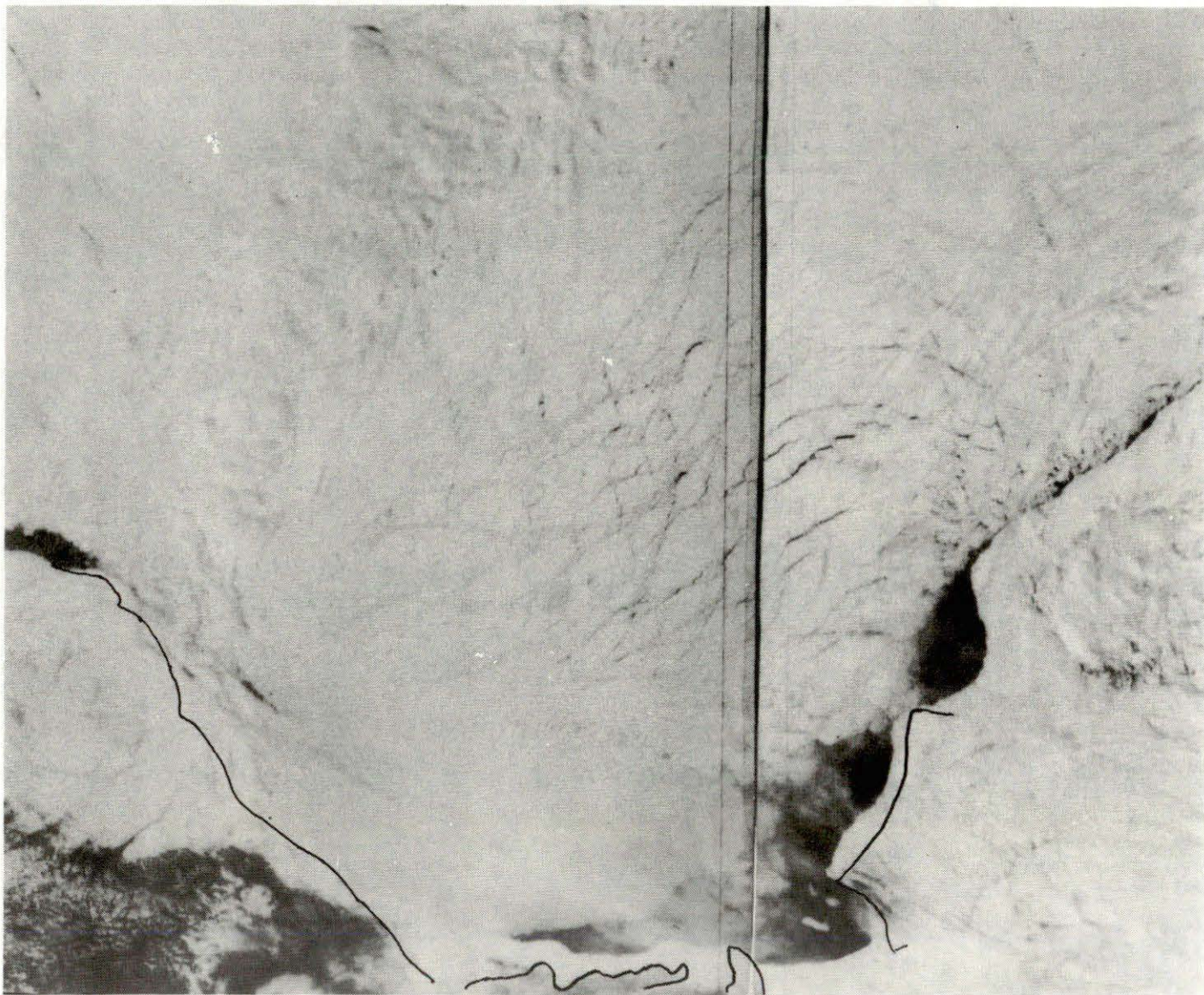
Figure 51.   A May 30, 1975 NOAA satellite image of the Canada Basin.   The old re-frozen March and new rectilinear north-south-tending leads are visible.

other refrozen leads in the pack ice. This property of the deep
water leads is not understood and could be intimately related to the
lead production mechanisms. In any case, following the motion of
these refrozen features (see Figure 52), it would appear that the
pack moved very roughly as a rigid body rotating about an axis in the
northeastern Canada Basin. New approximately rectilinear leads re-
developed (see Figures 49 and 50) oriented in the same northeast-south-
west and northwest-southeast directions of the leads seen in the March
15 image. Sets of more closely spaced north-south-tending leads are
also evident over the northern Chukchi Province in Figures 48 and 49.

The spatial-extent, -periodicity and persistence of the rectilinear
lead patterns strongly suggest that their generating mechanism may
be a fundamental feature of the Arctic Ocean environment. A direct
atmospheric effect seems most unlikely in view of the strong contrast
in the scales of the ice patterns and typical atmospheric phenomena.
Furthermore, the 100 km periodicity of the lead separation greatly
exceeds the wavelengths normally associated with flexural-gravity and
other waves in sheet ice (Wadhams, 1973; Press and Ewing, 1951).

There are at least two basic approaches which seem likely to explain
the origin of the observed rectilinear lead systems. The first of
these assumes the lead-generating medium to be the ocean and specif-
ically associates the leads with current shears inherent to planetary-
type waves (Rossby, 1938; Veronis, 1966) propagating in the under-
lying water mass. A description of such a mechanism will be given
below and in the Appendix together with an assessment of its success
in matching observations. This treatment will be followed by a brief
summary of a second mechanism now being actively investigated, which
assumes that the rectilinear leads are actually "strike-slip" faults
similar to those found in rock structures. In this case the lead
data may represent a new source of information on the rheological
properties of the ice cover and the stresses which act upon it.

Oceanic planetary waves are very low frequency, long-wavelength dis-
turbances linked to potential vorticity conservation in the presence
of the meridional gradient (β) of the Coriolis parameter and/or
variations in water density and depth. Apparently generated by
large scale ocean-atmospheric coupling, they have long been suspected
to play an important, if unconfirmed, role in general ocean dynamics.
Atmospheric fluctuations on smaller scales (roughly 10 to 100 km),
on the other hand, are capable of directly disrupting the regular
lead patterns which would otherwise mirror the low frequency currents
associated with these waves. This assumption is supported by the
fact that the directions of the calculated geostrophic surface winds
in September indicated a preponderant alignment (see the wind roses
of Figure 53) with the local mean flow of the Beaufort Sea Gyre.
This alignment, which would be expected to minimize internal dis-
locations within the pack, was not present in September 1973 (see
Figure 54) when no significant patterns were observed. Parallel
arrangements of the wind and mean currents appear to precede and/or
accompany periods characterized by significant rectilinear lead
patterns.
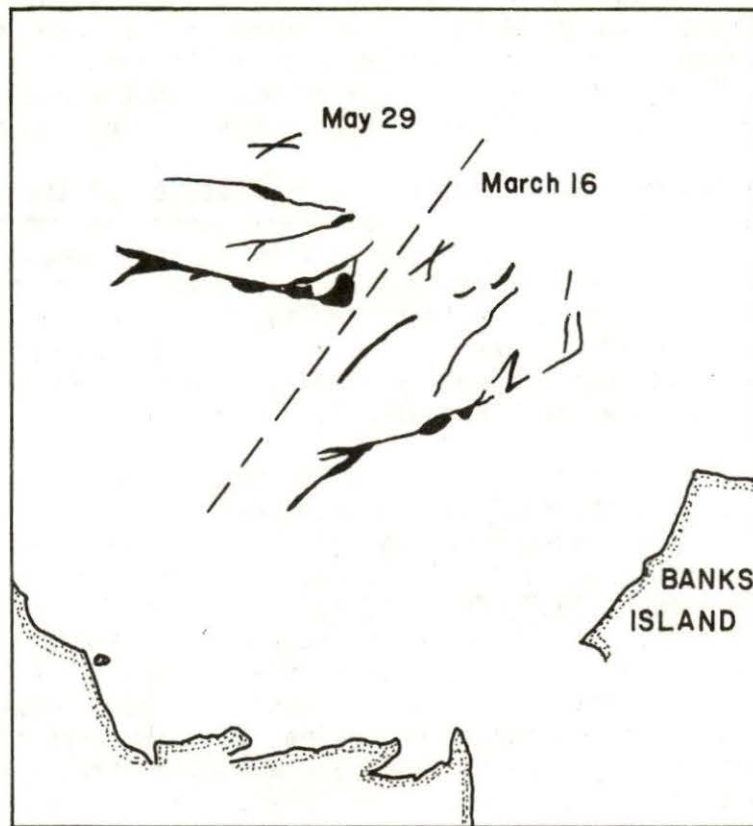
Figure 52. A sketch of equivalent sectors of the March 16, 1975 and May 29, 1975 lead patterns. The displacement is not a completely rigid one but can be very roughly approximated by a rotation about the northeastern corner of the Beaufort Sea.
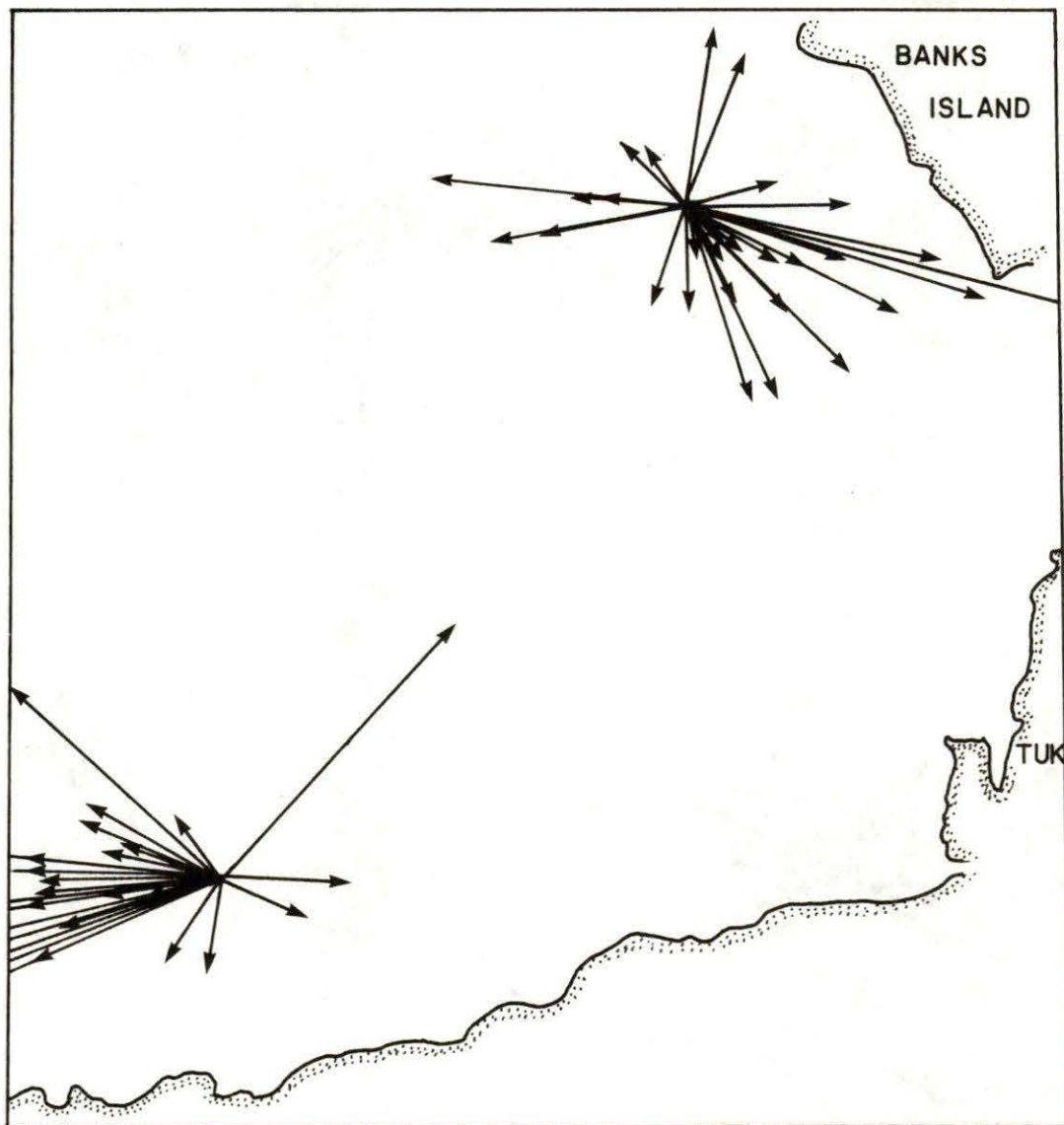
Figure 53. Wind roses for September, 1974.
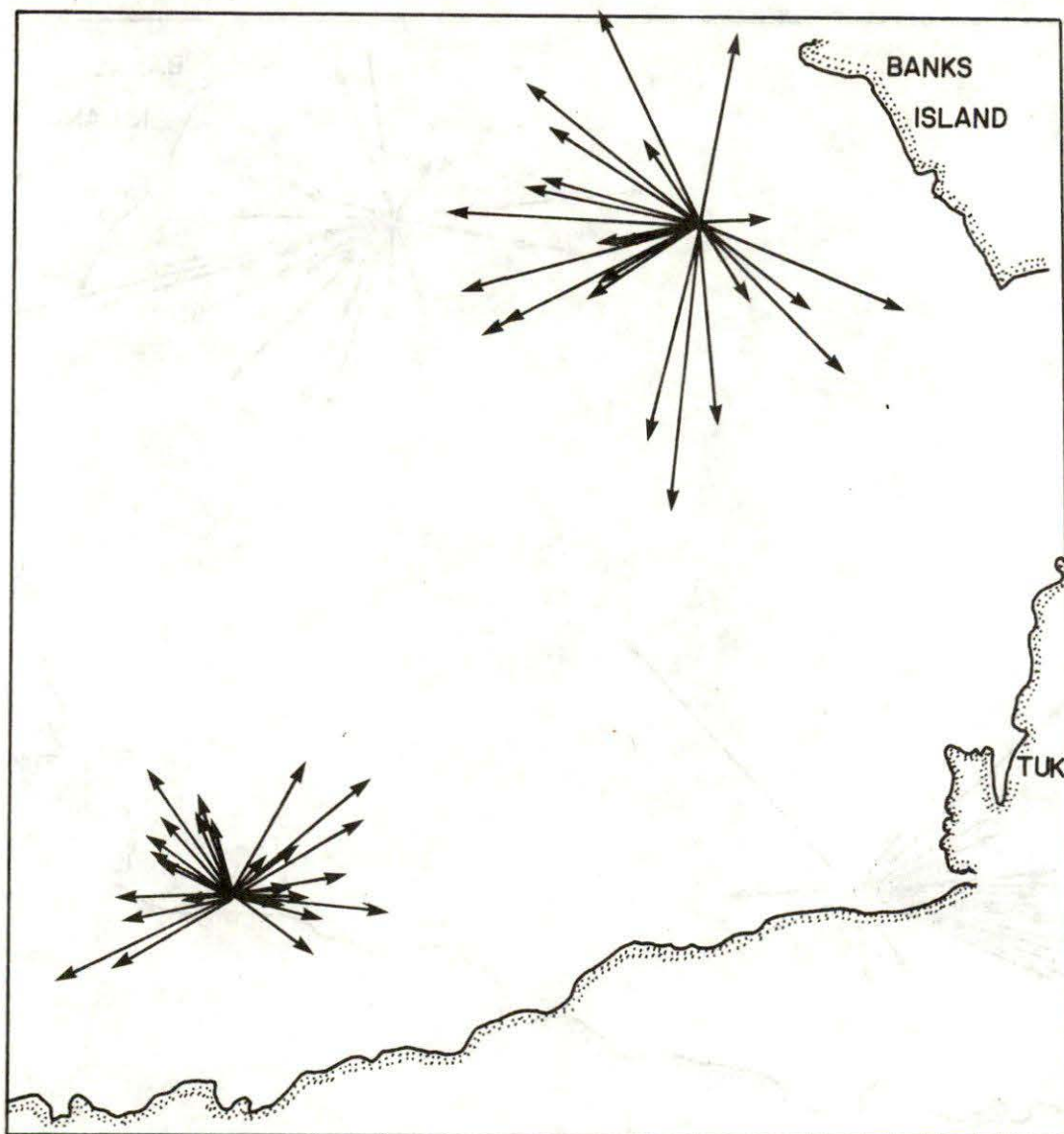
Figure 54. Wind roses for September, 1973.

Some evidence for the existence of oceanic planetary waves has recently been extracted from current meter records and geostrophic calculations in the Canada Basin (Newton, 1973) and over the Bering Slope (Kinder, Coachman and Galt, 1975). In the former investigation, baroclinic intermediate-scale features of the oceanic flow field had the appearance of north-south oriented plane waves with 100-200 km wavelengths. The wave period was estimated to be 16 to 32 weeks and its phase speed considered slow with respect to the mean gyral flow. The observed, near-surface, transverse current speeds were of the order of those noted above for the relative motions of adjacent ice fields. Although the deduced wave characteristics were somewhat consistent with the normal mode solutions derived for a circular, pole-centered basin (LeBlond, 1964), it is felt that such an explanation (Newton, 1973) is inappropriate to the partially enclosed southern Canada Basin. Moreover, it is impossible to reproduce the September-October lead pattern using the LeBlond model. A much more satisfactory approach is to interpret this pattern in terms of incoming and reflected waves analogous to the explanation offered for an observed system of geostrophic eddies within the Bering Slope Current (Kinder *et al.*, 1975). The data in that case were best understood in terms of a superposition of a south-southwesterly incident wave (of wavelength approximately 108 km) and its longer wavelength reflection from a discontinuity in the continental slope. A detailed mechanism is presented in the Appendix whereby lead patterns can be produced by surface current shears associated with planetary waves. Assuming multiple reflections of an original southward-propagating Rossby-wave, significant observed characteristics of the lead patterns are reproduced. The inadequacies of this approach arise in part from the greater speeds of the long term gyral motion relative to those generally associated with planetary wave propagation. It is difficult to maintain the rectilinearity required of the surface wavefronts under these conditions and alternative possibilities such as "phase-locking" may have to be introduced even within the framework of a planetary wave model (see Appendix).

The second basic approach, generally denoted as "rheological", may be more promising, although it seems even less likely to be encapsulated in a single, easily visualized picture. In this view the rectilinear leads constitute "strike-slip faults" in the ice cover associated with fracturing along two sets of lines whose common acute and obtuse angle bisectors respectively define the directions of the large and small principal stresses in the horizontal plane. Referring to Figure 43, this interpretation identifies a north-south compression and an east-west extension in the September 1974 ice pack. This possibility is consistent with the predominant southeasterly winds observed in the southern Canada Basin over this period (see Figure 53) and with the presence of considerable open water on the Siberian shelf capable of accepting the westward extension of Basin ice. However, at the present time, no analysis has been carried out to definitively link the lead patterns to any given force and the apparent periodicity of the patterns has not been reconciled with the very inhomogeneous nature of the ice cover. Within the rheological picture, however, the ubiquitous acute

angle, $\approx 28°$, associated with the lead intersections is equal to twice the angle of internal friction characteristic of the ice cover assuming the validity of the Navier-Coulomb-Mohr theory of failure in imperfectly elastic materials (Jaeger, 1971). The value of this parameter, together with the accompanying experimental evidence for highly localized shearing motions constitute important points of comparison with the viscous- and visco-elastic ice cover models now being developed within the United States-sponsored AIDJEX program.

Further satellite and ground truth observations would facilitate a choice of the most likely mechanism of lead generation. Progress on mechanism identification inevitably must be accompanied by similar progress in understanding the dynamics of the surface-water-ice system under the forcing atmosphere.

4. ICE AND SURFACE WATER STUDIES IN THE SOUTHEASTERN BEAUFORT SEA

Satellite imagery has been used to follow the movements of ice and silted water in the southeastern Beaufort Sea. The resulting data and observations will be discussed below after a brief summary of two more general studies pertaining to the size and wind dependence of ice floe motion.

4.1 Floe Size and Speed

It has been suggested (Venkatesh, personal communication) that an inverse relationship obtains between the speed and surface area of a freely floating, individual ice floe. ERTS imagery was used to follow clusters of widely spaced floes (separations of 5 km or more) having surface areas ranging from 1 km^2 to 10 km^2. Twenty-nine floes were included in the study and observations were confined to locations well removed from capes and shoreline features which might induce gradients in the velocities of wind and water currents. No significant surface-area to speed correlation was found.

4.2 Floe Velocity and the Wind Vector

During the summers of 1973-74, the movements of ice located in the vicinity of 71.5°N, 130°W (west of the entrance to Amundsen Gulf) were compared, with the wind-speeds and directions deduced from daily atmospheric surface pressure charts using the geostrophic assumption. Results are shown in Figures 55 and 56 to be generally consistent with Zubov's rule (1943) with a slightly larger than usual rightward rotation ($\bar{\theta} = 55°$). The decrease in the ice-speed to wind-speed ratio at higher wind speeds is also in accord with earlier results (Reed and Campbell, 1960). It should be noted that the ice floes included in this study were either not in physical contact with other floes or were embedded in small ice fields well removed from the vast Beaufort Sea pack. When these conditions were not satisfied, the effects of the internal pack ice forces appeared and anomalous drifts to the left of the wind could be observed (as cited in Subsection 3.2, Figure 34). The large value
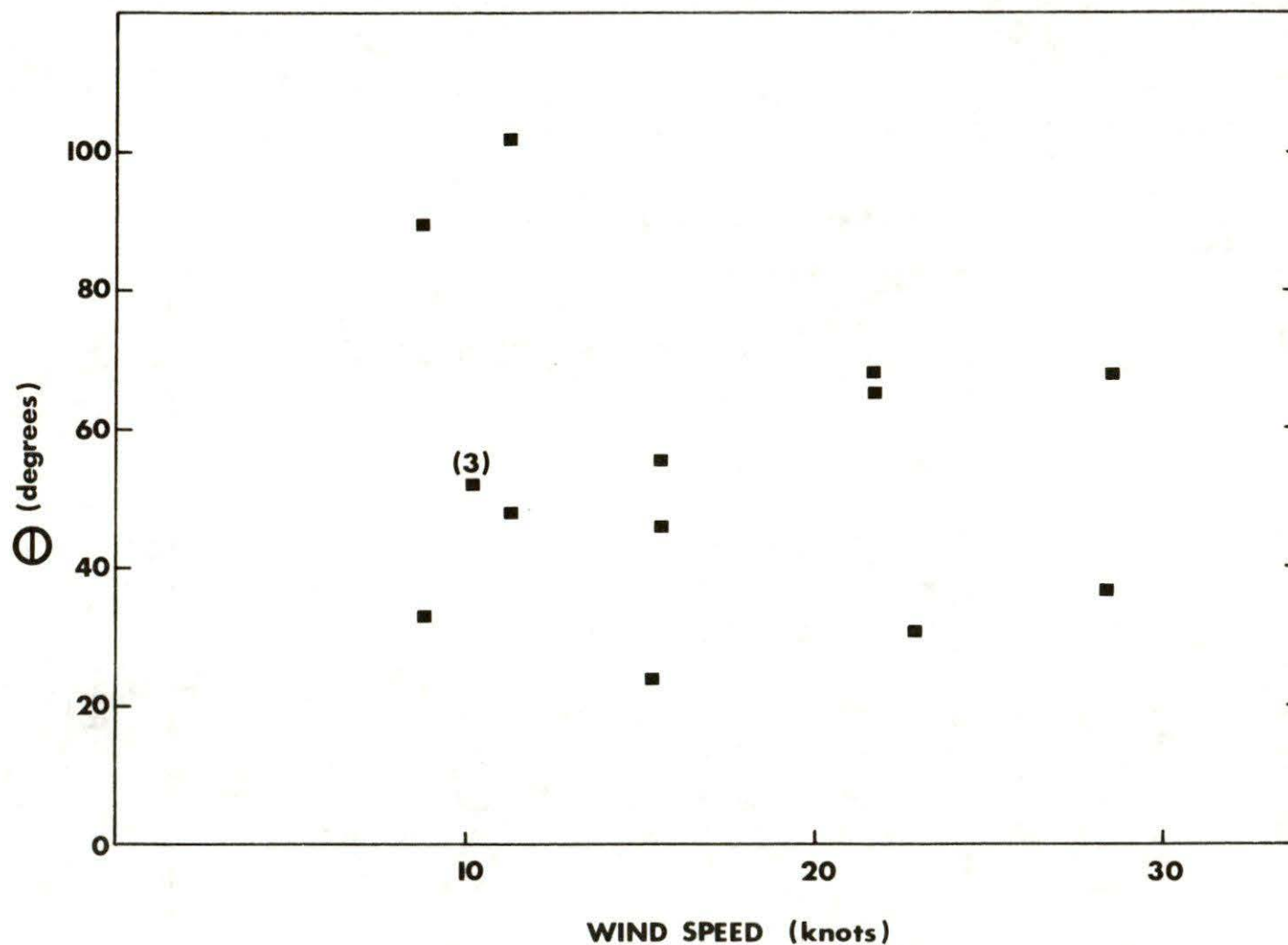
Figure 55. A plot of the angle between the daily ice displacement and calculated wind vectors as a function of wind speed. These data were obtained for floes in the southeastern Beaufort Sea and all corresponded to rightward deflections relative to the wind directions.
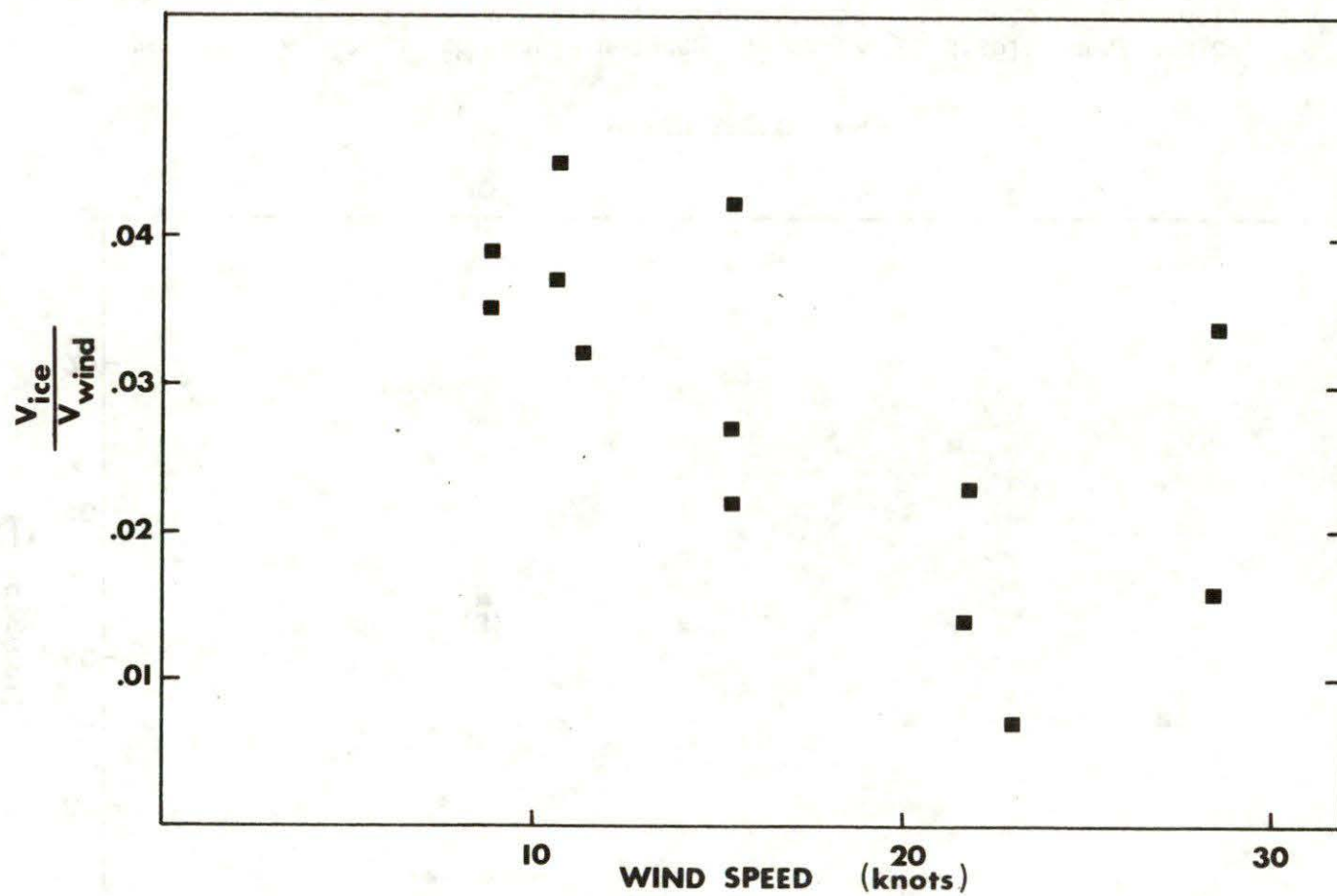
Figure 56. The ratio of ice and wind speed as a function of wind speed for floes in the southeastern Beaufort Sea.

of $\bar{\theta}$, relative to the results of Markham (1976), may be due to the intentional minimization of the effects of these internal ice forces which often appeared to be responsible for negative (leftward relative to the wind) floe deflections.

4.3 Ice and Surface Water Movements, 1973-1975

Surface waters in the southeastern Beaufort Sea move in response to local winds, rates of Mackenzie river flow, and are restricted by the motions and boundaries of the ice pack in the Canada Basin. Evidence indicates that the ice pack boundary can govern the thickness and areal extent of the low salinity surface water layer. The position of this boundary may be determined by conditions in the greater Canada Basin and the associated ice motions may differ considerably from those which obtain in the more inshore waters.

The positions of the pack ice boundary on selected 1973-5 dates have been sketched in Figures 57-59. Precise specification of boundary positions was particularly difficult in the neighbourhood of inhomogeneous ice tongues and eddies. Judgement was used in these cases to choose a representative demarcation line. Generally ice with a concentration greater than 5/10 was included in our pack ice category and the accuracy of the mapping should be better than 20 km.

The common element of the first two annual progressions in the ice-break-up is the general westward movement through August and September of a widening open water lead along the mainland coast beyond Herschel Island. In 1973 this was accompanied by a general eastward movement of ice in the eastern Basin toward the Banks Island coast and the entrance to Amundsen Gulf. The late and limited retreat of the 1974 pack, on the other hand, led to a continued late-summer westward movement of ice out of Amundsen Gulf and away from the coast of Banks Island. The proximity of the pack to the coast confined the low-salinity silted waters from the Mackenzie River to an unusually small area leading to a thickening of the surface water layer reported elsewhere (Herlinveaux and de Lange Boom, 1976). The ice dam thus formed eventually first broke in the Cape Bathurst area (see the sequence of NOAA images in Figure 60) leading to an apparently unusual flow of silted water eastward across Amundsen Gulf. This water was responsible for the mud-coloured ice found as far north as Sach's Harbour during the spring of 1975.

The most pronounced northward retreat of the eastern Beaufort Sea summer ice pack was observed in 1975. As a result, the fresh-water damming effects during and shortly after the Mackenzie River freshet (which peaks in early June) were significantly reduced even relative to the light 1973 ice-year. On the other hand, a late-summer, early-fall restriction of the still considerable river discharge may have been produced by the general eastward advance of the ice pack observed in August and September (Figure 59). This advance contrasted with the continued ice retreats of the two previous years and accounted for the late summer downturn in the corresponding open water ratio curve of Figure 1.
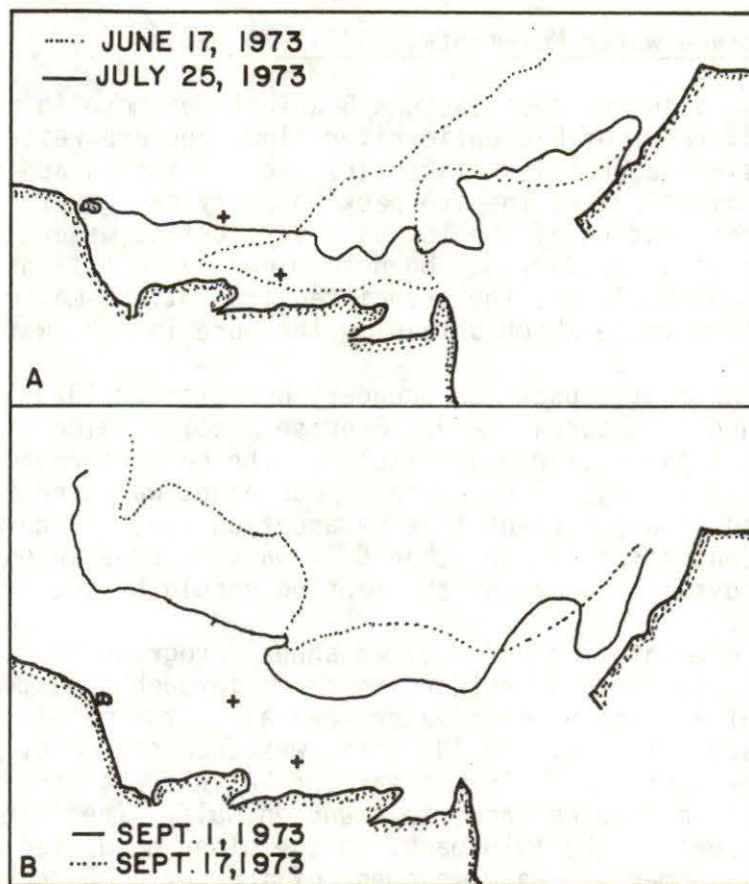
Figure 57. The dense (> 5/10) ice boundaries of the 1973 summer Beaufort Sea on: (A) (···) June 17; (A) (——) July 25; (B) (——) September 1 and (B) (···) September 17. The proposed 1976 drilling site locations are indicated by crosses.
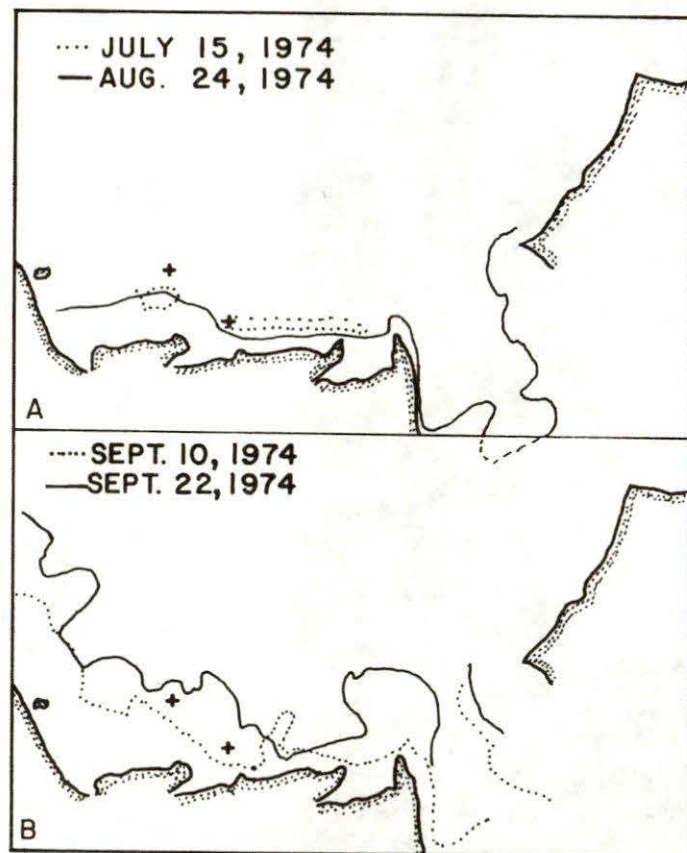
Figure 58. The dense (> 5/10) ice boundaries of the 1974 summer Beaufort Sea on: (A) (···) July 15; (A) (——) August 24; (B) (···) September 10 and (B) (——) September 22.
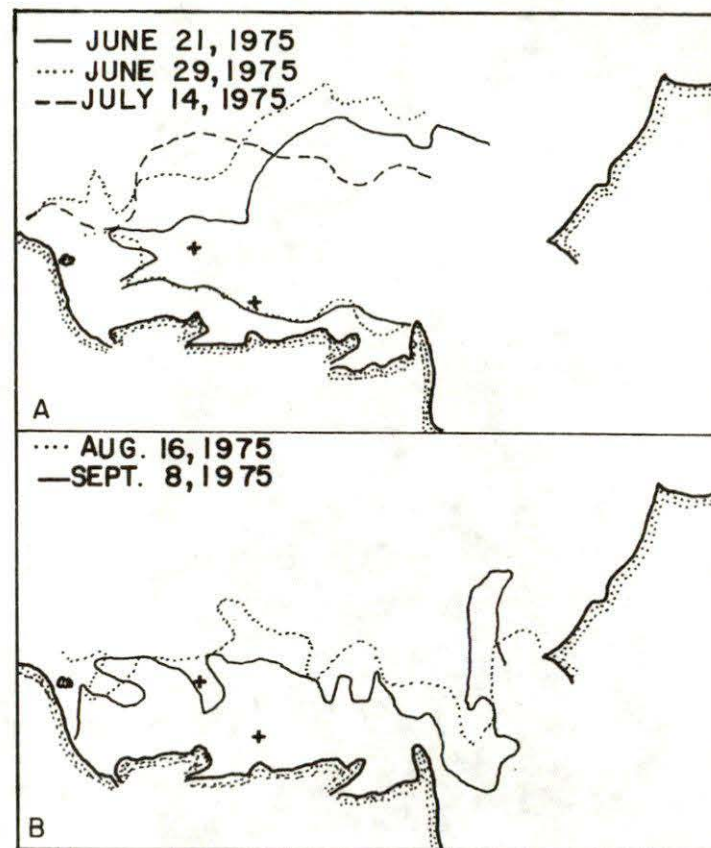
Figure 59. The dense (> 5/10) ice boundaries of the 1975 summer Beaufort Sea on: (A) (——) June 21; (A) (···) June 29; (A) (---) July 14; (B) (···) August 16 and (B) (——) September 18.
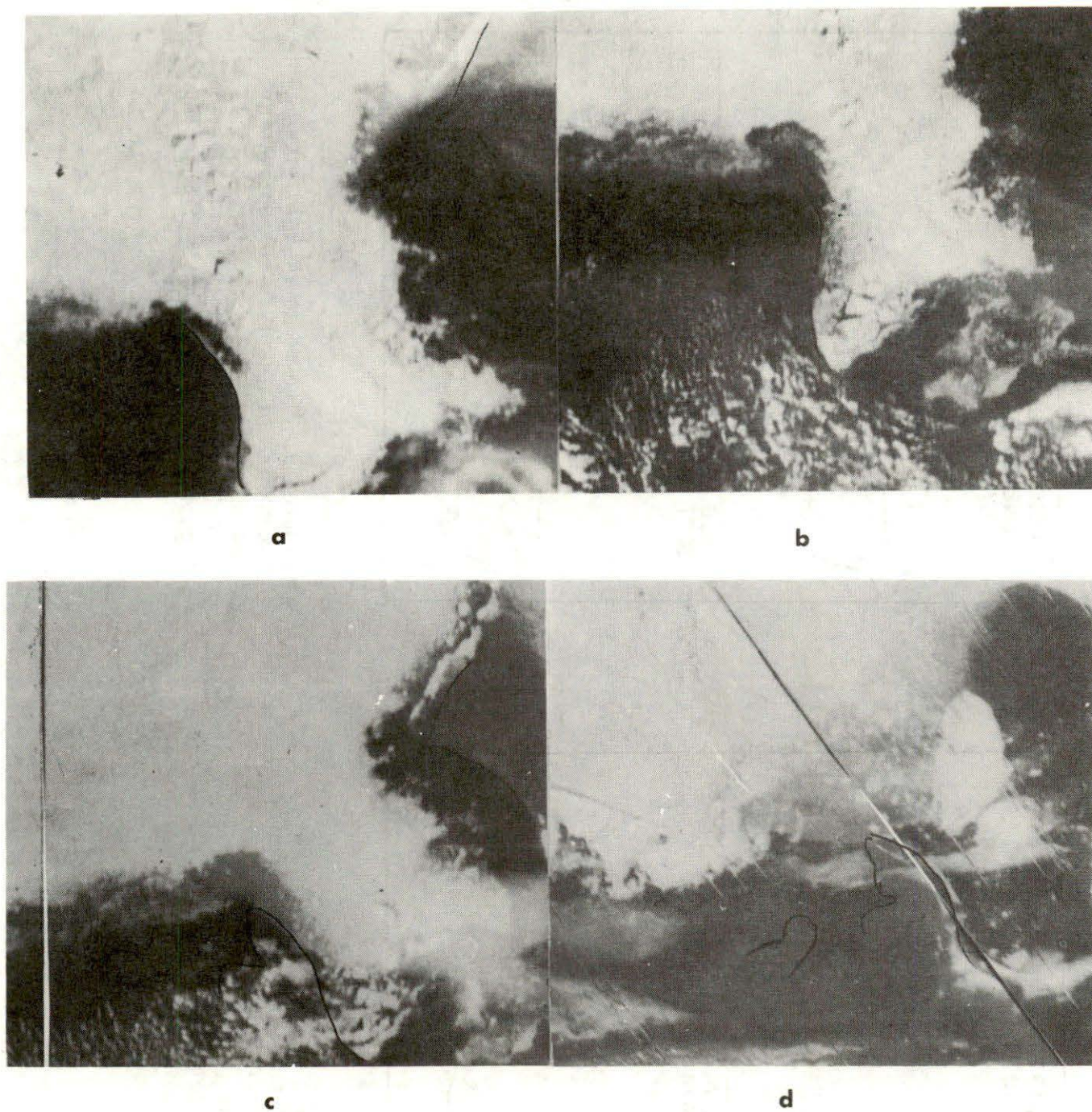
Figure 60.   The entrance to Amundsen Gulf on (a) August 23, 1974; (b) August 24, 1974; (c) August 25, 1974 and (d) September 16, 1974.   The small stretch of open water near the head of the Bathurst Peninsula (in (a)) gradually extended itself to the eastward, thereby more or less "opening" the entrance to the Gulf.   The low salinity waters moving northeastward along the Tuktoyáktuk Peninsula were then able to drift across to the Banks Island shore.

The position of the central ice pack boundary controls the break-up and dispersal of the landfast ice. The great northward retreats of 1973 and 1975 resulted in coastal access to shipping during the first week in July. Contrasting coastal conditions for a closed and open year may be seen in Figures 61 and 62, respectively. The remaining landfast ice of 1974 dispersed very slowly into the narrow open water region separating it from the offshore pack. By August 7, 1974 the previously landfast ice had moved completely offshore, but the closeness of the rigid pack ice edge still gave rise to heavy coastal floe densities (Figure 63).

The seaward boundary of the landfast-ice may usually be identified by its coincidence with a persistent lead that, along the Tuktoyaktuk Peninsula, roughly follows the 30 m depth contour (see Figure 64) and changes its position very little from year to year. Variations in the position of the lead seaward of this landfast-ice boundary were, however, visible in southwestern Mackenzie Bay near Herschel Island (see the sketched boundaries of Figure 65).

Along Tuktoyaktuk Peninsula, the onset of the spring season usually corresponds to a progressive widening of the boundary lead which begins in Amundsen Gulf and works its way westward into Mackenzie Bay. The resulting open water region is part of the eastern terminal polynya discussed in Section 3. The stretch of ice and water between the boundary lead and the pack ice of the Gyre will be denoted, in this report, as the "transition zone". Relatively little is known of the characteristic surface water and ice motions in this area. They are clearly affected by the Gyre in the Canada Basin but are also closely tied to the details of the coastal river discharges, wind patterns and mass exchanges through Amundsen Gulf and McClure Strait.

At times it is possible to establish a northern boundary of the transition zone coincident with a characteristic lead or leads which run eastward from Point Barrow, roughly following the 500 m bottom contour, to an eastern terminal polynya at a point west of Sach's Harbour on Banks Island. Such a lead is visible in the March 26, 1975 image of Figure 48. It can be seen that the rectilinear lead formations discussed in Subsection 3.3 existed only on the north side of this characteristic lead south of the pack ice and the distinction of an intervening transition zone is self-evident. It is not always possible to differentiate between zones in this fashion as the east-west oriented leads often become unobservable and the orthogonal north-south leads may reach fully to the landfast-ice boundary. Nevertheless, the concept of a distinct transition zone retains some validity in terms of ice movement and will be retained for convenience in the remainder of my discussion.

Before presenting specific data on conditions in the transition zone it is useful to identify the locations of the proposed sites for wildcat drilling in 1976. These are positioned in Figures 66-68 which show June imagery of the years 1973-5. The eastern site, Site #1, is seen to be at the landward edge of the transition zone while Site #2 lies roughly 40 km beyond the landfast-ice boundary. These

Figure 61.   A July 7, 1973 ERTS satellite image of the Beaufort Sea and the
             northern Tuktoyaktuk Peninsula. The white areas along the left
             edge and the upper right corner of the image are cloud formations.
             Floes having linear dimensions up to several kilometres are seen
             to be scattered in a roughly coast-paralleling band with a con-
             centration area near Point Dalhousie.

Figure 62. A July 19, 1974 ERTS satellite image of the same area shown in Figure 65. A small area of open water is seen at the lower left between the still intact landfast- and the seaward pack-ice.
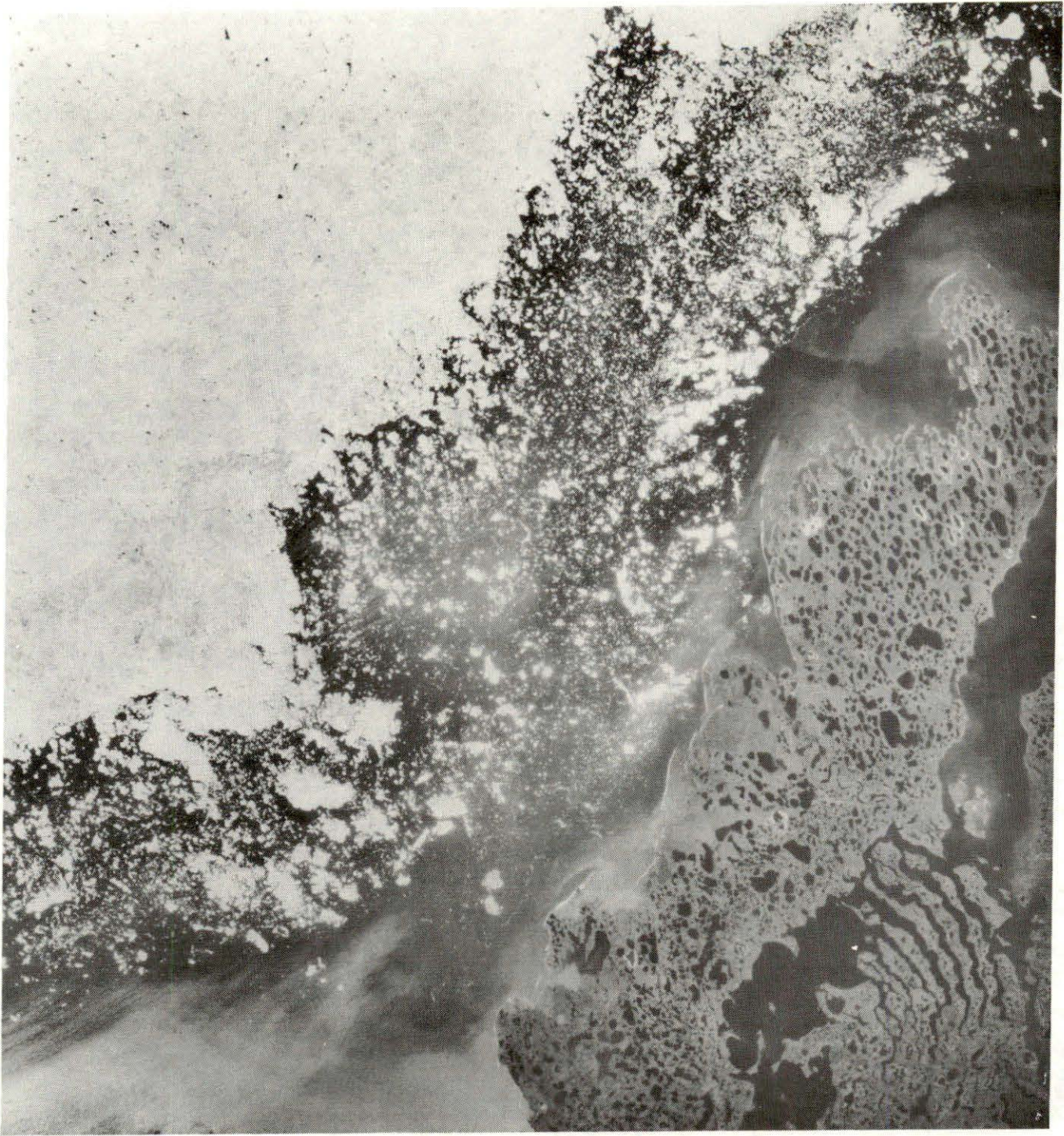
Figure 63. An August 7, 1974 ERTS satellite image of the area shown in Figure 66 and 67. A heavy concentration of floe ice remained inshore of the main pack.

NO. 2 ⊕

30 m
20 m

NO.1 ⊕

TUK
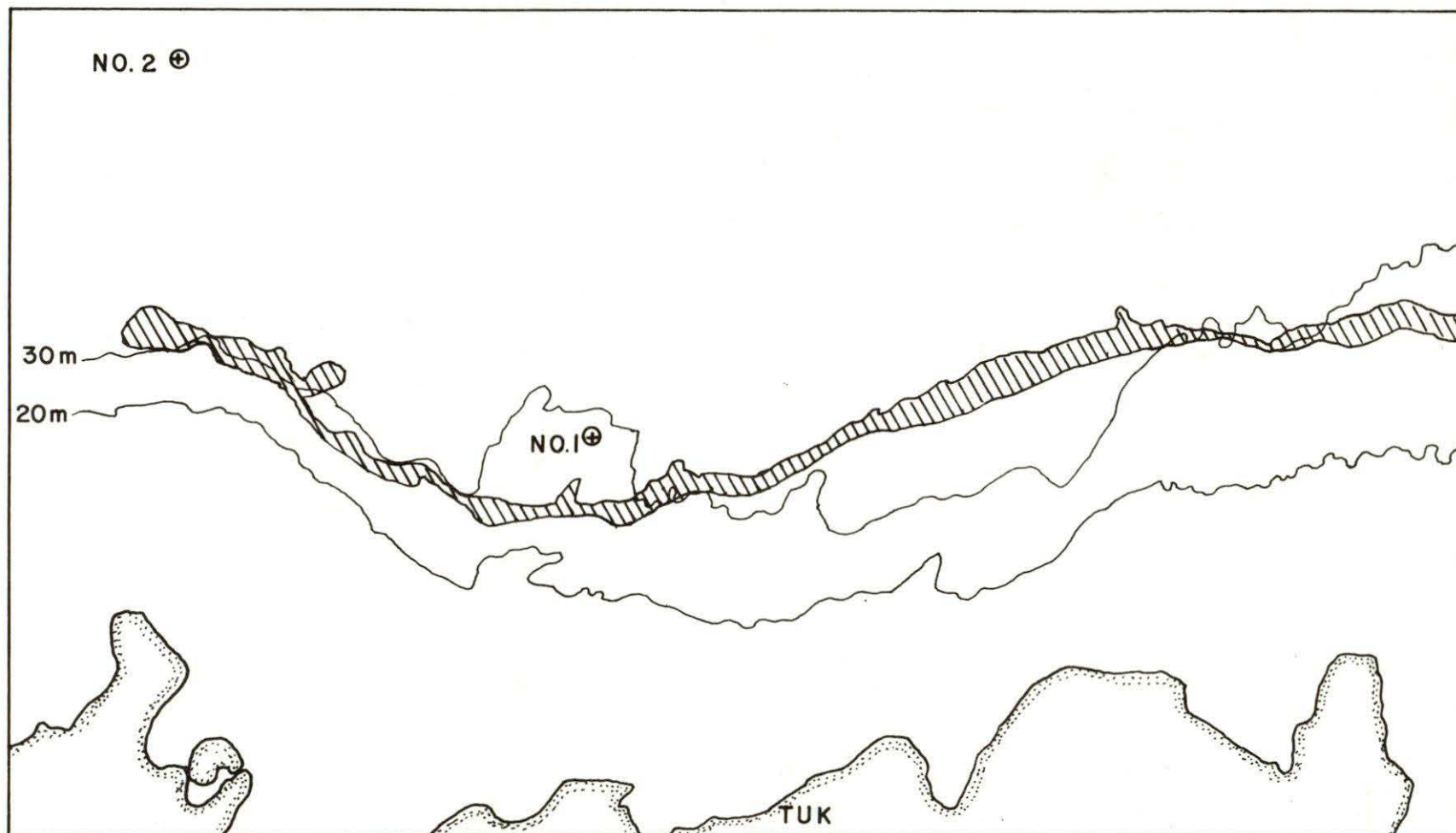
Figure 64.   A sketch of the bottom contours along the Tuktoyaktuk Peninsula
             and the landfast ice boundary lead as seen on a June 15, 1974
             ERTS satellite image.
             The positions of the proposed 1976 oil drilling sites are
             indicated.
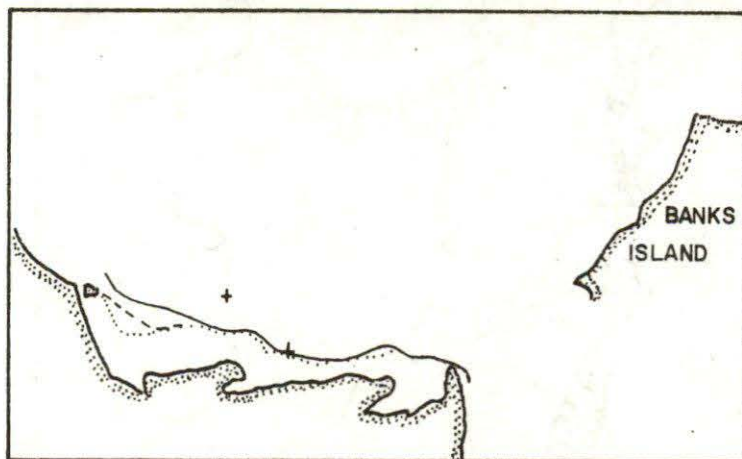
Figure 65.   A sketch of the landfast ice boundary lead in the southeastern
Beaufort Sea on June 29, 1973 ($\cdots$); May 16, 1974 (---) and May
21, 1975 (——).
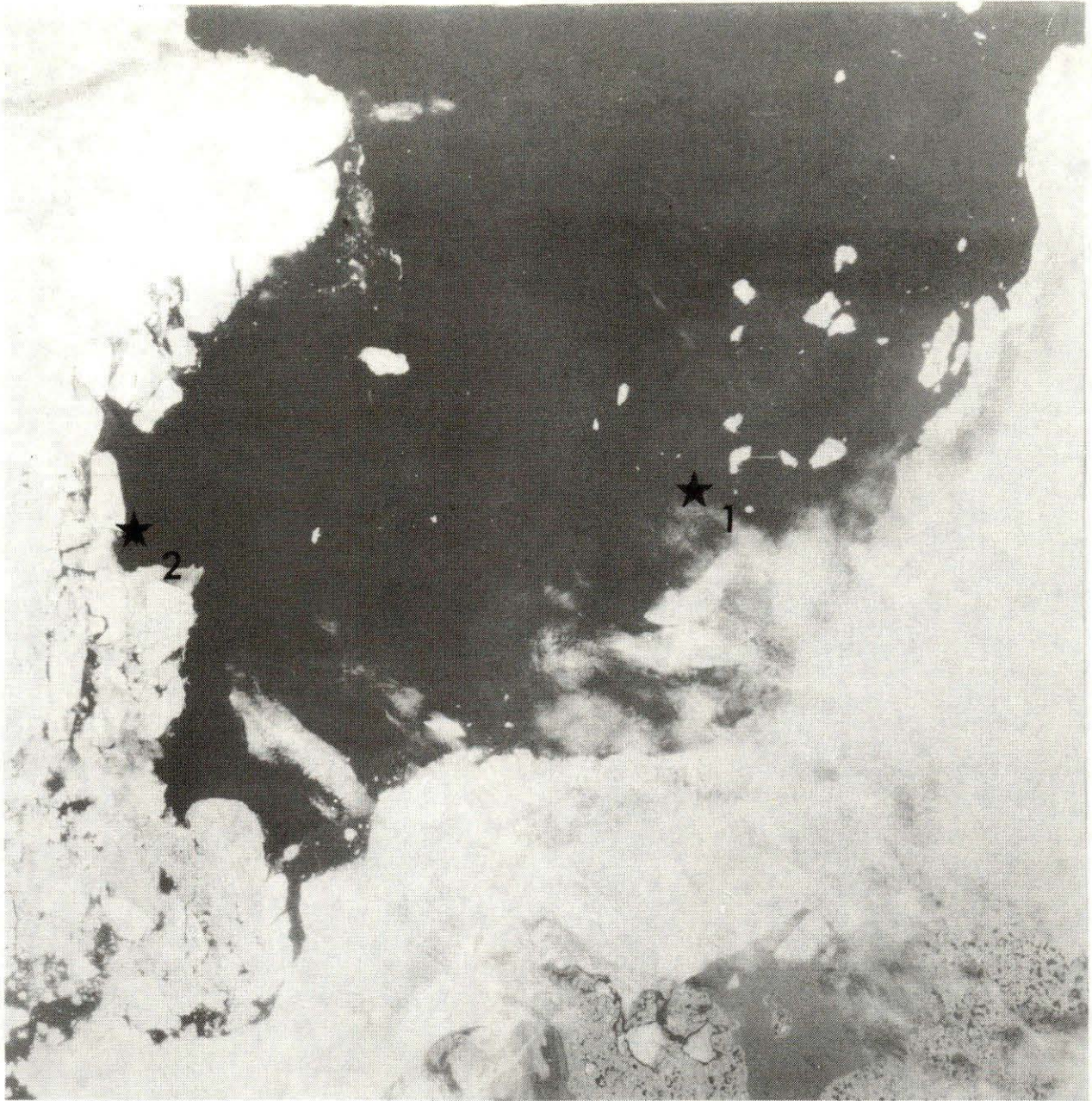
Figure 66. The proposed 1976 drilling sites relative to the landfast ice as seen on a June 20, 1973 ERTS satellite image.
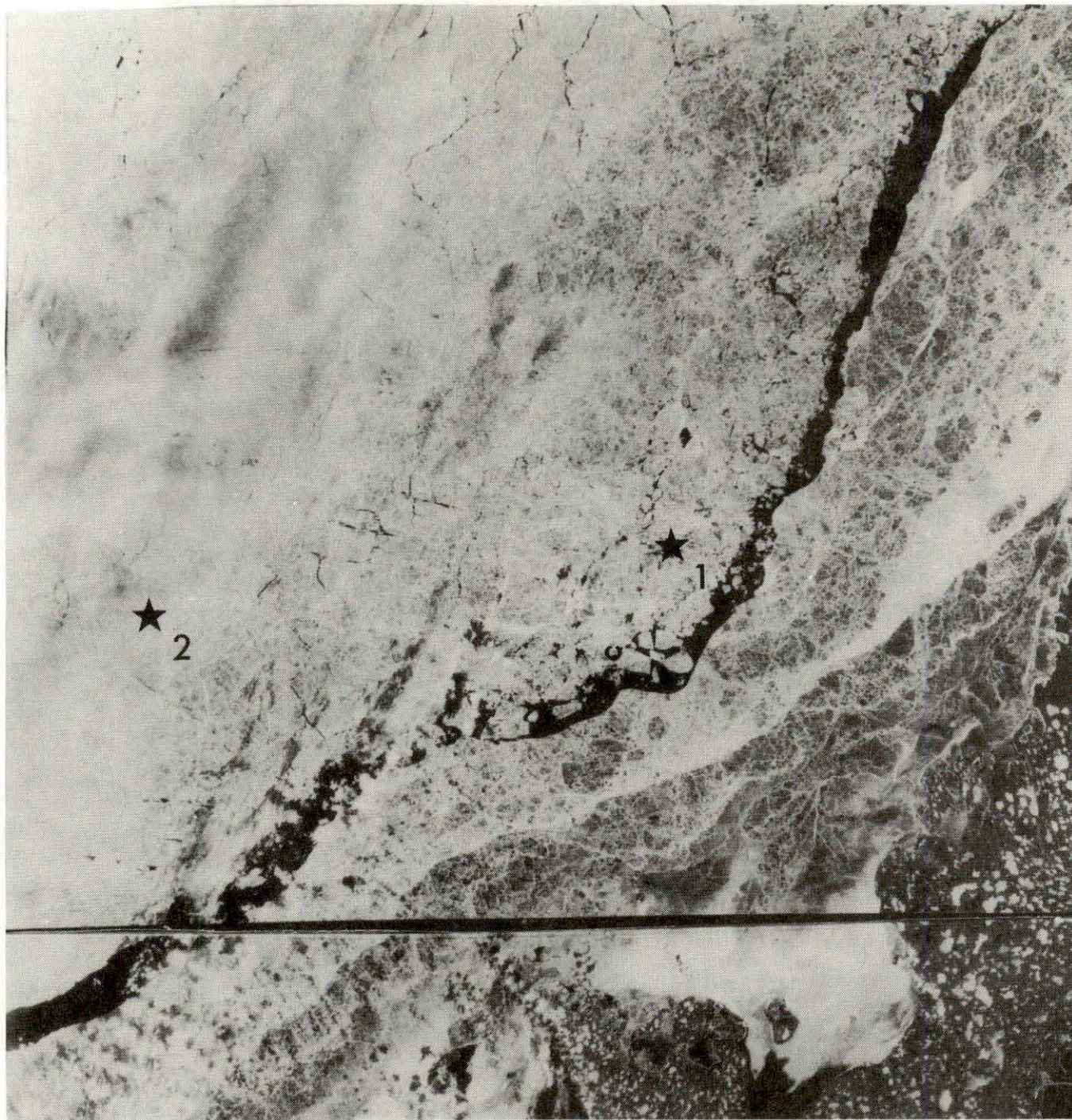
Figure 67.   The proposed 1976 drilling sites relative to the landfast ice as
seen on a June 15, 1974 ERTS satellite image.
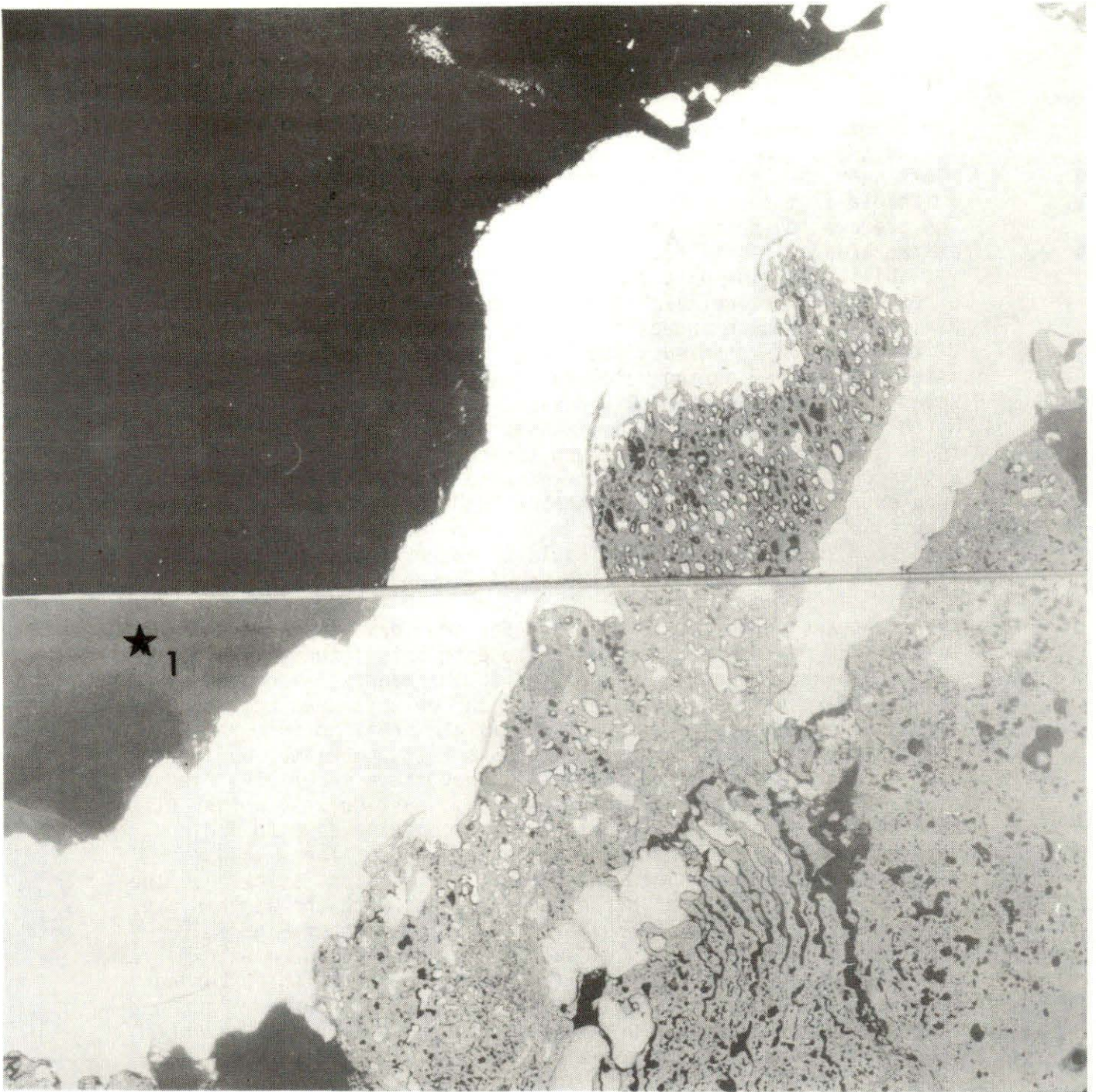
Figure 68.   The proposed 1976 drilling site #1 relative to the landfast ice
as seen in a June 26, 1975 ERTS satellite image.

circumstances guarantee, at least at Site #1, its continuous proximity to the open water of the landfast-ice boundary lead.

Ice displacements over successive intervals of a few days are plotted in the transition zone for a March 1975 period (Figure 69). The movements near the landfast-ice boundary are seen to be generally distinguishable from those which obtain in deep water areas to the north. The average ice drift speed, computed from the net 13-day displacement in the area near Site #2, was 7 kilometres per day. Because of the variability in flow direction, the daily drift speeds were usually in excess of this value. In fact, ERTS measurements made during this period showed these speeds to be greater than 15 km/day on three out of the four days studied. The largest daily drift speeds over this interval occurred during March 26-29 and corresponded to a mean daily speed of 25 km near Point Dalhousie. It is important to note that in March the ice movement in the transition zone north of Richards Island tends westward. It does not turn the corner to drift into Mackenzie Bay which, in fact, remains blocked with landfast-ice until its mid-June break-up (see also the sketched landfast-ice boundaries of Figure 65). As a result, transition zone ice would appear to move down from the Tuktoyaktuk Peninsula to enter the gyral flow somewhere along the eastern wall of the Herschel Canyon.

There appears to be some preference for smaller leads north of the Tuktoyaktuk Peninsula landfast-ice zone to orient themselves northeast-southwest or generally parallel to the landfast-ice boundary lead. The resulting open water leads and polynyi then act as natural pathways for the eastward spring wildlife migrations into the breeding and nurturing areas of Amundsen Gulf. However, any given configuration of leads and polynyi is inevitably short-lived and is usually unrecognizable within a few days. Particularly worthy of note are the open water channels which frequently develop and run perpendicular to the landfast-ice boundary lead. These leads appear to be prominent when the general pack motion "sticks" at the landfast ice boundary and often provide links with the north-south leads of the gyral pack. The March 15, 1975 image of Figure 10 provides excellent examples of such leads whose southern extremities curve eastward. The "knees" at the northern ends of these curved segments fall along the locus of the east-west lead of March 26 (Figure 48) which we have previously designated as the approximate seaward boundary of the transition zone. A close-up view of these "coast-perpendicular" leads is seen in the March 10, 1975 ERTS image of Figure 70. The rapidity of the transition to the orthogonal "coast-parallel" lead arrangement is illustrated in the following day's (March 11, 1975) ERTS image of Figure 71.

Although our observations in April 1975 were partly obscured by cloud and fog, a general slowdown of the ice drift to less than 4 km/day was observed in the transition zone. This result was in accord with the extensive lead refreezing evident in the eastern Beaufort Sea at this time.

As the season progressed through April and into May, continued melting and stress in the shear zone resulted in a much more finely-divided ice pack. Open water and melt-pools were almost evenly
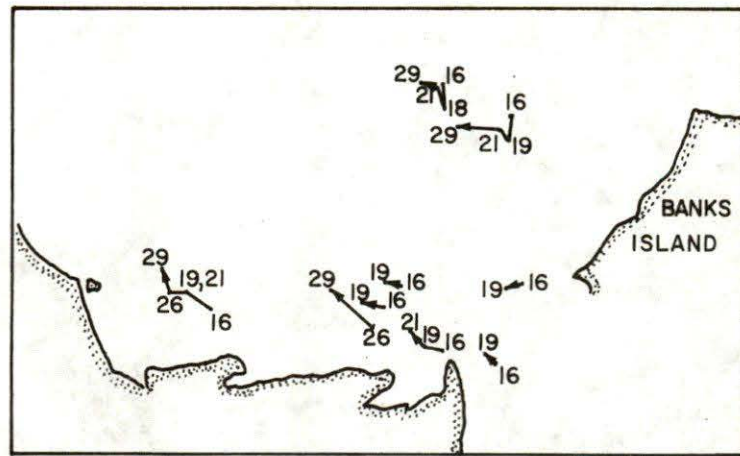
Figure 69.   Daily displacements of ice floes in the southeastern Beaufort Sea for the indicated March, 1975 dates.
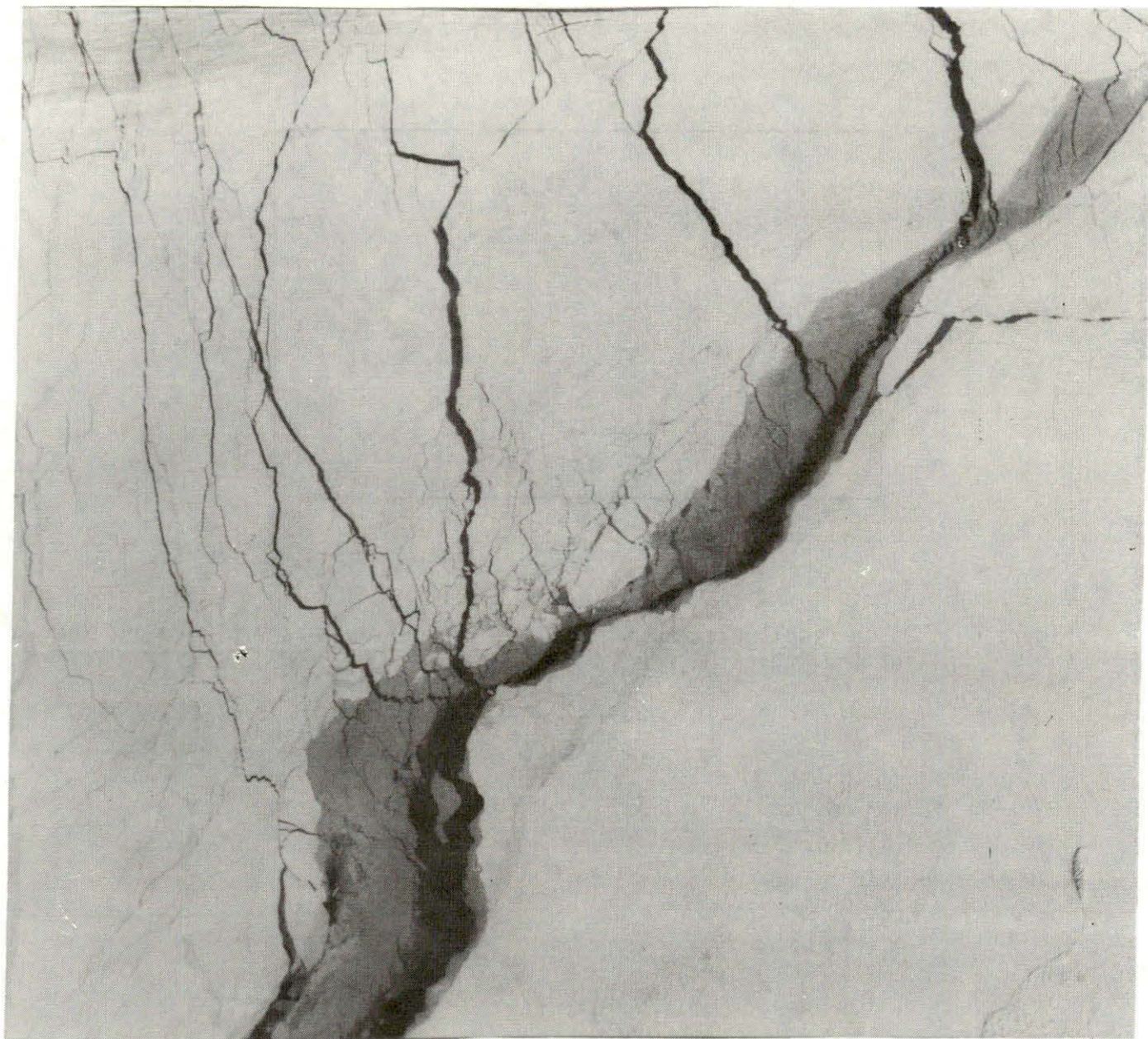
Figure 70. A March 10, 1975 ERTS satellite image of the landfast ice boundary
lead off the coast of the Tuktoyaktuk Peninsula. Other large
leads can be seen extending downward in directions nearly perpen-
dicular to this lead.
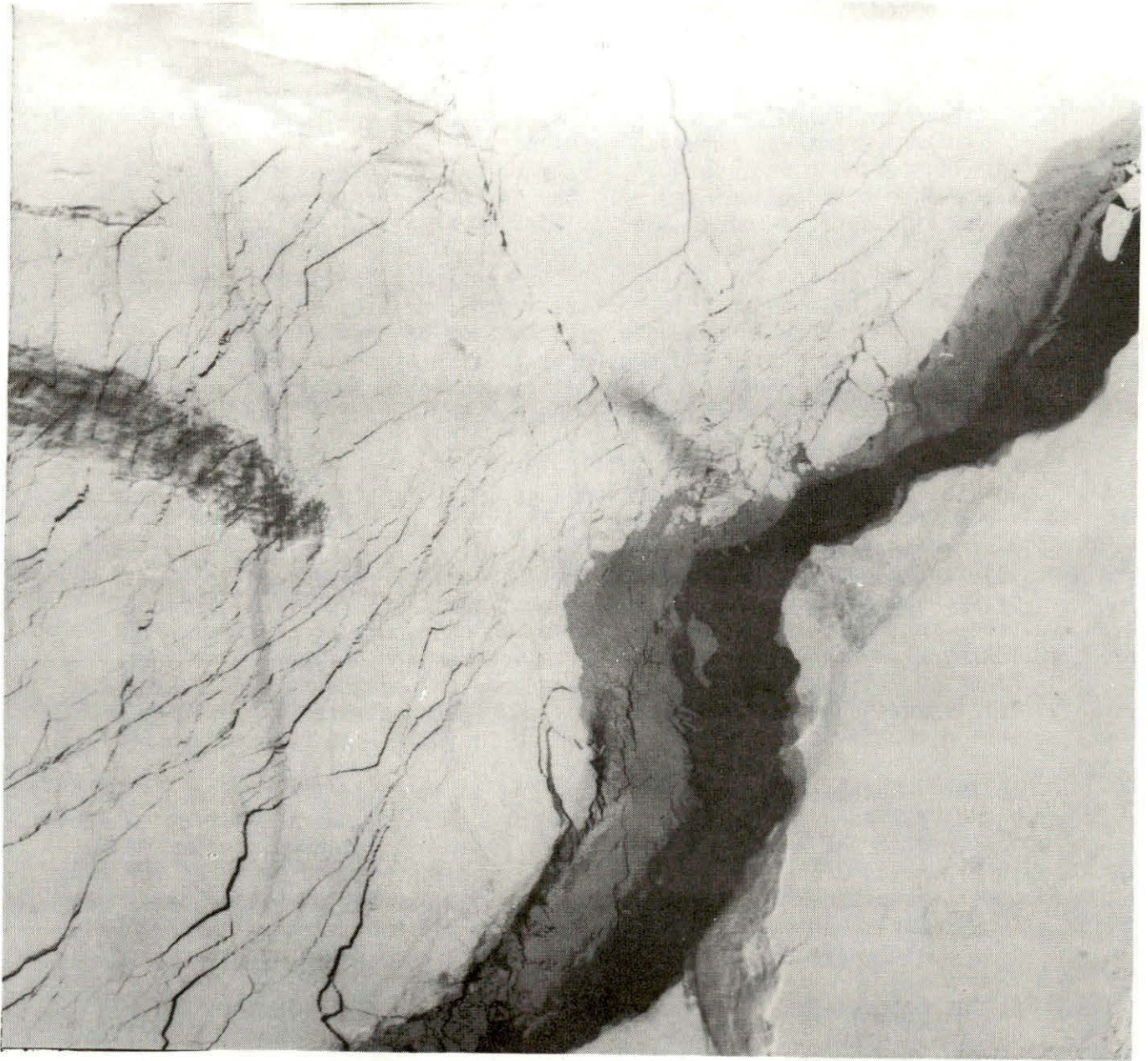
Figure 71. A March 11, 1975 ERTS satellite image of the same landfast ice boundary lead area pictured in Figure 70. The predominant lead orientation seaward of the boundary lead has changed from the perpendicular to the parallel configuration.

distributed throughout the pack and southwestward ice drifts with speeds of 10-15 km/day were common (see the successive-day image pair (May 21-22, 1975) of Figures 72 and 73). NOAA imagery measurements over a wider interval of time (see Figure 74) indicated a net displacement speed greater than 5 km/day and a particularly large (90 km) movement was observed over the May 25-30 period. The continuing tendency for southwestward movement is evident in the displacements sketched in Figure 75 for fixed points in the 10/10 transition zone ice of the June 11-16, 1974 period.

As referred to in Subsection 3.1, the configuration of the May 1974 transition ice zone was distinctive in that development of coast-paralleling leads did not occur at the edge of the landfast-ice. Instead, lead widening and a general fragmentation took place many kilometres further offshore and left a considerable extent of relatively unbroken ice beyond the landfast ice boundary lead (see Figures 8 and 39).

Some evidence of the mid-summer change in the eastern Beaufort Sea ice drift can be seen in Figures 76-78. In these Figures floe displacements have been plotted over intervals in the months of June, July and August of 1973, respectively, for the area immediately west of Amundsen Gulf. It would appear that the usual reversal of flow (from southwestward to northeastward) which occurs along the Tuktoyaktuk Peninsula coincides with a northward deflection of the Amundsen Gulf outflow. On occasion, however, northeastward coastal drifts were observed even in the presence of westward flow in the area directly opposite the entrance to the Gulf (see Figure 79).

In 1974, because of the extreme inshore position of the pack ice boundary, the northeastward late summer drift of individual floes was confined to the narrow coastal zone of open water (shown, for example, in Figure 64). The pack ice itself, even within 40 or 50 km of the coast, maintained an overall southwestward movement over the late August-early September period (see Figure 80) consistent with the 1974 late season movement of ice away from the entrance of Amundsen Gulf.

As indicated in the sketched boundaries of Figures 57-59 the summer and fall ice pack edges are often characterized by prominent extending tongues and eddies of floe ice. These irregularities can be generated by: (1) the rapid passage of local weather systems; (2) the movement of ice into regions of anomalous wind and/or currents; (3) back eddying in areas opposite Mackenzie River outlets and near promontories and islands. The forms of these intrusions in many cases resemble those of the turbid water swirls and tongues of the Mackenzie River plume.

The existence of ice floe intrusions in the region northwest of Kugmallit Bay results in a high probability for dense late summer concentrations of ice at the proposed drilling sites. This circumstance, evident in the plotted boundaries of Figures 57-59, is illustrated by reference to the ERTS imagery of the drilling sites taken at similar late August (mid-drilling season) dates during each of the years 1973-5 (Figures 81-83). As will be discussed in more detail in Section 5, high concentrations of ice can be seen to have

been present on all three occasions.

The daily movements associated with the discussed ice floe features
are illustrated in the August 5 and 6, 1974 images of Figures 84 and
85. These figures display the sudden and rapid movement of the ice
past the western coast of Baillie Island. Comparison of the images
indicates negligible corresponding displacements of the floes which
lie inshore of the 10/10 ice edge. Floes within the dense pack
underwent a uniform 8 km southwestward displacement. The much
larger displacements in the Baillie Island flow thus represent a very
local phenomenon, possibly produced by the anomalously high winds
often found in the area.

A similarly striking but much more consistent organization of the
surface motion was found in the southern end of Mackenzie Bay
(Shallow Bay) and particularly in the vicinity of Herschel Island.
Prominent, rather well-defined streams and eddies were often char-
acteristic of the floe ice and turbid water distributions in this
area. Examples of these are shown in Figures 86-88. The long
converging ice stream in Figure 86 consisted of small floes moving
westward toward a collecting area in the lee of Herschel Island.
This feature may be assumed to be associated with a water convergence
along the common boundary of a westward moving coastal current and
an opposing eastward flow in the waters further offshore and north of
Herschel Island. Both flows are visible in the successive day
(August 15-16, 1975) ERTS image pair of Figures 87 and 88. The
coastal current may be detected by following the westward advance of
the visible turbid water boundary near Kay Point. This boundary has
been observed to move as much as 30 km in a single day. The eastward
counterflow can be deduced by comparing the positions of the large
oval flow which appears in both images. The westward coastal current
past Kay Point is deflected to the north of Herschel Island and may
be the main avenue whereby the low-salinity surface waters of
Mackenzie Bay leave the area of the continental shelf and enter the
deeper region of the Beaufort Sea. This possibility is suggested by
the turbid water pattern of Figure 89 which shows the tremendous
westward extent of the visible plume and indicates a distinct flow
structure northwestward over the Herschel Canyon. The winds
immediately preceding this time were northeasterly, and evidently
drove southward a body of clear, saline water to account for the
darkened north-central plume. These winds would have also slowed
down the river discharge in northern Kugmallit Bay, thereby enhancing
the Shallow Bay flow which dominates the surface turbidity distri-
bution. In spite of the more inshore positions of the ice pack
boundaries, similar turbid water flows in the area off Herschel
Island were observed in July 1973 (see Figures 90 and 91).

The river plume of Figure 89 was the greatest westward extension of
turbid water observed during 1973-5. One might suspect that an even
greater spreading might have occurred at times closer to the roughly
June 1 time of maximum river discharge. However, it was not
possible to confirm this speculation because of the combined
observational obstructions provided by landfast-ice, the central ice
pack, and frequent concentrations of cloud and fog. Observations in
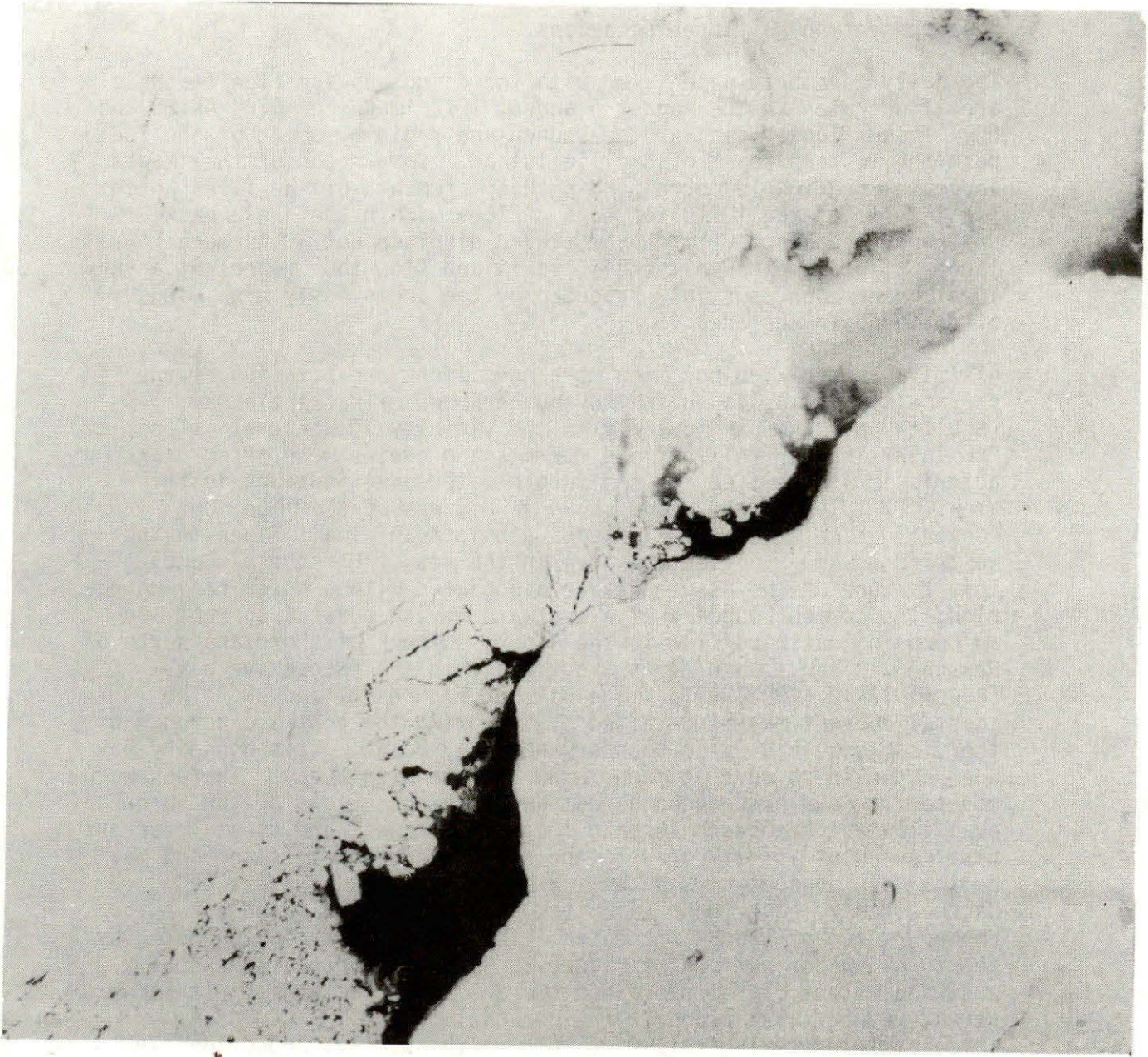
Figure 72.   A May 21, 1975 ERTS satellite image of the same portion of the landfast ice boundary lead pictured in Figure 70.
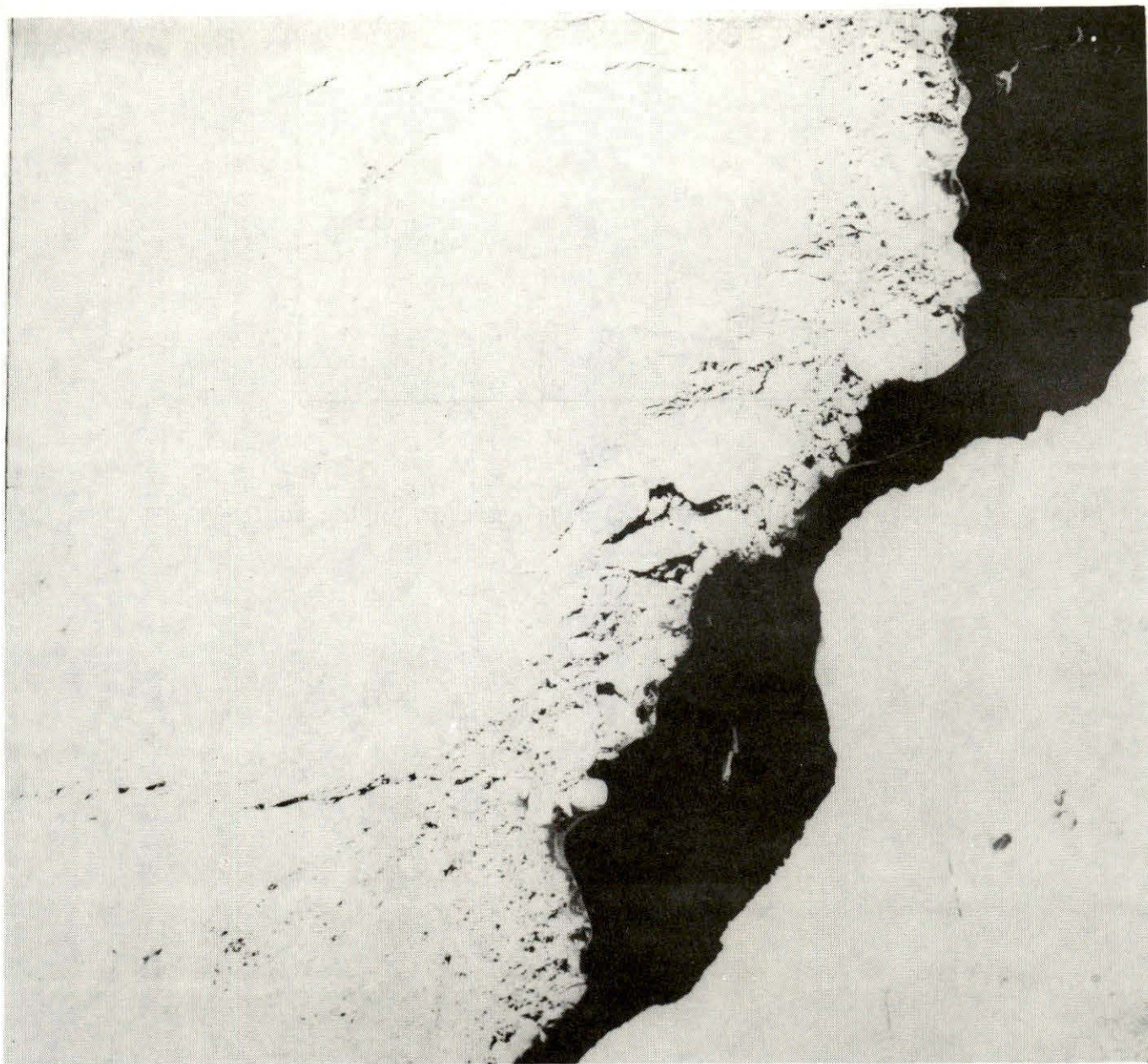
Figure 73. A May 22, 1975 ERTS satellite image of the same portion of the landfast ice boundary lead pictured in Figure 71.
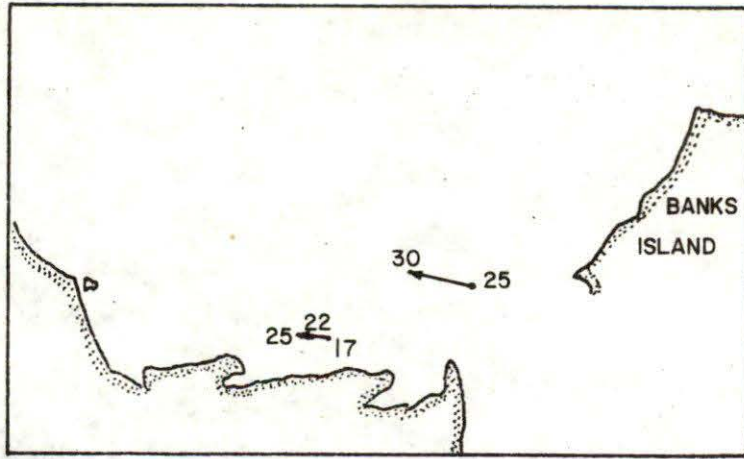
Figure 74.   A sketch of May, 1975 ice displacements in the southeastern
             Beaufort Sea.

16 ◄─────── 14
        15

16 ◄────── 15╱14
                ╲13

                    14
              15 ◄╱╲13

Landfast Ice Boundary

TUKTOYAKTUK   PENINSULA
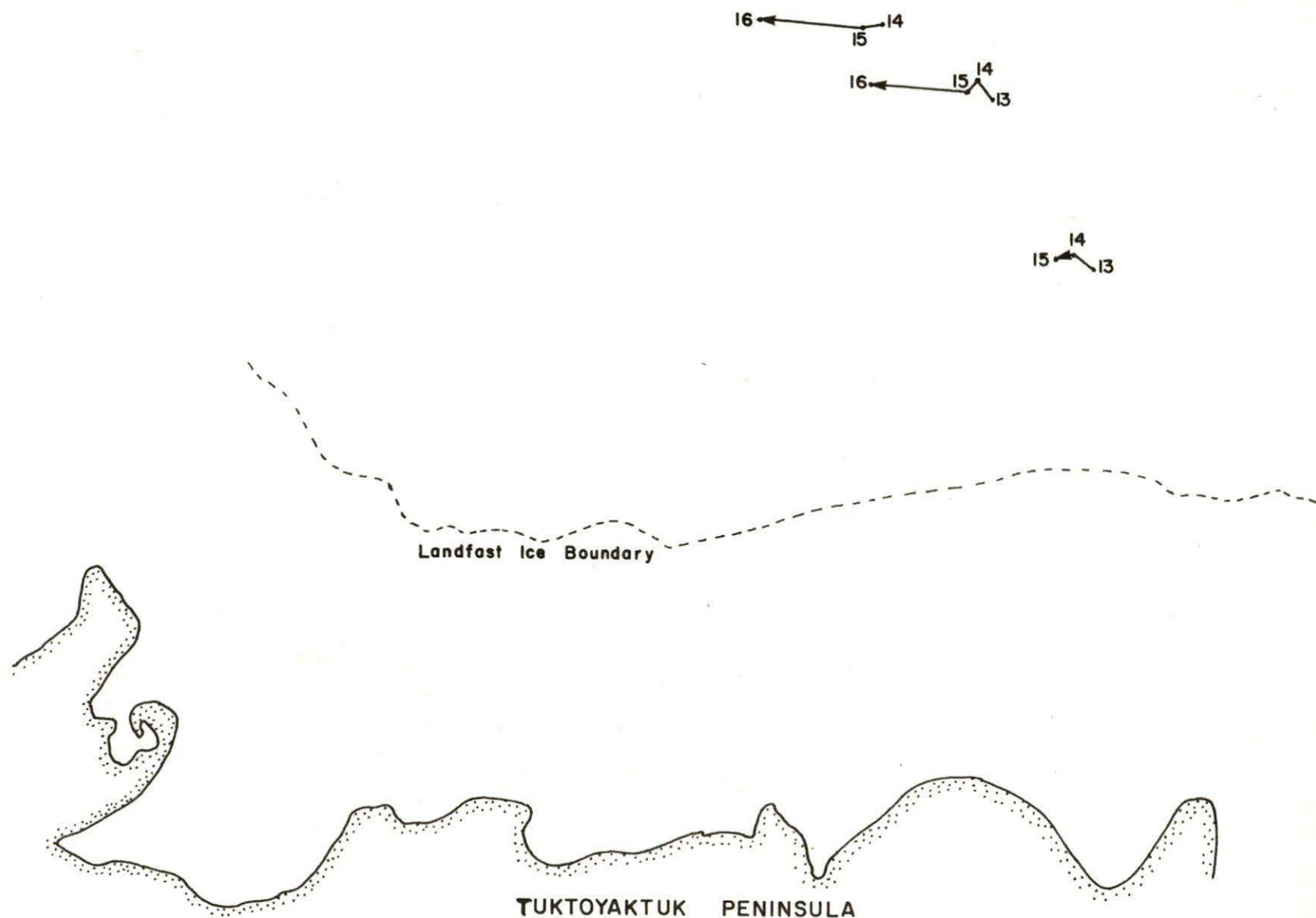
Figure 75.   A plot of ice floe displacements in the pack ice northwest of the
Tuktoyaktuk Peninsula during June 13-16, 1974.
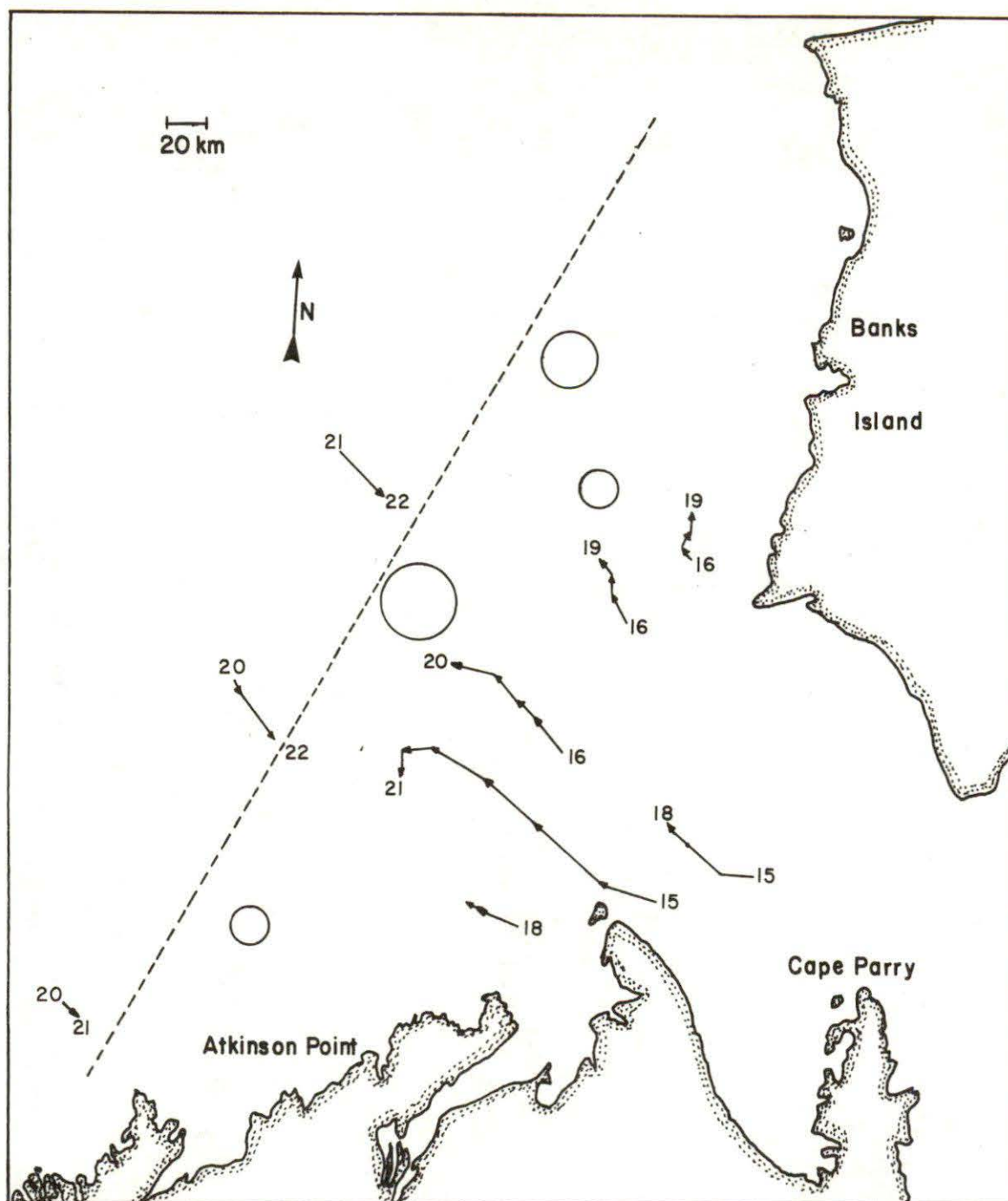
Figure 76. A plot of ice floe positions and displacements in the southeastern
Beaufort Sea on the designated June, 1973 dates. The uncertain-
ties in the position determinations are represented by circles and
the approximate positions of the dense (9/10 to 10/10) central ice
pack are indicated by the broken line.
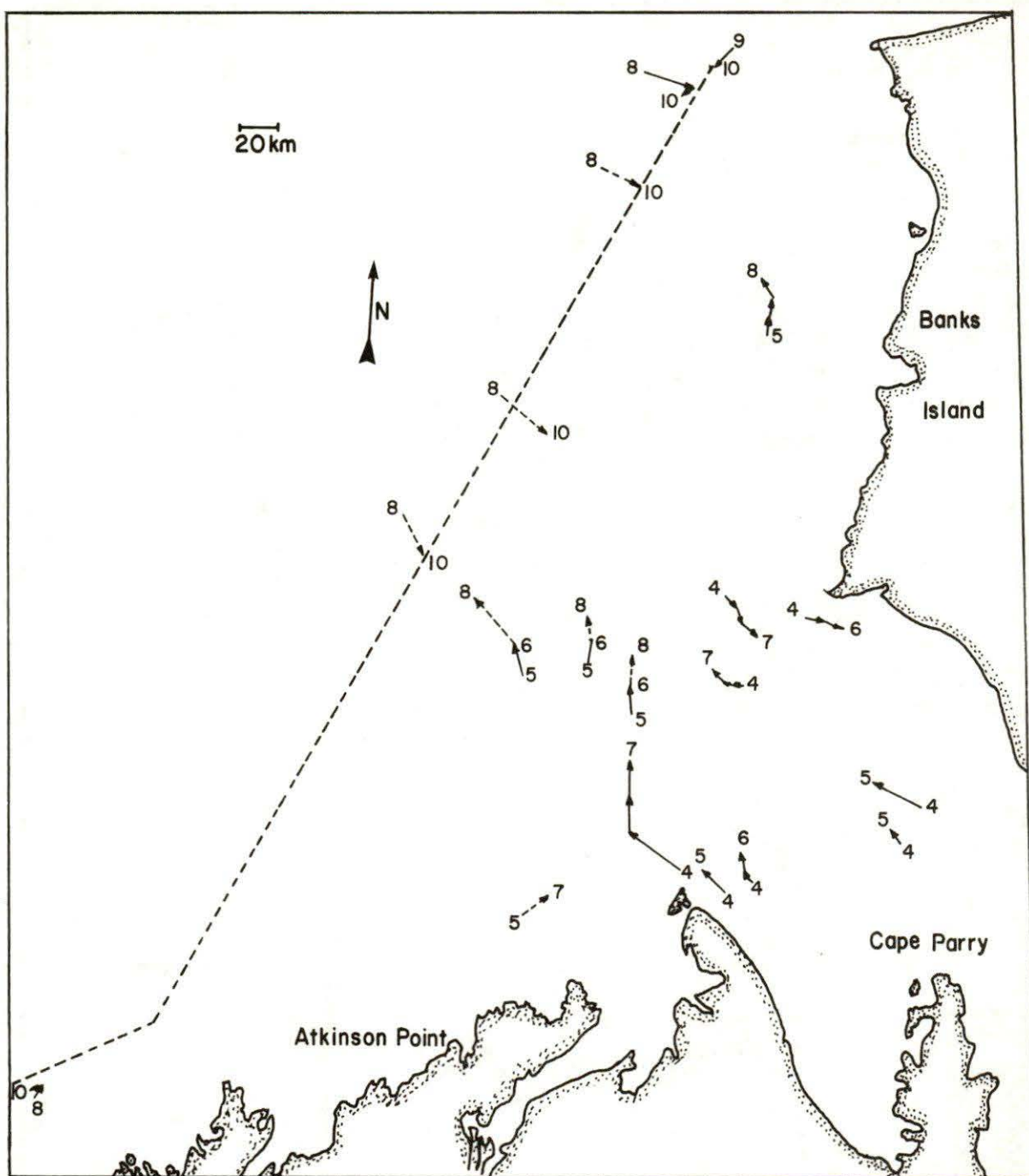
Figure 77. A plot of ice floe positions and displacements in the south-eastern Beaufort Sea on the designated July, 1973 dates.
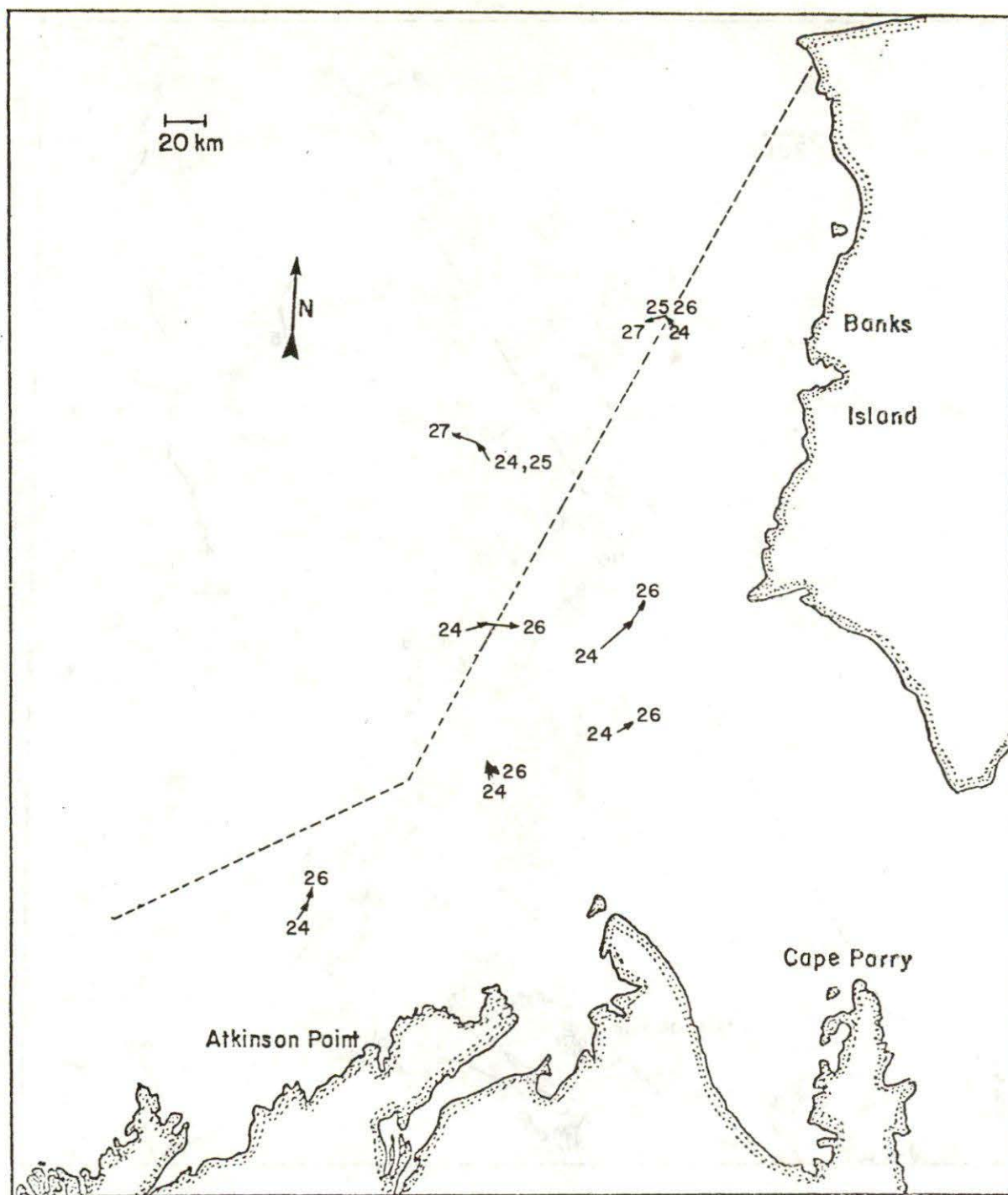
Figure 78. A plot of ice floe positions and displacements in the southeastern Beaufort Sea on the designated August, 1973 dates.
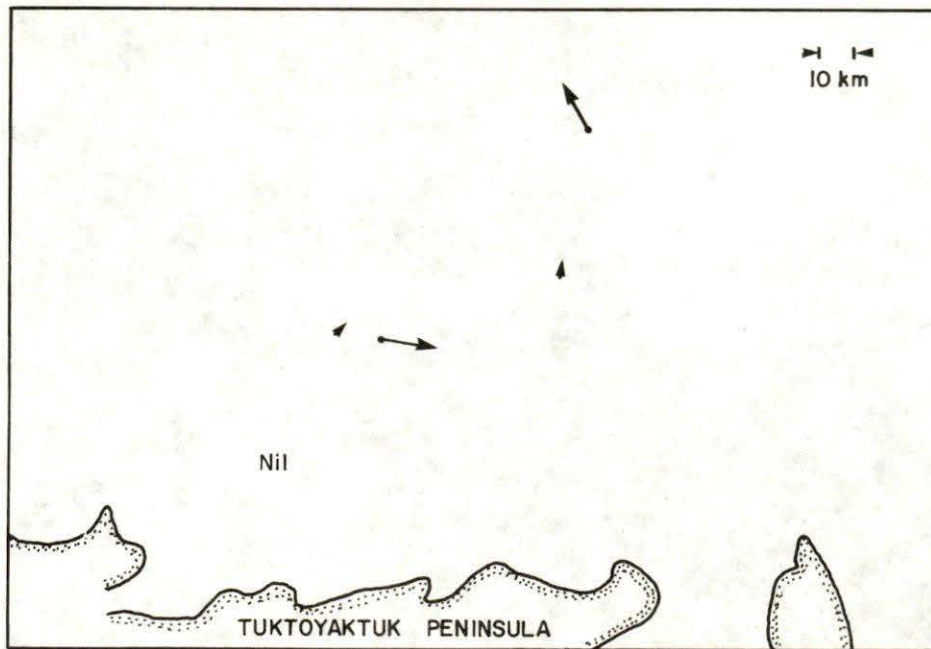
Figure 79. Displacements of isolated floes in the area northwest of the Tuktoyaktuk Peninsula over the August 19-20, 1975 interval.
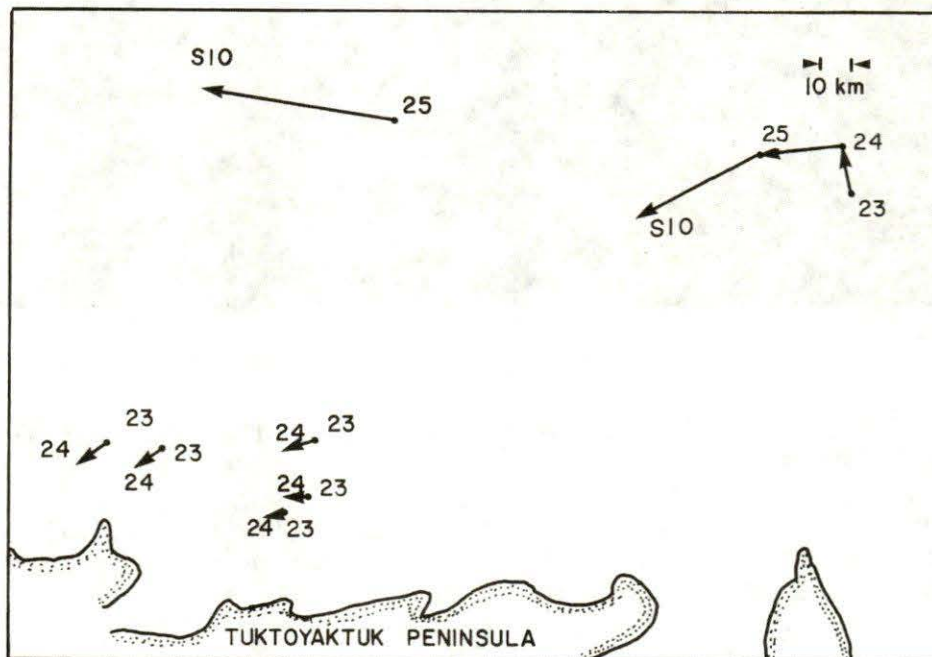
Figure 80. Displacements of recognizable ice floes in the ice pack northwest of the Tuktoyaktuk Peninsula over the August 23, 1974 to September 10, 1974 (denoted by § 10) interval.
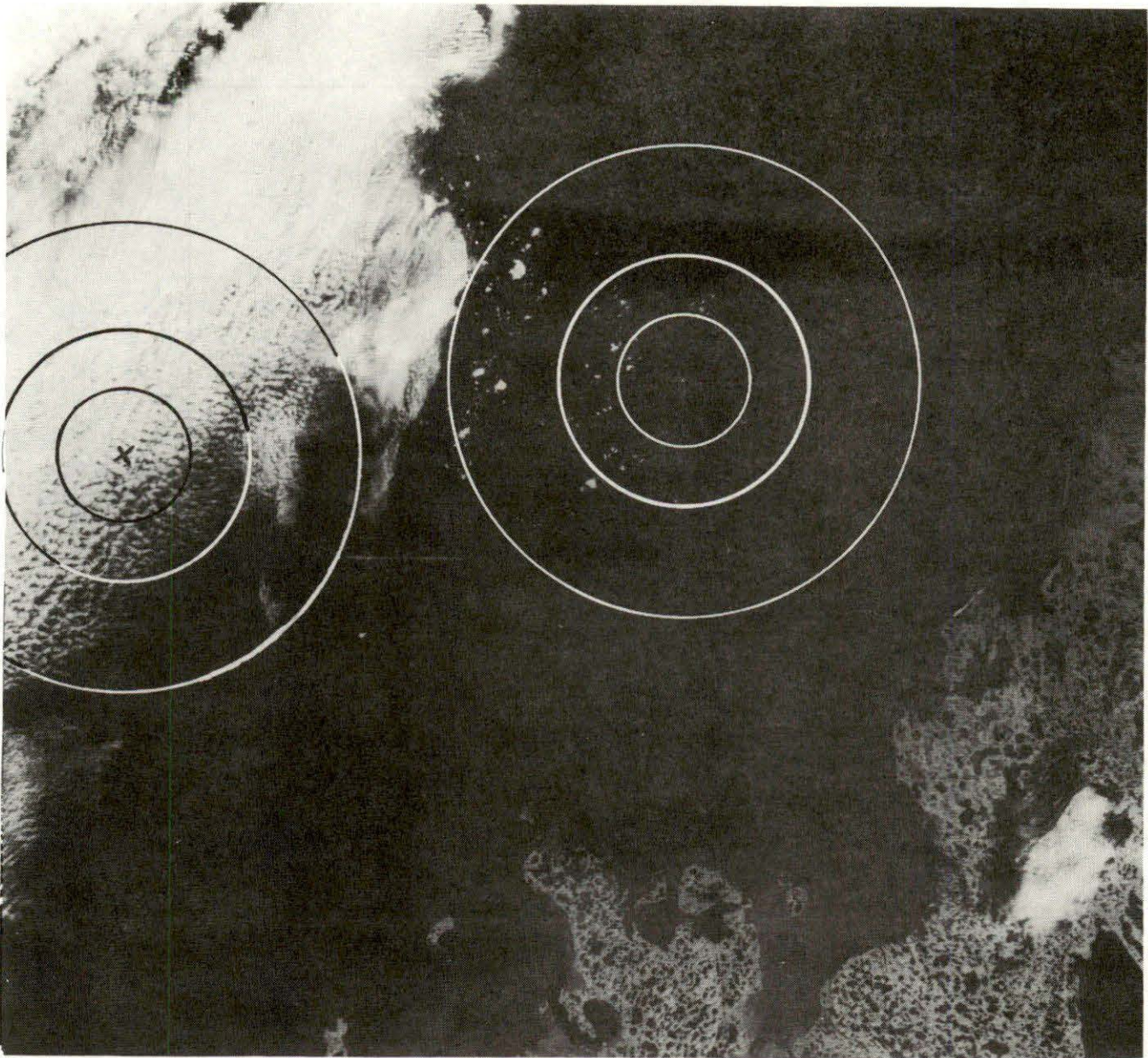
Figure 81.   An August 31, 1973 ERTS satellite image of the proposed 1976
             drilling sites and vicinities. The successive circles of decreas-
             ing radius respectively represent the boundaries of the 24-, 12-
             and 4-hour alert zones under an assumed (36% probability) existence
             of winds in the 10 to 20 knot range according to the procedures set
             out in the Canmar Ltd. safety program.
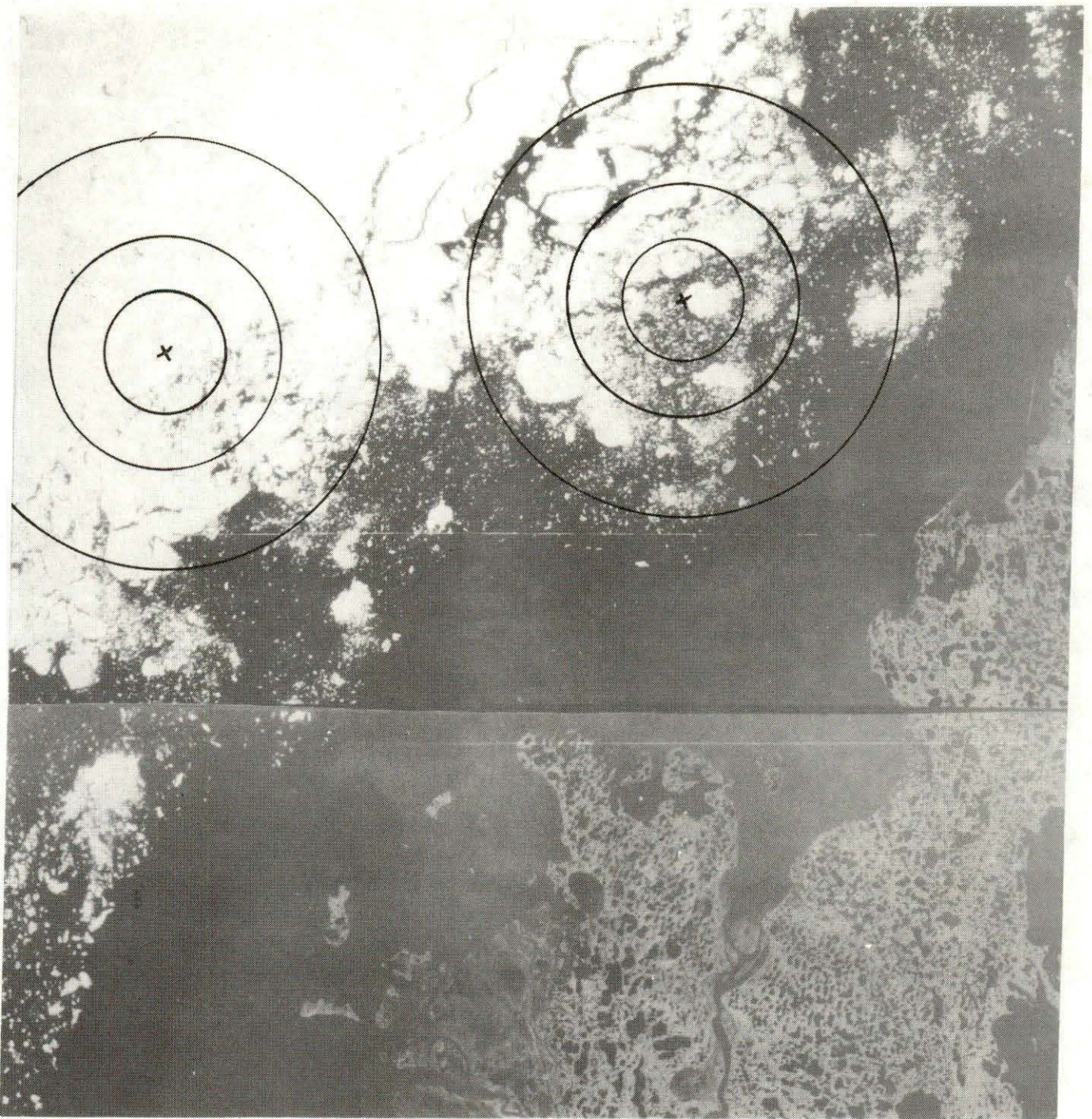
Figure 82. An August 26, 1974 ERTS satellite image of the proposed 1976 drilling sites and vicinities. The 24-, 12- and 4-hour alert circles are again included for the 10-20 knot wind range.
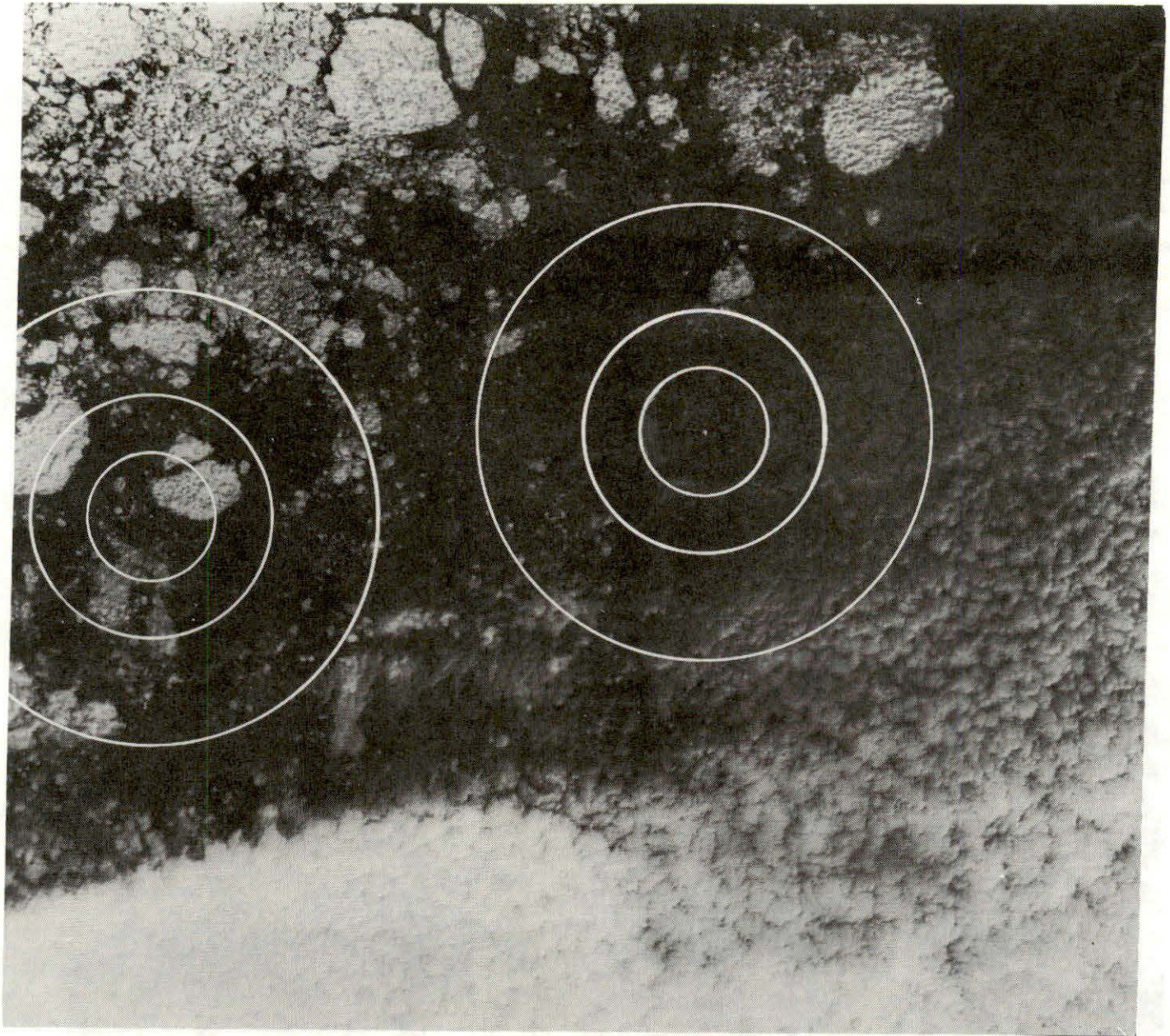
Figure 83. An August 30, 1975 ERTS satellite image of the proposed 1976
drilling sites and vicinities. The 24-, 12- and 4-hour alert
circles are again included for the 10-20 knot wind range.

Figure 84. An August 5, 1974 ERTS satellite image of the Cape Bathurst and
northern Tuktoyaktuk Peninsula region.

Figure 85. An August 6, 1974 ERTS satellite image of the area covered in Figure 84. A comparison of the two images shows little ice movement exclusive of the southward reaching tongue which moves along the western shore of the Baillie Islands (in the upper right-hand corner of the Figure).
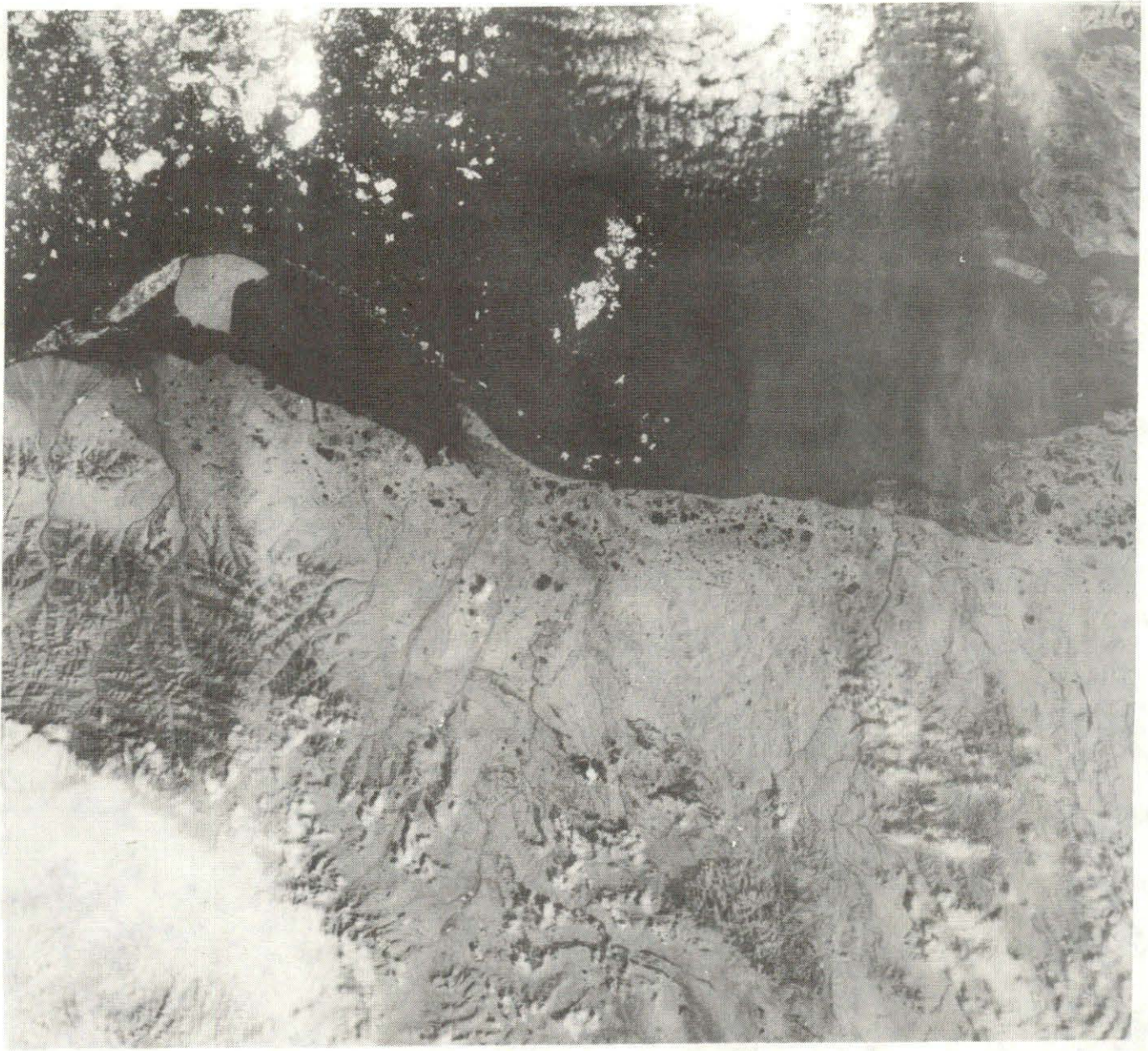
Figure 86. An August 10, 1974 ERTS satellite image of Mackenzie Bay. The westward flowing stream of ice is associated with a surface convergence in the Herschel Island area.

Figure 87. An August 15, 1975 ERTS satellite image of Mackenzie Bay near Herschel Island and Kay Point.
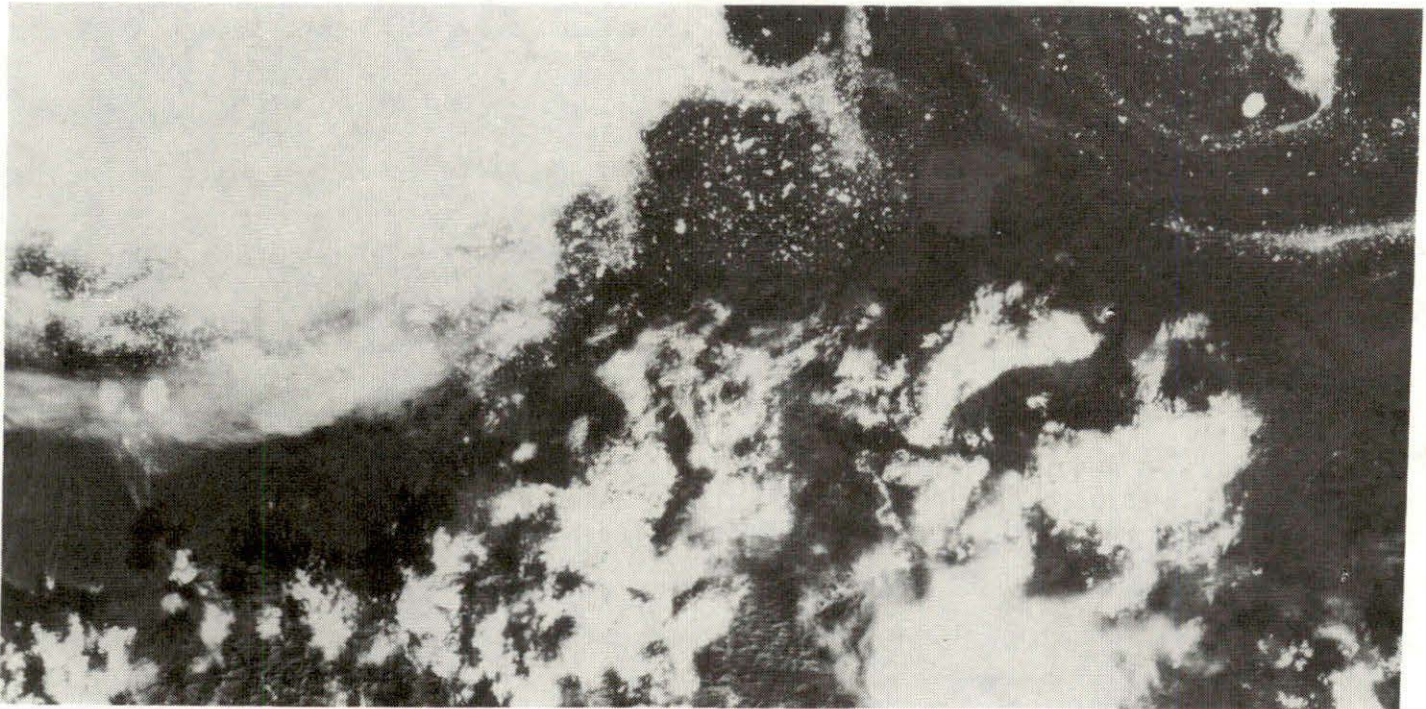
Figure 88. An August 16, 1975 ERTS satellite image of Mackenzie Bay near Herschel Island and Kay Point. A comparison of this image with that of Figure 87 indicates opposing movements in, respectively, the coastal silted water and the more off-shore ice floes.
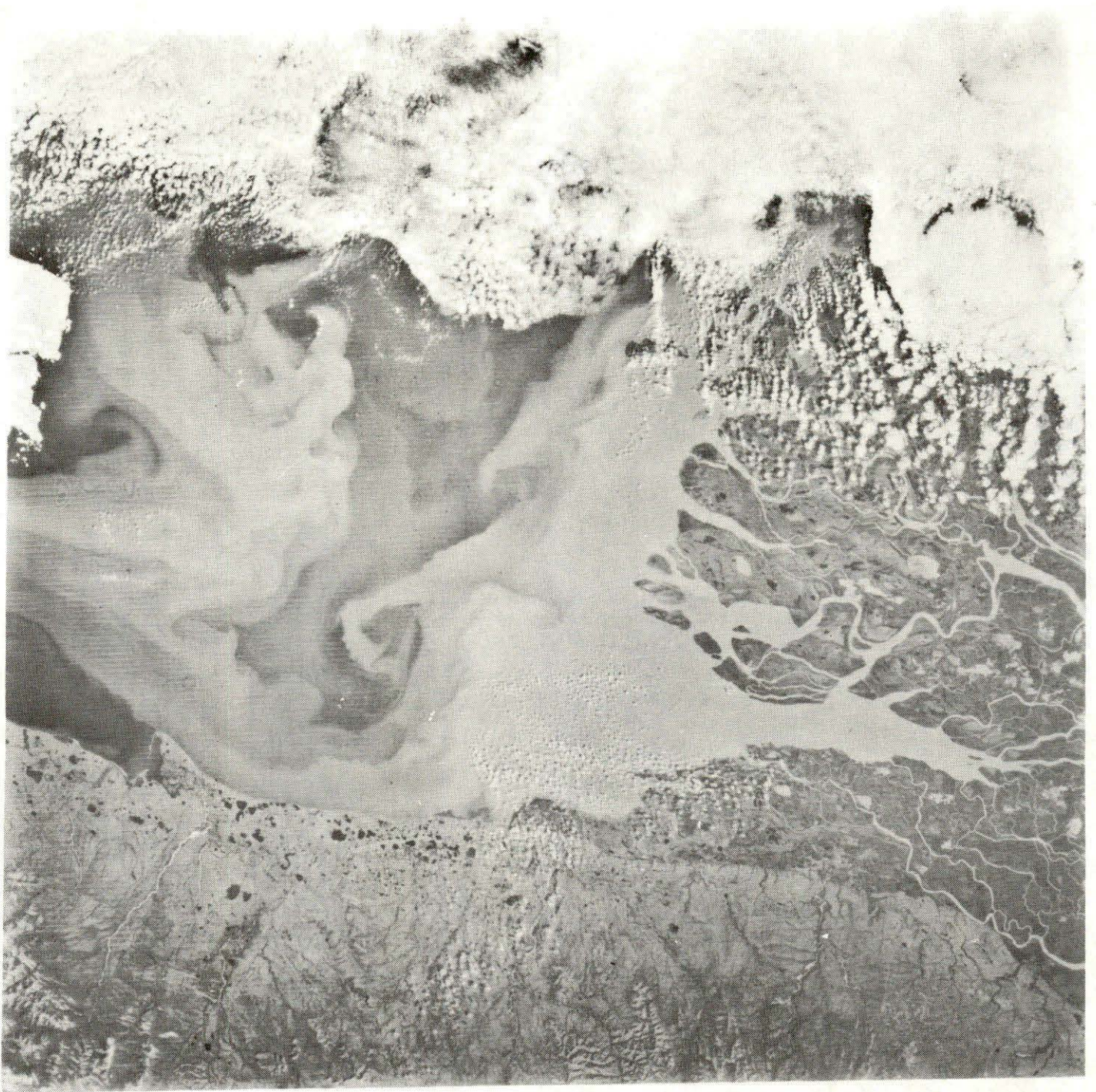
Figure 89. A July 17, 1975 ERTS satellite image of the Mackenzie Bay plume.

Figure 90. A July 10, 1973 ERTS satellite image of the Mackenzie Bay plume.
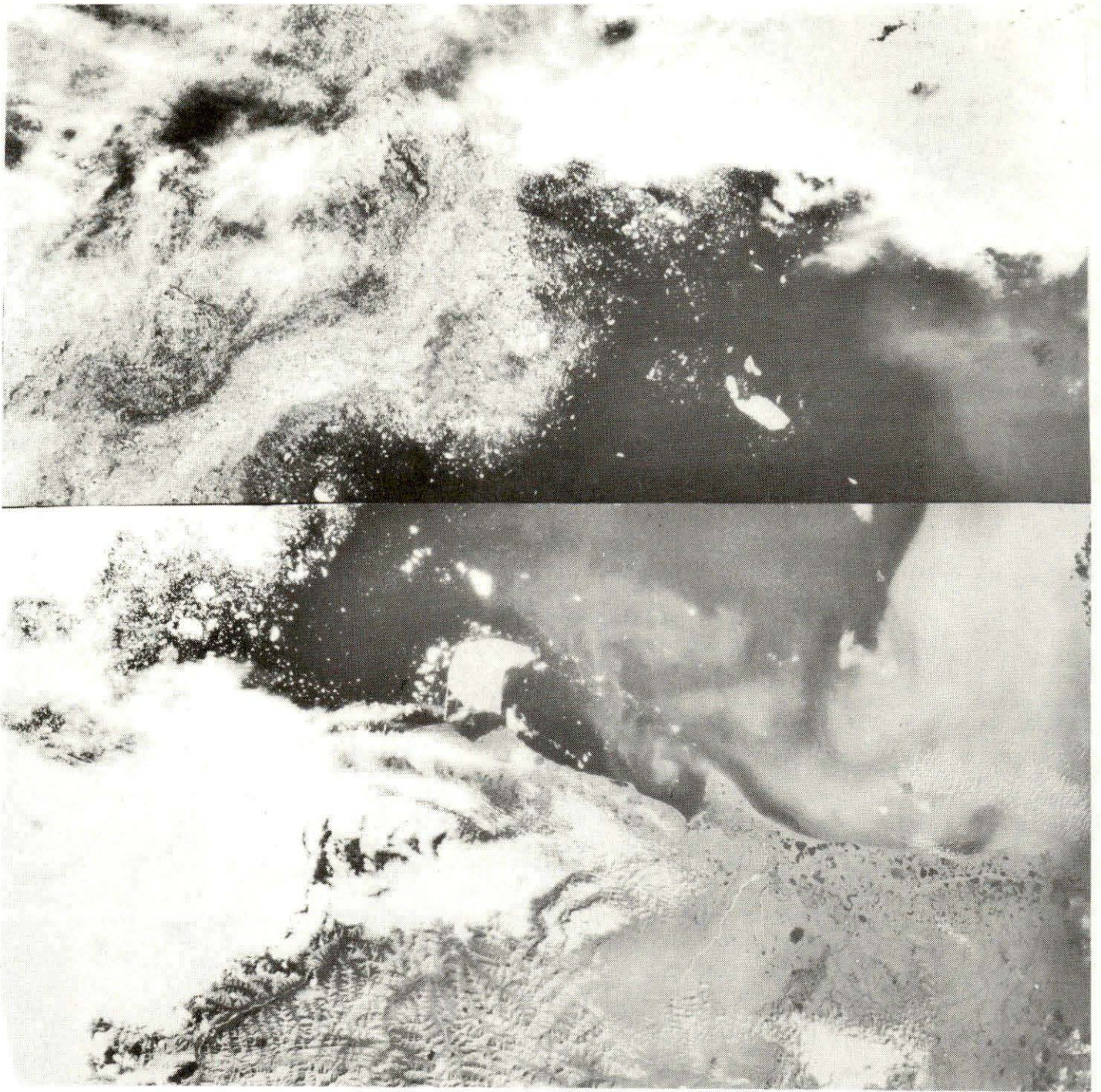
Figure 91. A July 29, 1973 ERTS satellite image of the Mackenzie Bay plume.

the late-summer and early-fall (Figures 92-95) indicated a general reduction in plume size relative to July (compare with Figures 89-91 and 96). There was evidence (Figures 92 and 94) of a continued flow from the main body of the plume outward toward Herschel Canyon. In the September 1, 1973 case (Figure 92) accompanying NOAA imagery shows that the river flow extended to the immediate vicinity of Herschel Island. The absence of a recognizable coastal flow in Figures 92 and 93 seemed to be associated with the presence of south-westerly winds.

A fairly consistent characteristic of the Mackenzie River plume is the presence of large extending eddies and intruding tongues of clear water along its perimeter. These are often seen to be directed to the south and southwest in line with the local flow direction of the neighbouring Beaufort Sea Gyre, and may thus depict lines of contact between coastal and deep water flows. One of the most persistent and far-reaching of these eddies was found north-northwest of Richards Island (see, for example, Figures 93 and 96). The existence of this eddy probably depends upon the Mackenzie River discharge into Kugmallit Bay. The turbid water of this river outlet is usually confined in two more or less distinct flows. The first of these flows westward across the north of Richards Island, while the other moves northeastward along the Tuktoyaktuk Peninsula. Both flows are usually present at any given time with their relative prominence being determined by preceding and contemporary wind conditions. Typical configurations in this area may be seen in Figures 95, 97 and 98.

Even in the absence of freshwater confinement by ice such as occurred in 1974, the turbid water can extend northward for hundreds of kilometres during the mid- to late summer months. An example of such flow near the northern end of the Tuktoyaktuk Peninsula is seen in the July 15, 1975 image of Figure 99. The distinctive small eddies seen in this image have cores of clear, saline water which drift northeastward with the prevailing late summer surface flow.

An examination was made of reflected light intensities in each of the four ERTS wavelength bands over the Shallow Bay sector of Mackenzie Bay. Analysis of the magnetic-tape recorded digital data indicates that the locus of maximum reflected light intensity is displaced to the eastward with increasing wavelength. As indicated by the mapping in Figure 100, the respective ridges of maximum intensity merge again and remain together in the areas north of 69°30'N. It is possible that this effect may be linked to variations in the local surface concentration of chlorophyll, which has a high infrared brightness. However, an equally likely, if less useful, possibility is that the observed behaviour arises from the simultaneous presence of light reflections from silt and optically thin cloud. The re-flected levels of infrared light change very little with variations in silt concentration relative to the known concentration sensitivity of the shorter wavelength reflections. As noted by Gower and Daniel (1974) this wavelength dependence is much weaker in the case of light reflected from thin cloud. It is easy to visualize cases where the non-coincidence of the locii of maximum cloud thickness and silt

Figure 92. A September 1, 1973 ERTS satellite image of the plume in Mackenzie Bay.

Figure 93.   A September 18, 1973 ERTS satellite image of the plume in
Mackenzie and Kugmallit Bays.

Figure 94.   An August 13, 1975 ERTS satellite image of the plume in Mackenzie and Kugmallit Bays.
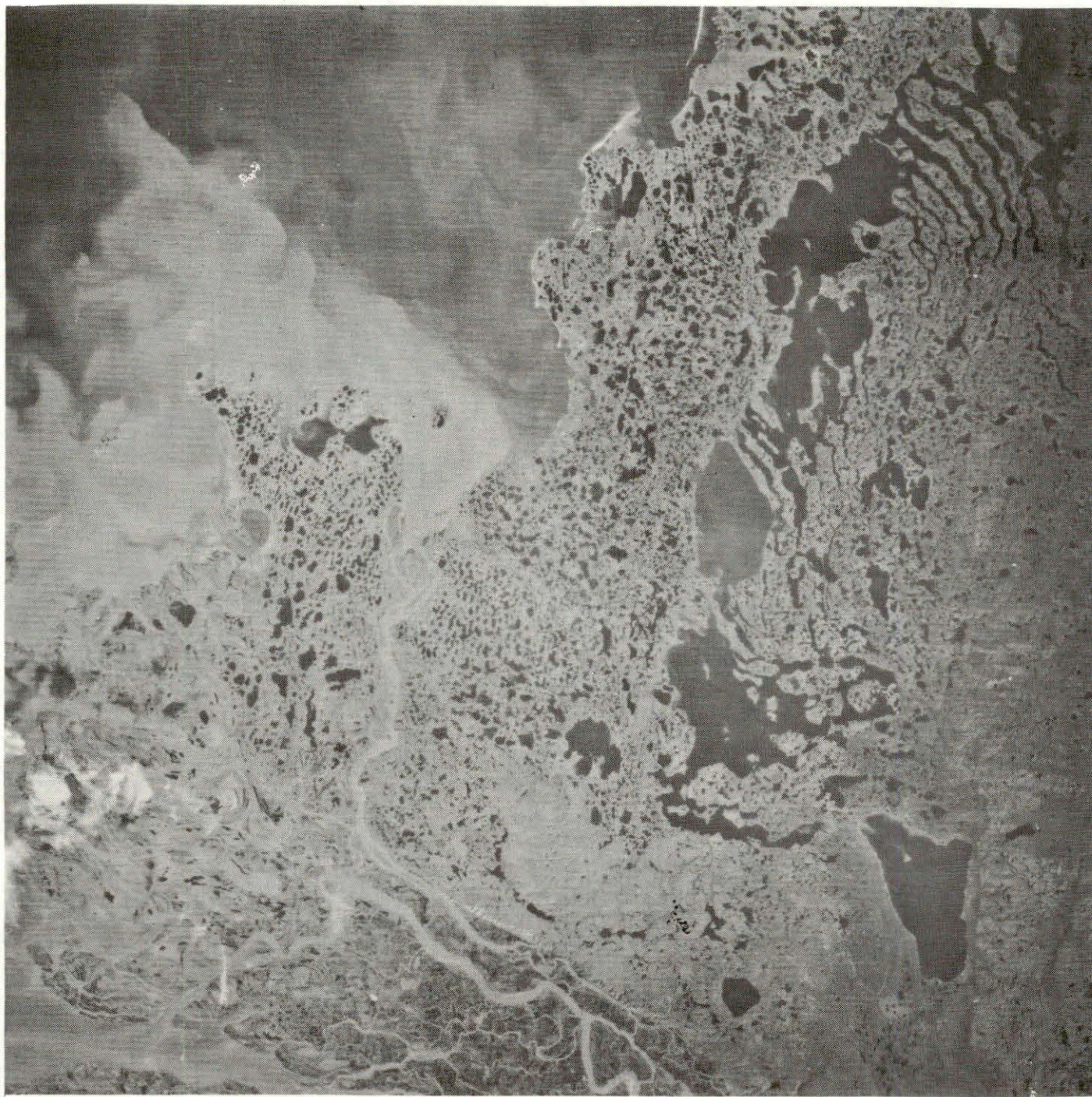
Figure 95.   A September 17, 1973 ERTS satellite image of the plume in
Kugmallit and northern Mackenzie Bays.

Figure 96.   A July 26, 1973 ERTS satellite image of the plume in Mackenzie and Kugmallit Bays.

114
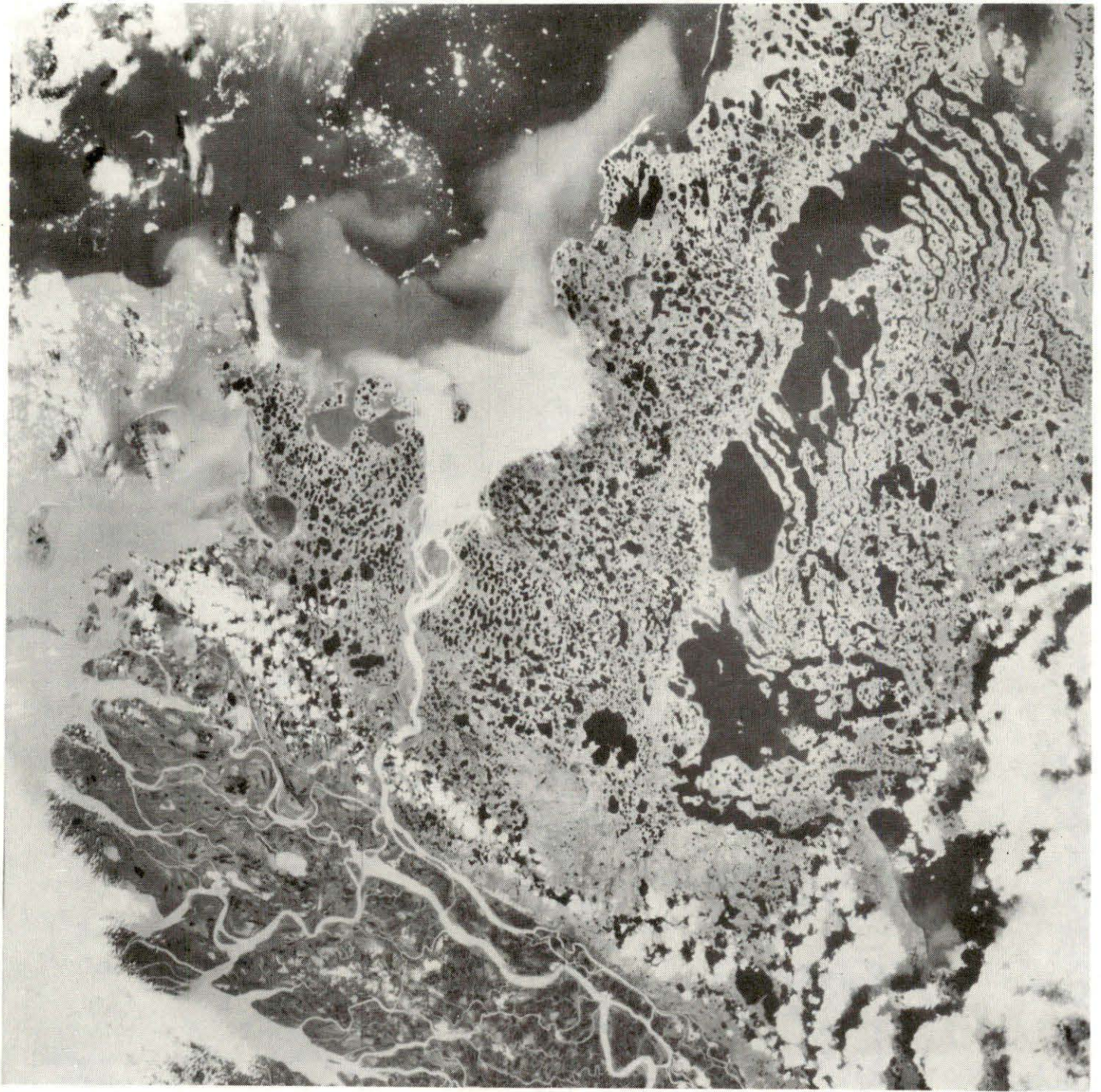
Figure 97. A July 7, 1973 ERTS satellite image of the plume in Kugmallit Bay.
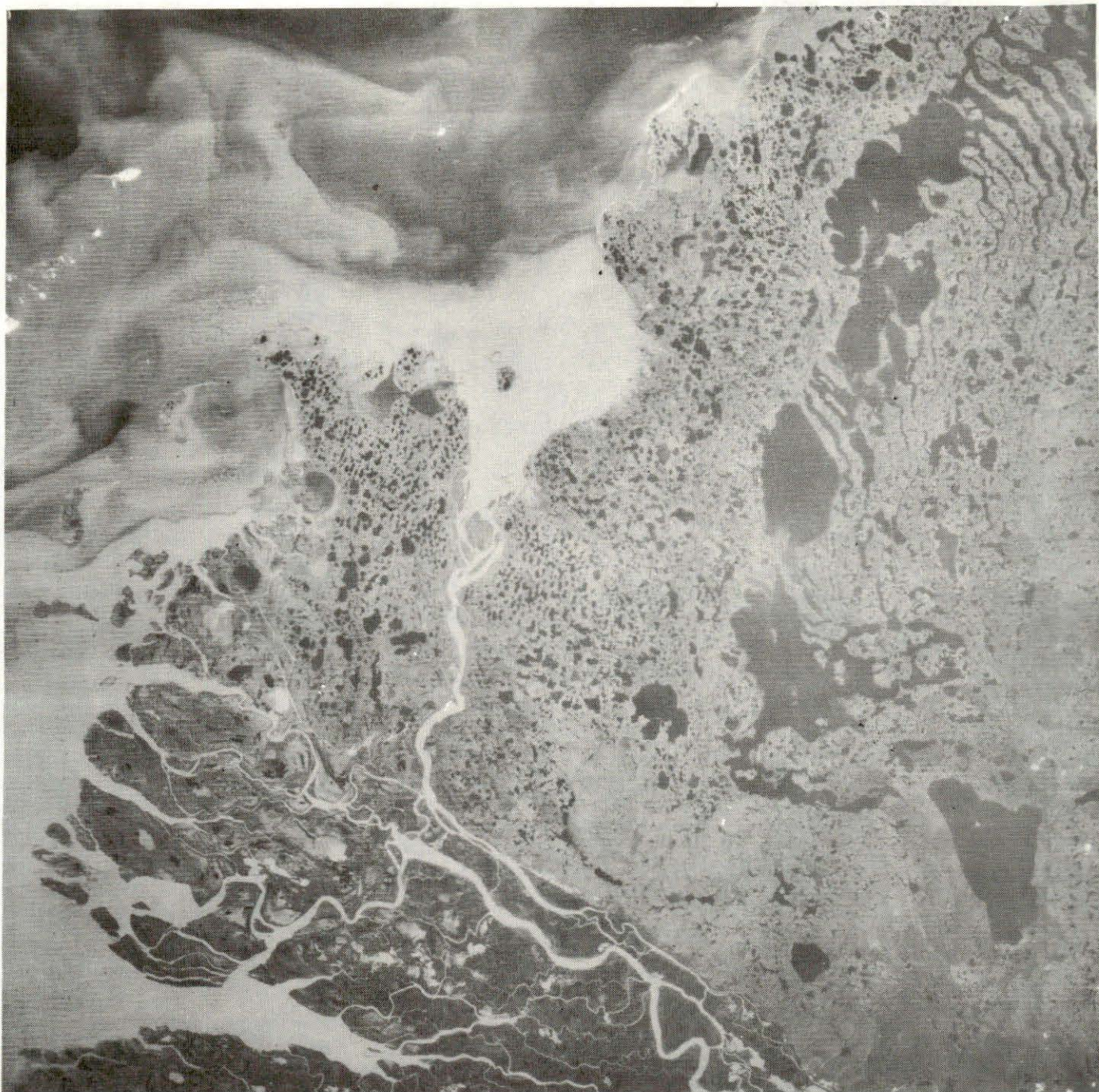
Figure 98.   A July 15, 1975 ERTS satellite image of the plume in Kugmallit Bay.

Figure 99.   A July 15, 1975 ERTS satellite image of silted water eddies off-
shore of the Tuktoyaktuk Peninsula.
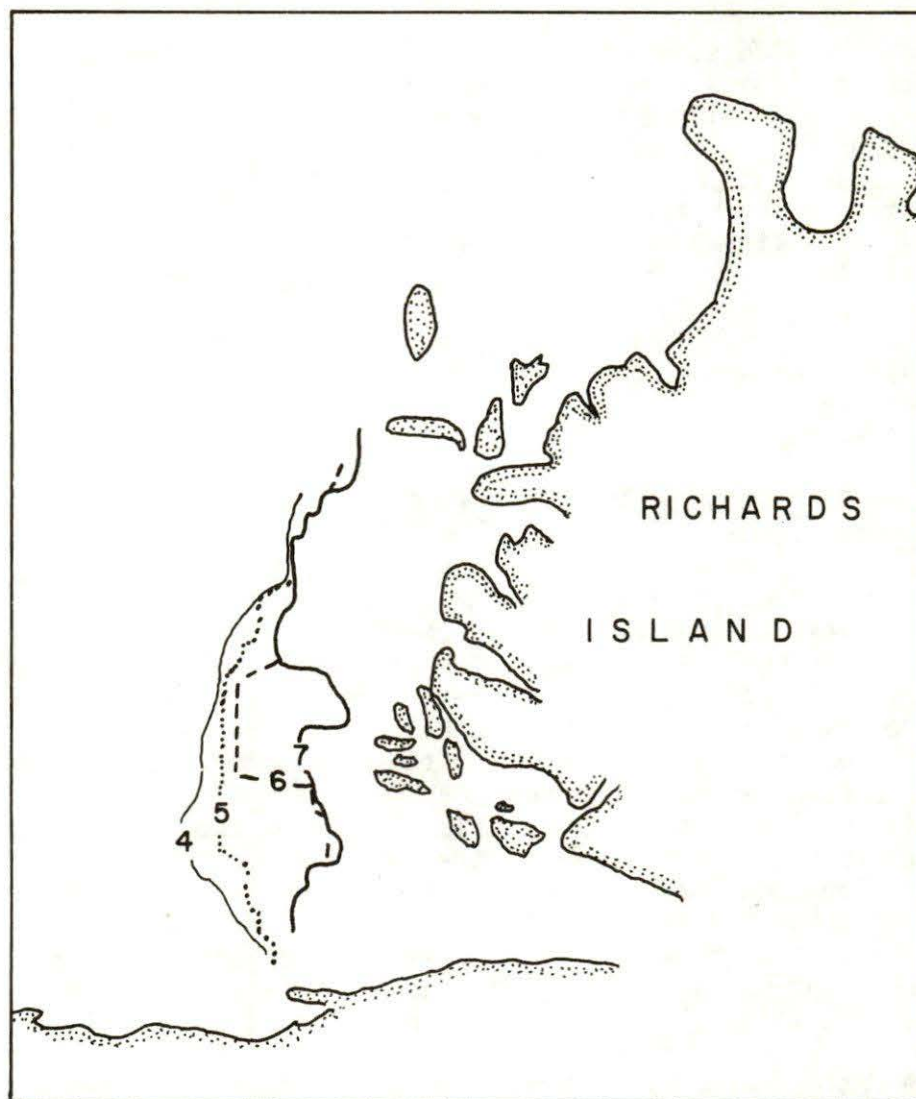
Figure 100. The loci of the maximum reflected light levels for bands 4, 5, 6 and 7 in Mackenzie Bay.

concentration produces a similar shift in positions of the maximum long and short wavelength light intensities.

Quantitative studies of the Mackenzie River plume, using digitally recorded brightness data, are presently greatly inhibited by the complexities associated with intervening cloud and fog formations. Progress on this problem clearly requires satellite-based studies of the various cloud and fog configurations. In this respect, it is relevant to note that line printer representations (see Figures 101 and 102) of "sliced" reflected light data (the measured absolute light levels for groups of 48 adjoining sampled ground points or "pixels" are broken down into ten categories) often show similarly shaped areas of maximum intensity which seem to be correlated with the presence of a characteristic bank of light cloud or fog in Mackenzie Bay.

5. CONCLUSIONS, RELEVANCE TO ENVIRONMENTAL PROTECTION AND RECOMMENDATIONS FOR FUTURE STUDY

The observations and data presented in this report deal with only a small fraction of the information contained in the three year compilation of satellite imagery. Emphasis has been given to observations of ice and surface waters while other aspects of the environment have largely been ignored. Some of these neglected phenomena such as the characteristic bank of light cloud over Mackenzie Bay or the mid-summer cloud concentrations over open water may, however, play critical roles in the environmental dynamics. Thus, for example, if oil on the sea, through its ability to retard evaporation, reduces the optical thickness of adjoining formations of cloud and fog, additional solar heating of the water would occur with a consequent disturbance of the natural energy balance. An environmental threat of this type could arise from chronic oil leakage or spillage which might maintain a pervasive surface film. A review of relevant data on this possibility is given by Walker (1976).

Detailed observations were taken over a period which included two summers (1973 and 1975) during which the Beaufort Sea was dominated by a vast open water area extending across its southeastern corner from McClure Strait on the north to Herschel Island on the west. The summer of the middle year, 1974, was characterized by a much smaller area of ice-free, low salinity water. The confinement of the Mackenzie River water by ice and its eventual release in September toward and across Amundsen Gulf resulted in an infusion of fresh water into the eastern Beaufort Sea which differed considerably from the steady, less localized mixing of the two "open" years. In spite of these differences, certain common elements of the annual ice-cover and surface water behaviour were identified and will be summarized below prior to discussion of their implications for future modelling programs, pollutant transport and future research work.

5.1 Ice Pack Characterization

The boundaries and characteristic seasonal motions of the three generic ice zones are represented in Figure 103. The landfast zone

ICE

RICHARDS IS.

SHALLOW BAY

●TENT IS.

●SHINGLE PT.
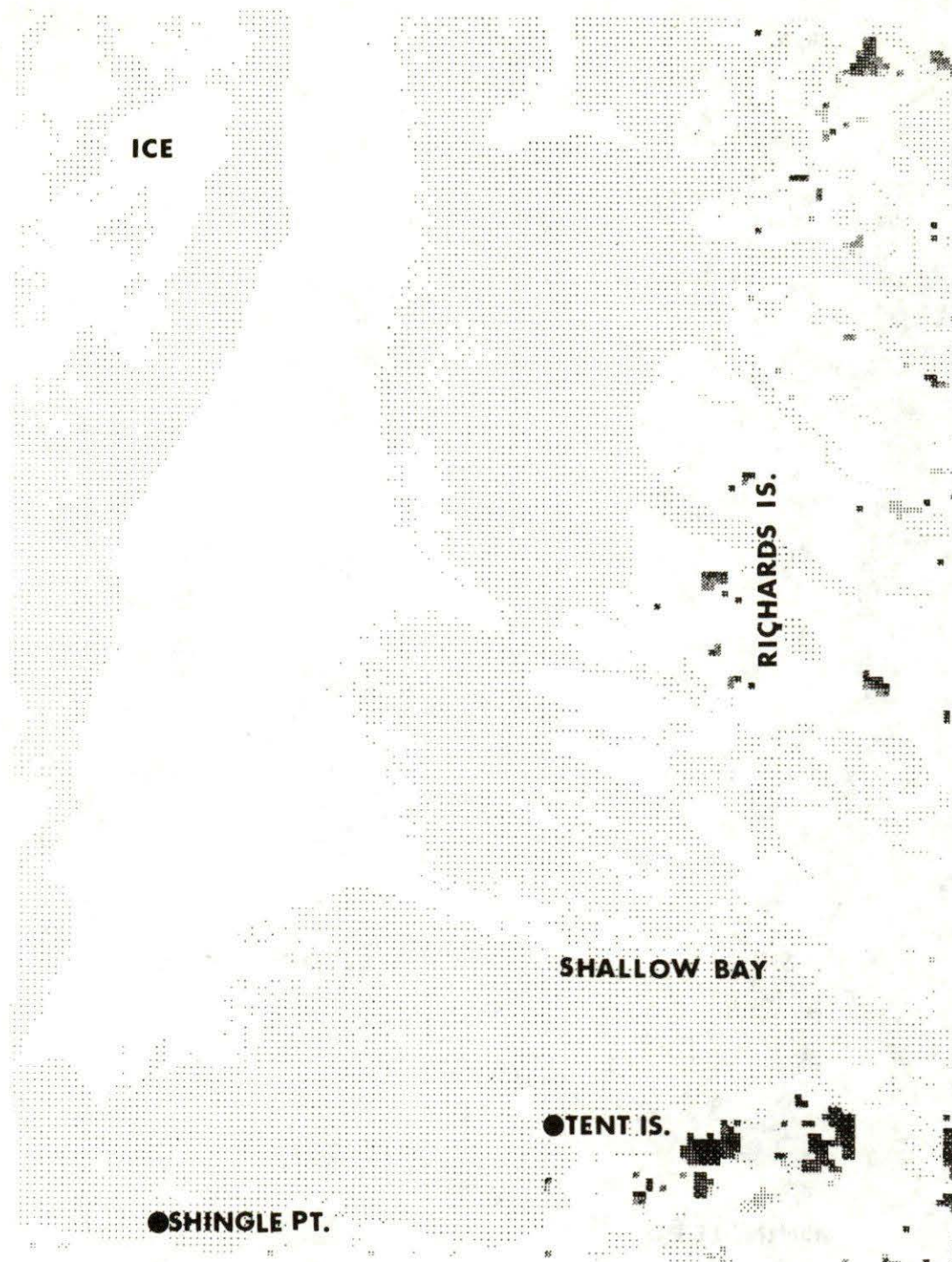
Figure 101. A line printer representation of the reflected light levels observed on July 10, 1973 in band 5 of the ERTS satellite system over Mackenzie Bay. At each point (representing an average over a group of 48 actual "pixels" or individual surface readings) a grey-level ranging from zero to 16 dots has been printer accordingly as the light level varies from its highest to its lowest values respectively. A distinctively shaped region of highest intensity (ranging upwards from $\approx$ 20% of the highest recordable level) is seen in the eastern end of Mackenzie Bay.
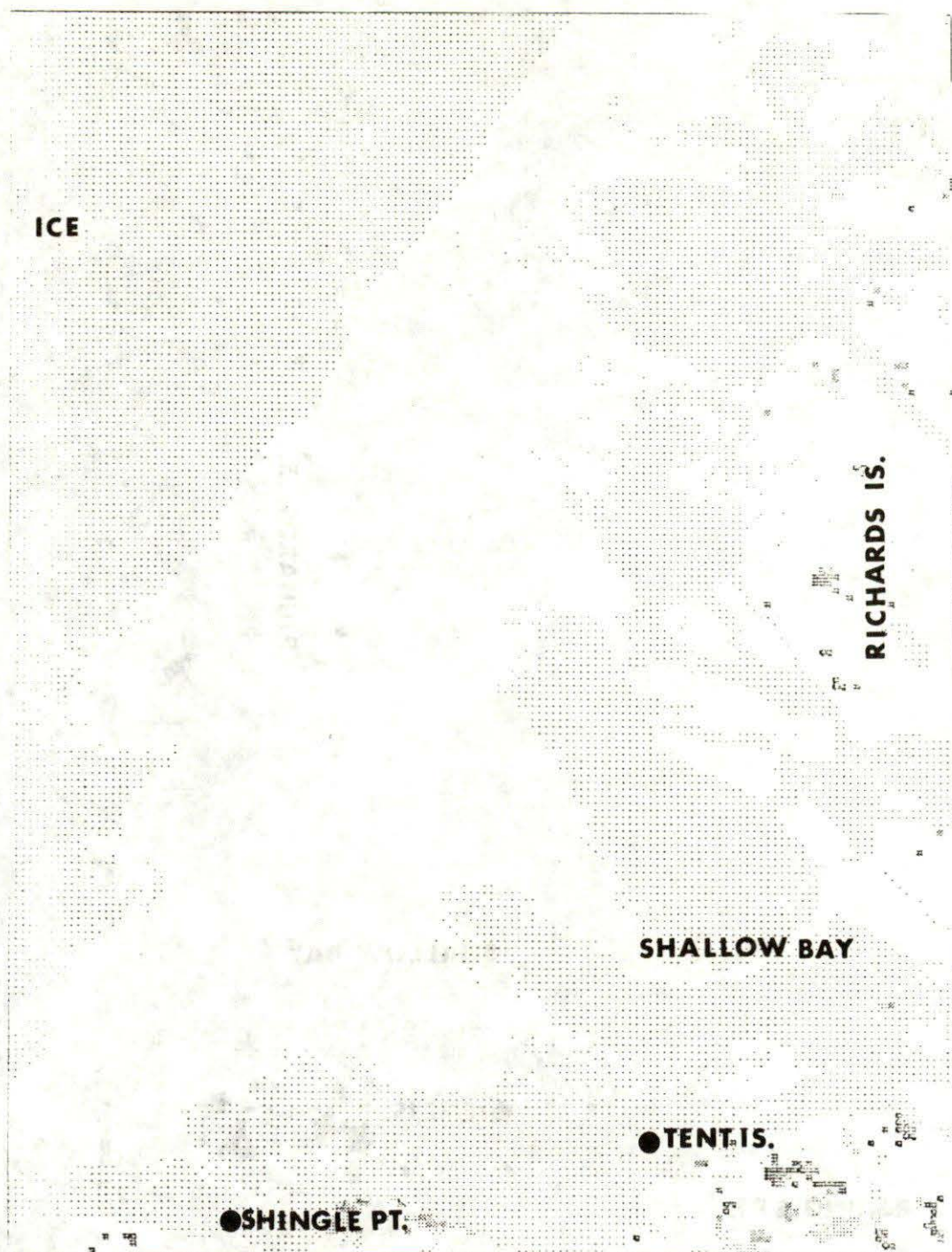
Figure 102. A line printer plot of the band 5 grey-levels on August 8, 1974. A great similarity is seen between the shapes and positions of the brightest water areas as observed on this date and on July 10, 1973 (Figure 101).

parallels the coast, extending out to approximately the 30 m contour
of depth. The comparatively stationary ice in this zone is separated
from the adjoining seaward transition zone by a boundary lead which
is present over most of the apparently normal November to July life-
span of the landfast ice. Little year to year variation was
observed in the position of this lead. The one month longer
extension of the landfast ice season observed in 1974 may be attri-
buted to either the extreme inshore position of the summer pack ice
and/or the large amount of thicker multiyear ice blown into coastal
areas during the 1973 freeze-up. The landfast-ice, although often
penetrated by small leads, generally acts to protect coastal areas
against floating and ice-fixed pollutants.

Observations of the transition zone in the areas of the proposed 1976
drilling sites indicate the existence of a seasonal shift from
southwestward to northeastward ice motion which occurs in late June
or July. The shift probably more or less coincides with a similar
transition in the basic trend of the offshore "gyral" flow. Studies
of the consecutive daily NOAA and ERTS images indicate that, in
months at least as early as March, daily displacements on the order
of 10 km were commonplace and at times exceeded 20 km. In the later
winter-early spring months, the ice configuration in this area
seemed to alternate between a high density of short coast-paralleling
leads and an orthogonal arrangement of longer, wider leads. The
latter channels of open water often appeared to be extensions of the
major north-south leads in the gyral pack which hence, in effect,
reached all the way to the landfast-ice boundary. By a progressive
widening process which propagated to the southwest and into
Mackenzie Bay, the landfast-ice boundary lead developed into the
designated eastern terminal polynya which constituted, in fact, the
bulk of the summer open water region of the Beaufort Sea. Motion of
the more-finely divided ice during the April to May period continued
to the southwest with speeds averaging on the order of 10 km/day and
rising to at least 55 km/day.

Although differences were noted in the late summer, early fall open
water distributions, in all three years the position and configuration
of the ice pack boundary was such that significant concentrations of
large floes occupied the proposed drilling sites during the mid-
drilling season period of late August. In 1973 this ice eventually
retreated to the westward, but in the other years extremely unfavour-
able operating conditions continued through the remainder of the
season. Overall conditions seemed to be slightly better at the most
eastern (#1) of the two sites. However, assuming the 43% probability
existence of winds in excess of 10 knots, the imagery and accompany-
ing circles of Figures 82-84 indicate that in each of the observed
years, mid-season drilling work could have only proceeded under the
12 or 4 hour alert procedures specified by Canmar Ltd. In view of
the short interval of time between the normal early July break-up of
the landfast-ice and the early October closing-down of the navigation
season, the apparent high likelihood of these interruptions would
appear to heavily prejudice the odds against the successful single
season inception and completion of a 15,000 foot drilling program.

Satellite observations of the gyral ice pack zone indicate rough agreement between the gyral contours of Figure 11 and the average motion over the spring to fall period. In 1975, however, distinct seasonal trends were observed with net displacements being westward and south-southeastward for the spring and summer seasons, respectively. A general summer speed-up was noted in the pack motion. Easterly wind allignments and large westward ice-drifts were closely correlated over the March-May periods, and tended to open large, nearly north-south flaw leads to the east of earlier major lead structures. However, no consistent relationship was found between the displacement field of the gyral ice pack as measured over one week intervals, and corresponding average atmospheric pressures.

The rigidity of much of the ice motion, i.e. relative displacements within the pack were much smaller than the corresponding absolute movements relative to fixed earth features, suggests the importance of collective effects and internal ice forces. These may play a critical role in the dynamics of the long rectilinear leads which were discovered to be common elements in the deep water ice cover. The observed periodicities and persistence of the patterns formed by intersecting parallel sets of these leads suggests that there are systematic elements in the ice pack dynamics. An offered planetary wave-induced current interpretation of these phenomena has been successful in several respects, particularly in explaining the relative lead orientations, their periodicity, and the apparent long-term continuance of shearing motion along their lengths. However, it is difficult to visualize a mechanism whereby the rectilinearity of the postulated current structures can be maintained in the presence of the known gyral surface water movements. An alternative mechanism, without this drawback, can be visualized on the basis of the rheology or mechanical properties of the complicated ice cover medium. In this approach the leads, considered as "strike-slip" faults, give a direct measure of the angle of internal friction, $\phi \approx 14°$, associated with the ice cover. Furthermore, the existence of two sets of intersecting leads arises quite naturally because of the two lines of yielding (separated by 2ϕ) which appear in any planar stress arrangement. However, neither the reproduction of the observed spatial periodicities nor the identification of the responsible stress fields has yet been achieved in these terms. In any case, regardless of the ultimate resolution of the lead generation question, the concentration of internal ice pack motion at the rectilinear leads makes them fundamental components in the meso- and macro-scale dynamics of the gyral ice cover.

5.2 Ice Modelling and Predictions

The availability of ice displacement data over thousands of square kilometres of the Arctic Ocean should encourage the development of modelling programs directed at the prediction of pack boundaries, coastal ice densities, etc. Such models would require, because of the more or less rigid pack motion, wind data over much of the western Arctic Ocean and some experimental and theoretical clarification of the basic current driving forces. In the latter respect,

GYRAL PACK ICE

TRANSITION ZONE

LANDFAST ICE

71°

70°

133

Herschel Is.

Richards Is.

Tuktoyaktuk Peninsula

Tuk

Mackenzie Bay
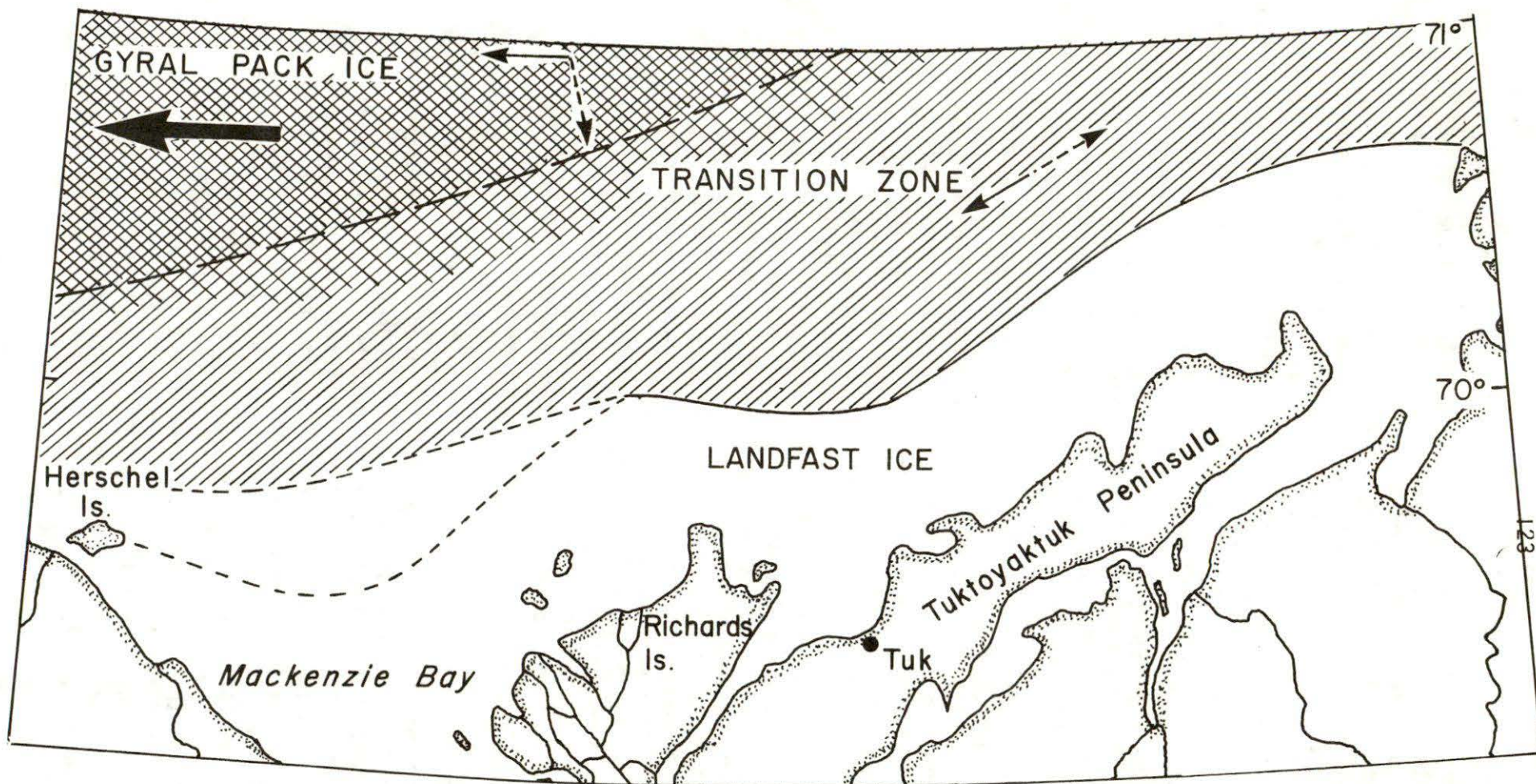
Figure 103. A schematic representation of the different ice zones of the southeastern Beaufort Sea. The large solid arrow indicates the direction of the prevailing average gyral motion while the lesser solid and broken-line arrows respectively represent the direction of the dominant motion in the winter-spring and summer-fall periods. The variable positioning of the landfast ice in western Mackenzie Bay is indicated by the broken line boundaries merging at Herschel Island.

particular attention must be paid to the possibility, suggested by Newton (1973), that identified barotropic ocean current components are not wind driven but are instead produced by the effects of atmospheric pressure gradients acting upon the uncompensated or level sea surface. The noted lack of correlation between the magnitudes of the ice and barotropic component currents may imply a need for a more sophisticated representation of the ice-water interaction than has been used in previous model calculations. The lack of any consistent similarity between the ice displacement fields measured in the present work, and the wind fields deduced from the average barometric contours is, at the very least, indicative of the complexity of the ice motion problem.

The very close correspondence noted between the production of major lead and polynya systems and significant easterly wind components would seem to raise questions concerning the efficacy of long-range ice condition prediction schemes which do not have, at their core, a similarly long-range weather forecasting program. Thus, although thickness, ridge-density, etc. do undoubtedly have an effect upon the response of ice to a driving atmosphere, these properties are likely to be less important to the eventual surface configuration and movement than the details of the extant weather system. A simple categorization of navigational seasons into qualitative groupings of "good", "fair" and "poor" tends to submerge important details of the variability within seasons and in different geographical locations which derives from the specific succession of driving conditions. For example, although the 1975 winter-spring atmospheric conditions led to the largely ice-free Beaufort Sea of early summer, the later mid- to late-summer wind and air pressure patterns drove ice into this same area and held it there for the remainder of the normal navigational season. The necessary secondary steps in a weather-forecast based ice condition prediction system requires a detailed representation of ice response under the forcing effects of wind, atmospheric pressure and surface water currents. As indicated above, the rate of development of the necessary general model of ice movement should be, in large part, determined by the availability of high quality, all-weather satellite coverage in the Arctic Ocean.

5.3 Implications for Pollutant Transport

An evaluation of the likely movements of oil leaked into the southeastern Beaufort Sea is complicated by the considerable year-to-year variations observed in basic parameters such as the ice-covered to open-water ratios and the extent of the Mackenzie River plume. In spite of accompanying elements of constancy in seasonal flow-directions, landfast-ice boundary positions, etc., it is difficult to derive meaningful average ice and water configurations. However, in lieu of more complete data, these repetitive aspects of the environment, together with some allowances for possible extreme situations, must be the basis upon which pollutant transport predictions may be founded. A scenario is developed below assuming an oil blow-out occurs during the late August to early October period when drilling areas may be under or close to large concentrations of floe ice (see Figures 82-84).

Throughout this interval of time there should be considerable open water interspersed among the huge year-old and multi-year floes which dominate the area along the edge of the pack. Moreover, when some consolidation of the pack occurs, wide leads can appear oriented in directions perpendicular to the coastline. Since a landfast-ice barrier cannot be expected to develop, as in Figure 104, until late October or early November, coastal contamination in the interim period is likely from floating oil which moves down these leads and/or percolates through other more irregular pathways of open water. Winds may also be expected to drive contaminated ice into the very shallow water regions. The prevailing currents and ice movements at this time would tend to carry the contaminated ice and slicks to the northeast at rates which depend upon the wind velocities but average out to net daily displacements on the order of 10 km. It would be difficult to maintain an oil burnoff over the well head at this time because of the high concentration of rapidly-moving large floes.

At some time during the unobserved winter season a reversal occurs in the prevailing northeastward water and ice flow along the shelf of the southeastern Beaufort Sea. It is possible that this reversal follows the rapid drop in river discharge which normally occurs in late September and early October. In this case the previously accumulated northeastward swath of contaminated ice and open water patches would begin a southwestward movement, eventually over-running and co-mingling with the "new" oil produced at the wellhead. Presently, no estimates of the winter flow rate are available but, on the basis of our March observations, a net daily displacement of 5 km seems reasonable. At this rate, contaminated ice produced at either of the two proposed drilling sites would move quite quickly (in less than a month) across the northern reaches of Mackenzie Bay and into the gyral pack whose motion parallels the mainland coast west of Herschel Island. A comparable avenue for oil dispersal would be provided by the landfast-ice boundary lead. The various changes which occur in the exact position and edge contours of this lead may be expected to bring it either directly over or within a few kilometres of Site #1. Leads in the transition zone oriented in both the parallel- and perpendicular-to-coast directions could in any case maintain an intermittent leakage of oil into this boundary channel from Site #1, as well as from the more seaward Site #2. The currents should carry the oil westward along the length of the boundary lead. Inevitably a slow flow of oil into this lead will be maintained from reservoirs in the cracks and channels near the edge of the landfast-ice. Periods of intense ridge formation occasioned by severe winter storms may force contaminated ice and floating slicks into the body of the landfast ice and closer to beach areas. In the spring, the main environmental threat would come from the concentrations of floating, weathered oil in the boundary lead and in other small leads to its seaward which serve as the obvious wildlife pathways into Amundsen Gulf. Again, the prevalence of large floes and sizeable, approximately 10 km/day, ice speeds greatly complicate any attempts at a burnoff of the surfacing oil. The tendency of the barrier lead to grow into the summer open water area would seem to guarantee the retention of weathered floating oil offshore of the lower Tuktoyaktuk Peninsula. A June break-up of the partially contaminated shorefast
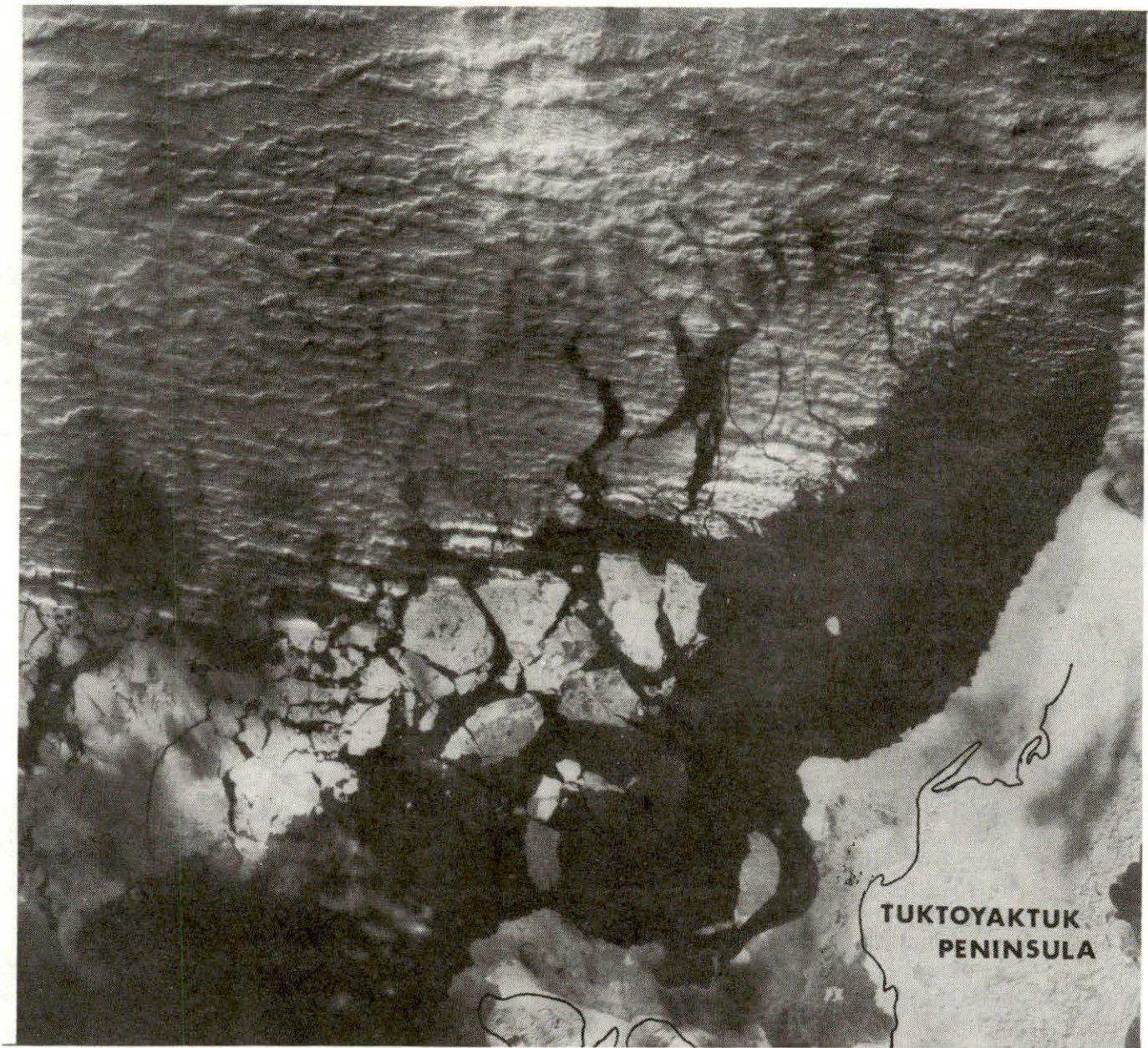
Figure 104.   An October 24, 1974 ERTS satellite image of the Kugmallit and
              northern Mackenzie Bays.

ice and the mid-summer resumption of a northeastward flow would then gravely threaten the biologically critical beaches of the Peninsula and the waters of Amundsen Gulf with both old and newly surfaced oil.

By July, the westward reaching swath of disconnected patches of blackened ice may reach (assuming a 3 km/day gyral motion) 700 to 800 km along the mainland coast to the Alaskan north slope. The width of this swath and its incursions into inshore areas will be determined by the accumulated changes in the coastal and gyral pack wind fields as well as by more complex current structures such as those observed by Newton (1973) which may be associated with the rectilinear leads and localized ice shearing. This width may be very conservatively estimated to be 100 to 200 kilometres.

The existence of rectilinear leads in the southern Beaufort Sea (see Figure 47) provides a mechanism whereby oil may be rapidly led into the body of the gyral ice pack. In the short run, this oil is removed as a threat to coastlines and wildlife migratory routes. However, the full effects of its presence in the essentially in-accessible pack ice are not easy to assess. This oil will certainly increase the absorption of radiant energy and enhance melting in the comparatively cloud-free central pack area. Whether this in turn will significantly affect the thermal and/or macroscale mechanical properties of the pack remains an open question, depending critically, of course, upon the quantities of injected oil. Clearly any permanent or semi-permanent change in the seasonal or spatial distri-bution of even very small open water areas would represent an important variation in the parameters and character of the Arctic environment.

In summary, the proposed 1976 drilling sites appear to be particularly hazardous to the environment from two nominally opposite points of view. First, they are located in an area of relatively high late-summer ice density. This circumstance, of course, increases the probability of a spill, shortens the drilling season, and reduces the prospects for successful relief well drilling during the second summer. On the other hand, it is the proximity of both these sites to the barrier lead and other related areas of open water which make them particularly effective threats to the biota of the offshore and coastal areas.

The offered scenario of pollutant transport obviously does not exhaust all possibilities. Depending upon the specifics of any given season, the environmental consequences of a spill can be either con-siderably greater or smaller than those described. The true extreme and most probable situations can be more clearly estimated by the continuance and extension of Beaufort Sea research in the directions recommended in the following and final section of this report.

5.4   Recommendations for Future Research

5.4.1   Ice Movement

The existing data on ice movement in the western Arctic
Ocean cannot provide an adequate basis for a detailed ice-
cover modelling program. The density and frequency of the
displacement data grid should be increased through better
analysis techniques using aids such as the Bausch and Lomb
Zoom Transfer Scope which correct some of the geometric dis-
tortions introduced by satellite image-scanning systems.
Continued compilation of displacement data, both on the ERTS
and NOAA satellite scales is essential to increasing our
general knowledge of the ice-cover dynamics as well as en-
hancing our ability to identify and explain the origins of
unusual events such as the extremely wide-spread and spatially
regular lead patterns of September-October 1974. Particular
effort should be directed toward obtaining winter data from
the thermal infrared wavelength sensor of the NOAA satellites.

5.4.2   Ice Character and Leads

The details of lead growth, disappearance and general
behaviour remain poorly known and appear germaine not only to
the dynamics of the ice cover but also to questions of energy
and mass exchange between the atmosphere and the ocean. It
should prove possible to relate lead production to the over-
all field of ice motion and to the spatial distribution of
the various ice-types (year-old, multi-year, new),
surface moisture levels and temperature. The four wavelength
band facility of the ERTS satellites has not yet been fully
exploited in Beaufort Sea ice-type identification. It should
now be applied to specific problems of immediate interest such
as the seasonal and year to year variations in the composition,
ridge-density, etc. of transition zone and landfast-ice, as
well as toward the anomalous persistence of low reflectivity
refrozen leads in the central ice pack.

A need remains for more complete time dependence data on the
shearing motions associated with rectilinear leads. Values
should be obtained for the lifetimes of such leads and obser-
vations carried out to detect the spatial migration of the
localized shearing motions as some rectilinear leads close
and others open. These studies would be facilitated by the
present existence of two orbiting ERTS satellites which thus
offer an average 50% probability of daily coverage for any
point in the Beaufort Sea. All-weather microwave sensor data
from planned Canadian and U.S. aircraft over-flights should
be available and research program development is necessary in
anticipation of the near-daily receipt of similar data from
the Seasat-A satellite package scheduled for a 1978 launch.

5.4.3 Peripheral Open Water Areas

Present practical interests in the Arctic Ocean are heavily concentrated in the relatively narrow strip of water that develops each spring and summer along the coastal periphery of the Beaufort Sea ice pack. The extents and configurations of these waters determine, in part, biological productivity, wildlife migration routes, sea state and contribute to the global weather. Studies of these and other problems would be aided by continued observation of the movement of coastal ice floes and silted water. Specific interest would be centered on Mackenzie, Kugmallit and Liverpool Bays where a small number of characteristic flow patterns have been identified (Herlinveaux and de Lange Boom, 1976; MacNeill and Garrett, 1976). Such a program would allow a general expansion of a very limited data base and could lead probability estimates for the occurrence of specific configurations or events such as the appearance, in 1974, of low salinity, Mackenzie River water off the southern coast of Banks Island.

5.4.4 General

A satellite-based observation and data-taking program directed toward the three cited areas of interest should proceed simultaneously with corresponding surface data gathering and theoretical and/or numerical modelling efforts. Cooperation of this kind has been thus far largely confined to the recti-linear lead problem where theoretical and satellite obser-vation efforts have proceeded at a coordinated pace but still in the absence of relevant surface data. The more ambitious programs involving ice-motion modelling clearly need large amounts of surface data. Some of this data, particularly in the landfast and transition ice zones, can be obtained from manned field stations. However, the overall information demand is such that telemetering buoys and radiosonde baloons are essential components of a viable research program. Con-current development is proceeding on meteorological models of surface winds and pressures based upon expected improvements in the grid of Arctic telemetering stations. It is antici-pated that the outputs of such a model, based on perhaps a 50 km grid, would be adequate to derive the surface stress fields applicable to the interpretation of the observed ice and water motions.

In conclusion, it seems clear that satellite imagery can make significant contributions to our understanding of the Beaufort Sea and the encompassing Arctic Ocean. Further progress toward a truly quantitative Arctic science now requires the coordination of such observations with the more traditional ground-truth and theoretical methods of oceanography.

APPENDIX

POSSIBLE RELATIONSHIP BETWEEN RECTILINEAR LEAD PATTERNS AND PLANETARY WAVES

In developing a specific planetary wave interpretation of the observed recti-
linear lead phenomena, our attention has been concentrated primarily upon the
diamond-shaped ice structures observed in September and October of 1974. We
have assumed that the leads form along the junctions of oppositely directed
current regimes. Each of the two lead sets of Figures 42 and 43 (identified
as "1" and "2" in Figure 44) thus establishes the phase propagation direction
of a corresponding transverse wave. Using a wavenumber diagram appropriate to
planetary waves controlled by the β-effect (Figure 105) wave "1" was found to
have a southward group velocity, corresponding to a disturbance originating
in the northern sector of the Canada Basin. Its apparent reflection from the
southern continental shelf may be identified with wave "2" whose group
velocity advected energy to the northeast. Current structures formed by the
simultaneous presence of these two wave sets have been sketched in Figure 106
together with solid lines representing the loci of the corresponding maximum
shears. As required, the arrangement of these lines closely resembles the
observed lead patterns, while the specified directions of phase propagation
are consistent with earlier deductions made from oceanographic data (Newton,
1973).

The wave model is satisfying for a number of reasons. First of all, meridion-
ally propagating waves over a large portion of the southern Basin would be
moving over a region of almost uniform depth and would therefore be expected
to be governed by the β-effect. Secondly, the incident and reflected group
velocities are consistent with the requirement of no net energy flux across
the southern boundary. In addition, the waves satisfy the condition that the
wavenumber component parallel to the boundary be conserved. They also have
wave-number magnitudes which are nearly equal, as implied by the observed
lead spacings. Moreover, as our model requires adjacent leads to be separ-
ated by one-half wavelength, the 200 km wavelengths suggested by Figure 106
consistent with the value obtained in the previous investigation (Newton,
1973). Applying to wave "1" the standard expression for the frequency σ
(Longuet-Higgins, 1964)

$$\sigma = \frac{\beta k}{k^2 + \ell^2} \tag{1}$$

where k and ℓ are respectively the east and north components of the wave-
number, gives a characteristic period of 450-600 days (1.2 - 1.6 years). The
corresponding phase and group speeds are roughly 0.5 cm s^{-1} and 0.3 cm s^{-1},
respectively, for both wave components. Since planetary waves incident upon
the eastern boundary would also be reflected by the steep continental slope,
the absence of rectilinear leads in the ice cover of the continental shelf in
this region adds further support to our interpretation. Unlike the incident
waves at this boundary, the reflected waves produce no detectable lead
pattern because of their exceedingly long wavelengths (> 600 km). Finally,
the observed tendency toward parallel-to-boundary allignment of the reflected
wave crestlines could be due to an increased topographic influence in the
region of the continental rise.
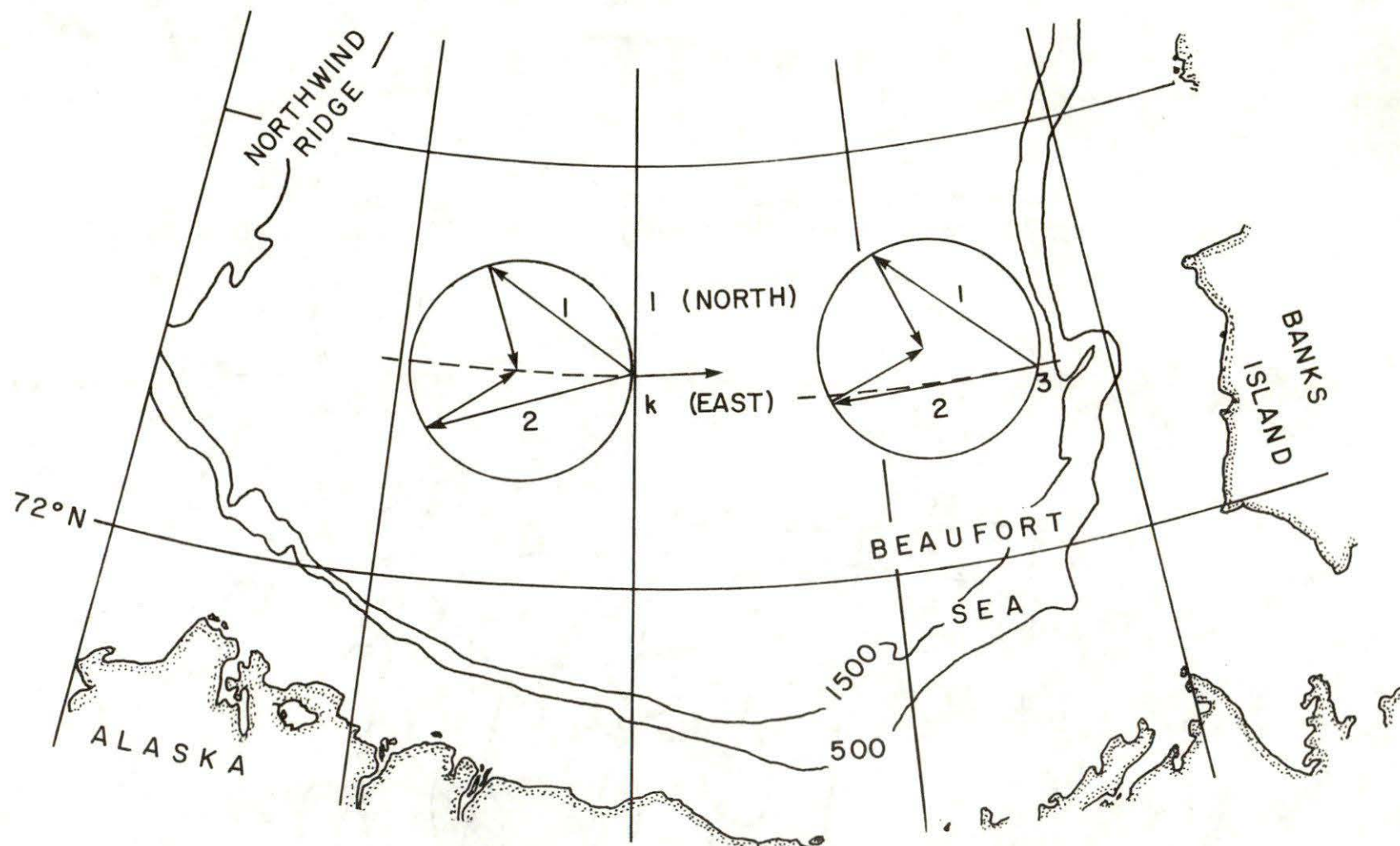
Figure 105.   Circles giving the wavenumber loci at constant frequency for planetary waves in the southern sector of the Canada Basin. Group velocities are directed from the tip of the wavenumber vectors to the circle centers.   Incident energy flux is associated with phase propagation direction 1, its reflection from the southern boundary with phase propagation direction 2.   The left-hand circle is applicable to waves unaffected by bottom topography, while the right-hand circle applies near the eastern boundary where topography is not fully compensated by baroclinicity.   At this boundary, wave 2 is reflected as an undetectable very large wavelength disturbance.
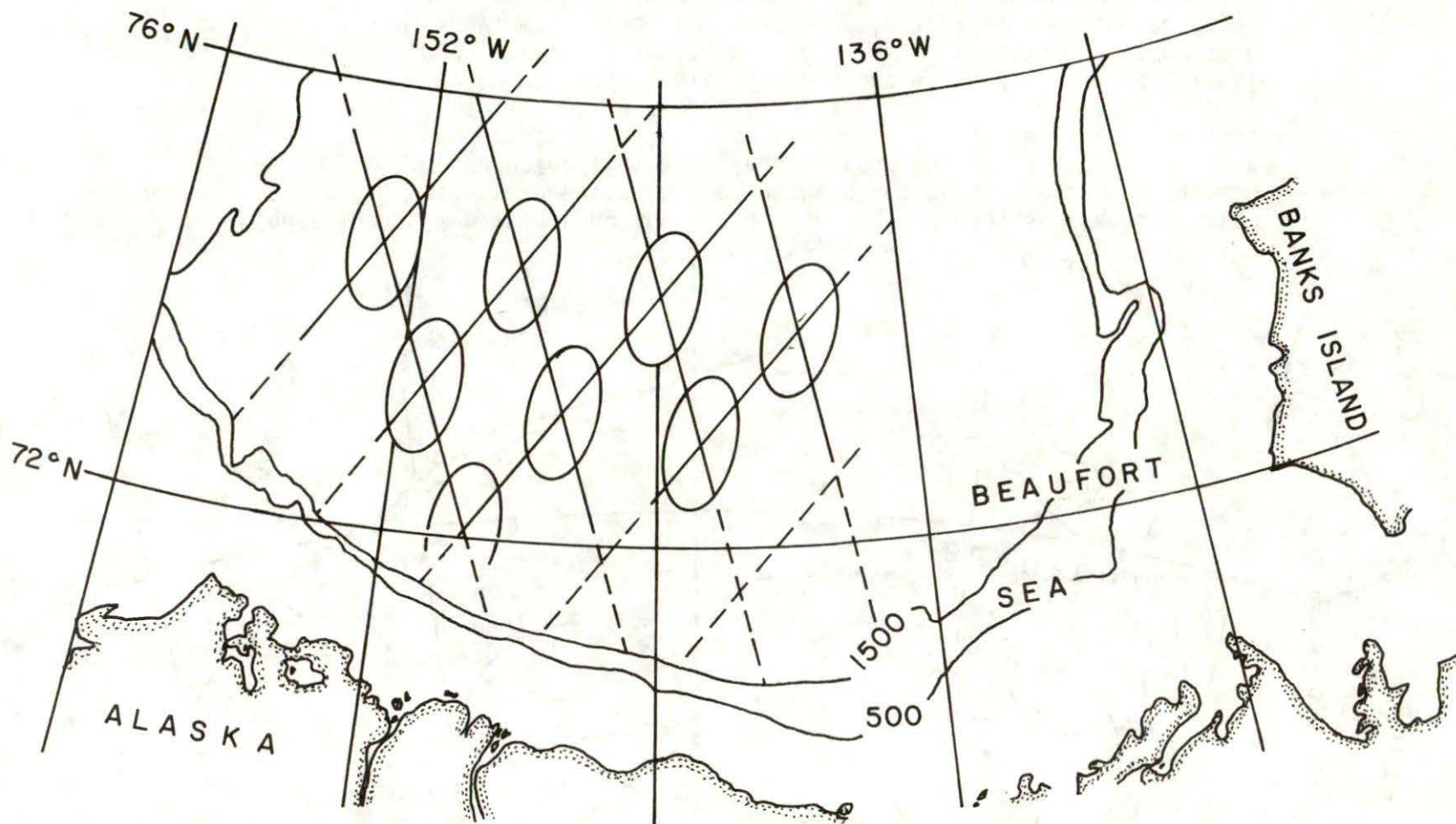
Figure 106. The lines of maximum shear associated with the individual wave sets "1" and "2". Representative resultant eddy currents are also shown for part of the Basin.

Our very simplistic model of the wave properties within the Basin is only valid if the depth-induced vortex stretching does not dominate the β-effect. For purely barotropic Rossby-type waves, the magnitude of the former effect is simply determined from spatial variations in the fluid depth, h, so that its effectiveness as a restoring force is given by the ratio $R = f|\nabla h|/\beta h$ where f is the Coriolis parameter. Over the continental rise where R >> 1 such waves would be totally controlled by the topography and would have substantially shorter periods than those inferred from Equation 1. For baroclinic waves, on the other hand, R needs to be redefined in terms of an effective depth, h*, whose space-time variations are determined by the water density structure. Topographic influence may then be partially or fully compensated by adjustments in the density field. It is difficult to explain the observed lead orientations on the basis of purely barotropic waves or to account for their observed extension west of the Northwind Ridge which forms the western boundary of the Basin (since $\nabla hf/h\sigma$ >> 1 at this boundary if σ is given by (1), it acts like a rigid wall (Rhines, 1969)). The fact remains that at least in 1974 and 1975 lead patterns were seen in shallow (< 200 m) areas of the Chukchi Province where long wavelength planetary waves, such as those proposed for the Canada Basin, would normally be expected to be critically damped. The resolution of these difficulties may lie in the baroclinic nature of the waves, which according to Newton's observations are confined to the upper 200 metres of the water layer. In such cases topographic effects might be nearly compensated everywhere in the Basin except in the area of the eastern continental rise. On the other hand, one other very serious objection to our simple Rossby wave interpretation may be resolvable by invoking topographical rather than β-effect control in critical slope areas. The difficulty in question was pointed out by Dr. Coachman (personal communication) and amounts to the expectation that, because of the low wave speeds predicted from (1) relative to the local mean flow, the resultant wave fronts would not retain a rectilinear character. A barely recognizable lead pattern would be produced and in the southern sector the reflected wave component would apparently be propagating against a more rapid mean flow.

Alternate, more rapidly propagating planetary-type disturbances such as Sverdrup-, Poincaré-, and Kelvin-waves would not present the latter difficulties. However, such rapidly moving waves would not be consistent with the observed slow linear advection of the lead pattern in the southern portion of the Basin, nor be capable of producing the needed localized stress on the ice cover.

One possibility is that topographical control of the planetary waves on the continental slopes gives rise to a phase-locked or quasi-permanent wave structure in view of the fact that the favoured direction of phase propagation is anti-clockwise and hence opposed to the anti-cyclonic mean flow. The situation would be much as obtains in the atmosphere where a fixed wave-like pressure pattern results corresponding to the appropriate phase-locked Rossby wave. In the oceanic case, the current structures would be more or less permanent features of a given local area of the Basin. It is conceivable that this mechanism could explain the generation in May 1975 of new, similarly oriented rectilinear leads in the region in which the now refrozen and advected-away leads appeared a few months earlier (see Figures 10, 48-51). The exploration of this and other approaches requires further data on the nature of the surface advection and ice-evolution processes. It should be noted that the passive role assigned to the ice in this model is clearly an

oversimplification. The ice state (thickness, compactness, etc.) appears to affect the magnitudes of the shearing motions and almost certainly is an important factor in determining the extent and definition of the lead patterns. Similarly, it is probably the internal, cohesive ice forces which ensure that each of the lead-delineated ice fields moves as a single rigid unit, eliminating any possible uniformly parallel allignment of the ice and underlying water motions. A representation of these forces is necessary if the simple motions sketched in Figure 44 are to be quantitatively related to the flow structure. Some observations were made of new lead formation, which, as part of an internal pack rearrangement process, apparently maintained the criss-cross pattern in the presence of the steady, effectively unidirectional shearing displacements. However, the amount of data available is presently inadequate to allow the characterization of these processes or for that matter to clarify the other cited ice physics problems. A finite duration of the observed shearing motions might allow us to understand the patterned ice-cover as an advecting replica or "snap-shot" of a stationary quasi-permanent current structure. Alternatively, the long-term continuance of such motions would support the detailed advecting current structure picture developed above.

The origin and properties of the shallow water leads need to be carefully examined and their relationship, if any, to the Basin phenomena, established. Higher order effects such as wave trapping by sea mounts (Rhines, 1970) and current structure advection have not yet been considered. Fortunately, current data should be relatively easy to obtain in the Chukchi Province shallow water zone since this area is commonly ice-free for three to four months of each year. Canada Basin current data from the 1975 AIDJEX program should also be forthcoming shortly. Hopefully, these various bits of information can be put together with the available satellite ice observations to construct a fully self consistent model of repeating rectilinear lead generation in the Canada Basin and adjoining areas of the Arctic Ocean.

REFERENCES

Ackley, S.F. and W.D. Hibler, III (1974). Measurements of Arctic Ocean deformation and fracture patterns. Presented at SCOR/SCAR Polar Oceans Conference, Montreal.

Campbell, W.J. (1965). The wind-driven circulation of ice and water in a polar ocean. J. Geophys. Res. 70, 3279-3301.

Campbell, W.J. and L.A. Rasmussen (1972). A numerical model for sea ice dynamics incorporating three alternative ice constitutive laws in sea ice. Proceedings of an International Conference, Reykjavik, Iceland, May 10-13, 1971. Thorbjörn Karlssen (ed.). National Research Council of Iceland, Reykjavik, 176-187.

Campbell, W.J., P. Gloersen, W. Nordberg and T.T. Wilheit (1974). Dynamics and morphology of Beaufort Sea ice determined from satellites, aircraft and drifting stations. In: *Approaches to Earth Survey Problems Through the Use of Space Techniques.* P. Bock *et al.* (eds.). Berlin, Akademaie-Verlag, 311-327.

Carstensen, L.P. (1967). Some effects of sea-air temperature differences, latitude and other factors on surface wind-geostrophic wind ratio and deflection angle. Technical Report #29, Fleet Numerical Weather Facility, Monterey, Calif.

Crowder, W.F., H.L. McKim, S.F. Ackley, W.D. Hibler, III and D.M. Andersen (1974). Mesoscale deformation of sea ice from satellite imagery. In: *Comp. Advanced Concepts and Techniques in the Study of Snow and Ice Resources.* H.S. Santeford and J.L. Smith (eds.). Washington, D.C., National Academy of Sciences, 563-573.

Gower, J.F.R. and I. Daniel (1974). The use of ERTS-1 computer-compatible tapes with respect to marine research. Pacific Marine Science Report 74-2.

Herlinveaux, R.H. and B. de Lange Boom (1976). Physical oceanography of the Southern Beaufort Sea. Beaufort Sea Project Technical Report #18.

Hunkins, K.L. (1974). Subsurface eddies in the Arctic Ocean. Deep Sea Res. 21, 1017-1033.

Jaeger, J.C. (1971). *Elasticity, Fracture and Flow.* 3rd edition. Halsted Press (New York).

Kinder, T.H., L.K. Coachman and J.A. Galt (1975). The Bering Slope current system. J. Phys. Oceanog. 5, 231-244.

LeBlond, P.H. (1964). Planetary waves in a symmetrical polar ocean. Tellus 16, 503-512.

Longuet-Higgins, M.S. (1964). Planetary waves on a rotating sphere. Proc. Roy. Soc. London A279, 446-473.

MacNeill, M. and J.F. Garrett (1976). Open water surface currents. Beaufort Sea Project Technical Report #17.

Markham, W.E. (1976). Ice climatology in the Beaufort Sea. Beaufort Sea Project Technical Report #26.

Marko, J.R. and R.E. Thomson (1975). Spatially periodic lead patterns in Canada Basin sea ice: A possible relationship to planetary waves. Geophys. Res. Lett. 2, 431-434.

Maykut, G.A. and N. Untersteiner (1971). Some results from a time-dependent thermodynamic model of sea ice. J. Geophys. Res. 76, 1550-1575.

Newton, J.L. (1973). The Canada Basin: Mean circulation and intermediate scale flow features. Doctoral Dissertation, University of Washington, Seattle (inpublished).

Newton, J.L. and L.K. Coachman (1973). Observations of ice motion and interior flow field during 1971. AIDJEX Pilot Study, AIDJEX Bulletin #18, 5-30.

Press, F. and M. Ewing (1957). Propagation of elastic waves in a floating ice sheet. Trans. Am. Geophys. U. 32, 673-678.

Reed, R.J. and W.J. Campbell (1960). Theory and observations of the drift of Ice Station "Alpha". Final Report, Office of Naval Research Task No. NR 307-250.

Rhines, P.B. (1969). Slow oscillations in an ocean of varying depth, Part I: Abrupt topography. J. Fluid Mech. 37, 161-190.

Rhines, P.B. (1970). Edge-, bottom-, and Rossby waves in a rotating stratified fluid. Geophys. Fluid Dyn. 1, 273-302.

Rossby, C.G. (1938). On the mutual adjustment of pressure and velocity distribution in certain simple current systems, II. J. Mar. Res. 1, 234-263.

Rothrock, D.A. (1973). Circulation of an incompressible ice cover. AIDJEX Bulletin No. 18, 61-68.

Veronis, G. (1966). Rossby waves with bottom topography. J. Mar. Res. 24, 388-394.

Wadhams, P. (1973). Attenuation of swell by sea ice. J. Geophys. Res. 78, 3552-3563.

Walker, E.R. (1975). Oil, ice and climate in the Beaufort Sea. Beaufort Sea Project Technical Report #35.

Zubov, N.N. (1943). Arctic ice. (English trans. National Technical Information Service No. AD 426972, 491 pp.).

ACKNOWLEDGEMENTS